13. SITE 681[1]

Shipboard Scientific Party[2]

HOLE 681A

Date occupied: 0115 L, 7 November 1986

Date departed: 2400 L, 7 November 1986

Time on hole: 22 hr 45 min

Position: 10°58.60′S, 77°57.46′W

Water depth (sea level; corrected m, echo-sounding): 150.5

Water depth (rig floor; corrected m, echo-sounding): 161.0

Bottom felt (m, drill pipe): 161.3

Penetration (m): 187.0

Number of cores: 20

Total length of cored section (m): 187.0

Total core recovered (m): 112.4

Core recovery (%): 60

Oldest sediment cored
Depth (mbsf): 187.0
Nature: diatomaceous mud and mud turbidite
Age: Pleistocene
Measured velocity (km/s): 1.64

HOLE 681B

Date occupied: 0000 L, 8 November 1986

Date departed: 1315 L, 8 November 1986

Time on hole: 13 hr 15 min

Position: 10°58.60′S, 77°57.46′W

Water depth (sea level; corrected m, echo-sounding): 150.5

Water depth (rig floor; corrected m, echo-sounding): 161.0

Bottom felt (m, drill pipe): 161.9

Penetration (m): 143.5

Number of cores: 16

Total length of cored section (m): 143.5

Total core recovered (m): 97.3

Core recovery (%): 67.8

Oldest sediment cored
Depth (mbsf): 143.5
Nature: Sandstone
Age: Pliocene–Miocene (?)
Measured velocity (km/s): 1.64

HOLE 681C

Date occupied: 1315 L, 8 November 1986

Date departed: 1800 L, 8 November 1986

Time on hole: 4 hr 45 min

Position: 10°58.60′S, 77°57.46′W

Water depth (sea level; corrected m, echo-sounding): 150.5

Water depth (rig floor; corrected m, echo-sounding): 161.0

Bottom felt (m, drill pipe): 161.9

Penetration (m): 91.4

Number of cores: 10

Total length of cored section (m): 91.4

Total core recovered (m): 86.24

Core recovery (%): 94.4

Oldest sediment cored
Depth (mbsf): 91.4
Nature: Not studied
Age: Quaternary
Measured velocity (km/s): 1.53

Principal results: Of the three sites (679, 680, and 681) along the east-west transect crossing the upwelling deposits of the Peruvian shelf and upper slope, the most landward (and consequently the shallowest) is Site 681. This site is also located nearest the origin of coastal upwelling centers around the headlands near 11°S; its depth nearly coincides with the top of the oxygen-minimum zone. Thus, an ex-

[1] Suess, E., von Huene, R., et al., 1988. *Proc. ODP, Init. Repts.*, 112: College Station, TX (Ocean Drilling Program).

[2] Erwin Suess (Co-Chief Scientist), Oregon State University, College of Oceanography, Corvallis, OR 97331; Roland von Huene (Co-Chief Scientist), U.S. Geological Survey, Branch of Pacific Marine Geology, 345 Middlefield Rd. M/S 999, Menlo Park, CA 94025; Kay-Christian Emeis (ODP Staff Scientist), Ocean Drilling Program, Texas A&M University, College Station, TX 77843; Jacques Bourgois, Département de Géotectonique, Université Pierre et Marie Curie, 4 Place Jussieu, 75230 Paris Cedex 05, France; José del C. Cruzado Castañeda, Petroleos del Peru S. A., Paseo de la Republica 3361, San Isidro, Lima, Peru; Patrick De Wever, CNRS, Laboratoire de Stratigraphie, Université Pierre et Marie Curie, 4 Place Jussieu, 75230 Paris Cedex 05, France; Geoffrey Eglinton, University of Bristol, School of Chemistry, Cantock's Close, Bristol BS8 1TS, England; Robert Garrison, University of California, Earth Sciences, Applied Sciences Building, Santa Cruz, CA 95064; Matt Greenberg, Lamont-Doherty Geological Observatory, Columbia University, Palisades, NY 10964; Elard Herrera Paz, Petroleos del Peru, S. A., Paseo de la Republica 3361, San Isidro, Lima, Peru; Phillip Hill, Atlantic Geoscience Centre, Bedford Institute of Oceanography, Box 1006, Dartmouth, Nova Scotia B2Y 4A2, Canada; Masako Ibaraki, Geoscience Institute, Faculty of Science, Shizuoka University, Shizuoka 422, Japan; Miriam Kastner, Scripps Institution of Oceanography, SVH, A-102, La Jolla, CA 92093; Alan E. S. Kemp, Department of Oceanography, The University, Southampton SO9 5NH, England; Keith Kvenvolden, U.S. Geological Survey, Branch of Pacific Marine Geology, 345 Middlefield Rd., M/S 999, Menlo Park, CA 94025; Robert Langridge, Department of Geological Sciences, Queen's University at Kingston, Ontario K7L 3A2, Canada; Nancy Lindsley-Griffin, University of Nebraska, Department of Geology, 214 Bessey Hall, Lincoln, NE 68588-0340; Janice Marsters, Department of Oceanography, Dalhousie University, Halifax, Nova Scotia B3H 4J1, Canada; Erlend Martini, Geologisch-Paläontologisches Institut der Universität Frankfurt, Senckenberg-Anlage 32-34, D-6000, Frankfurt/Main, Federal Republic of Germany; Robert McCabe, Department of Geophysics, Texas A&M University, College Station, TX 77843; Leonidas Ocola, Laboratorio Central, Instituto Geofisico del Peru, Lima, Peru; Johanna Resig, Department of Geology and Geophysics, University of Hawaii, Honolulu, HI 96822; Agapito Wilfredo Sanchez Fernandez, Instituto Geologico Minero y Metalurgico, Pablo Bermudez 211, Lima, Peru; Hans-Joachim Schrader, College of Oceanography, Oregon State University, Corvallis, OR 97331 (currently at Department of Geology, University of Bergen, N-5000 Bergen, Norway); Todd Thornburg, College of Oceanography, Oregon State University, Corvallis, OR 97331; Gerold Wefer, Universität Bremen, Fachbereich Geowissenschaften, Postfach 330 440, D-2800 Bremen 33, Federal Republic of Germany; Makoto Yamano, Earthquake Research Institute, University of Tokyo, Bunkyo-ku, Tokyo 113, Japan.

panded Quaternary record was obtained at Site 681 for studies of temporal changes in the main upwelling parameters, with particular focus on fluctuations in the upper boundary of the oxygen-minimum zone.

Three holes were drilled at Site 681; Hole 681A penetrated to 187.0 mbsf and >90% of the sediment record (to 139.5 mbsf) was recovered. The section to this depth consisted of repeated sequences of dark olive gray diatomaceous mud containing laminae of diatom ooze, and massive dark gray terrigenous muds with some degree of bioturbation. Below 139.5 mbsf to the bottom of Hole 681A (at 187.0 mbsf), recovery was poor in the section, which was dominated by dark gray silty sand intercalated with sparse units of diatomaceous mud. At Hole 681B, the same Quaternary sequence was piston-cored with excellent recovery to 143.5 mbsf. The Brunhes/Matuyama boundary and the Blake event were recognized in both holes, and numerous floral and faunal markers and phosphorite lag deposits facilitated chronostratigraphic and lithostratigraphic correlations. At Hole 681C, 86.2 m of core was recovered. The samples were frozen without splitting to complete whole-round sampling for geomicrobiology, organic-geochemistry, and physical-properties projects that were not finished at Site 680.

The pore-water and dissolved-gas chemistries of this sediment reveal many intense early diagenetic processes. Throughout the recovered section, organic matter has been remineralized by microbial sulfate reduction. Authigenic dolomite (as rhombs, nodular and blocky zones, and thinly bedded layers) is the main product of diagenesis. Both friable yellowish and dark nodular phosphorites are common and attributed to *in-situ* formation and reworking, respectively, as the mechanisms for concentrating carbonate-fluorapatite at certain stratigraphic zones. Early diagenetic processes are affected by highly saline pore fluids, similar to those discovered at Site 680, where chloride and other dissolved major ion contents increased to concentrations twice those of seawater. The distinctly higher rate of sedimentation at Site 681, compared with Site 680, drives microbial sulfate reduction to completion at 25 mbsf, and a zone of methanogenesis develops between 25 and 85 mbsf. Below this depth, methanogenesis again is inhibited by sulfate replenished from the subsurface brine.

Preliminary studies of Site 681 indicate that the recovered section contains a high-resolution Quaternary record of the Peruvian coastal upwelling regime. This is reflected in well-preserved and abundant diatom floras that occur in laminated muds alternating with bioturbated silty muds. Synchronous with these different facies are alternations in the amount and type of sedimentary organic matter. The frequency of alternation appears similar to that of major glacial/interglacial cycles. The large amplitudes of sea-level fluctuations have not erased the upwelling record at Site 681 because tectonic subsidence during deposition apparently maintained optimal water depth for deposition of this facies.

BACKGROUND AND SCIENTIFIC OBJECTIVES

Site 681 is the most landward site of the east-west transect of three sites (679, 680, 681) across the Peruvian upwelling center at 11°S latitude. The water depth is only 146 m; the site is situated above the depositional center of the outer shelf (Fig. 1). Our scientific objectives relate to the history of coastal upwelling as recorded in Quaternary sediments and were discussed in detail in "Background and Scientific Objectives" of the Site 680 chapter (this volume).

At Site 681, the seafloor intersects the oxygen-minimum zone near its upper boundary. By collecting closely spaced sediment samples, we will be able to reconstruct in detail this sensitive interface through time. We expected that the upwelling facies at Site 681 would be the most complete and expanded section of the transect at 11°S. Changes in the lateral facies along the "average" trail of upwelling plumes observed at Sites 679 and 680 were to be evaluated against the "standard" section of upwelling sediments drilled at Site 681. Furthermore, we expected the sediments at Site 681 to reflect in great detail the seaward–landward shift of upwelling centers during changes in sea level. This shift may have been so dramatic in the past that the most landward part of the shelf may have been entirely removed from the influence of coastal upwelling during extremely low stands of sea level. Because this site is located nearest the origin of coastal upwelling centers, the expected upwelling characteristics of sediments deposited here included the lowest temperature and salinity signals, the highest dissolved-nutrient signals, and extreme apparent oxygen utilization.

The objectives related to geomicrobiology and early diagenesis were expected to take on a new importance at Site 681 because of highly saline pore fluid in the Holocene and late Pleistocene sediments discovered at Site 680. There, salinities of pore waters increased steadily downhole to more than twice the concentration of normal seawater (see "Inorganic Geochemistry" section, Site 680 chapter). The implications for the geomicrobiology program and the objectives related to early diagenesis are profound. Conceivably, the subsurface supply of dissolved sulfate (either by diffusive transport from a subsurface evaporite source or by advection of the brine) (1) will stimulate the activity of sulfate-reducing microbes deep in the sediment, (2) will control dolomitization, and (3) may be the reason for the unexpectedly low rates of methanogenesis in the organic-rich sediments off Peru. Thus, both our geomicrobiology and pore-water sampling programs were intensified at Site 681.

Using the APC and XCB, three holes were drilled at this site to about 200 meters below the seafloor (mbsf). This was expected to provide sufficient samples for the geomicrobiology objectives as well as for the high-resolution studies of the uppermost sediment sequence. The seismic data across the site showed the Pliocene and Quaternary sections encountered at Site 679 to be thicker at Site 681 by about 50 to 100 m. We interpreted most of the expanded section as uppermost Quaternary sediments. The seismic image implied seaward-prograding beds that are about 100 m thick, which we hoped would provide one of the most complete and expanded Quaternary sections from any coastal upwelling regime.

OPERATIONS

After completing Site 680, the ship was under way at 0350 UTC, 7 November 1986, to survey Site 681 using our 80-in.^{3} water-gun and 3.5-kHz acoustic transducer. The geophysical survey proceeded along the line of direct approach between Sites 680 and 681. One reason for the shallow seismic survey was to ascertain that no acoustic turbulent features, "wipe-out" zones, or "pull-down" structures were present in the subsurface to signal free methane gas in these organic-rich sediments of the Peru upwelling zone. We saw no indications of any such features. Instead, the 3.5-kHz record showed excellent penetration into the uppermost mud facies, which continued to increase in thickness (>100 m) but eventually thinned out as the survey line passed landward beyond Site 681. The air-gun record showed two distinct faults with little vertical offset. These faults are confined to the Pliocene/Pleistocene sequence previously drilled at Site 679 and obviously predate deposition of the uppermost mud facies. The faults are about equidistant between Sites 680 and 681.

We dropped a spar-buoy at 0524 UTC in a water depth of 151 m (Fig. 2). Upon retrieving the geophysical gear, the positioning beacon was lowered on a taut wire, and global dynamic positioning (GPS) was attained at 0700 UTC. From that time until 1000 UTC, the vessel waited for confirmation of its exact position by GPS and SatNav systems. A useful GPS window did not begin until after 1400 UTC. Unfortunately, we missed a SatNav positioning fix on the ship's receiver system at about 1200 UTC, although that position was received by the system installed in the underway geophysics laboratory. We tried visual and radar sightings but were not successful. This situation caused an unnecessary delay of approximately 3 hr before our position was finally confirmed by SatNav. The first APC core spudded at 0700 L (1200 UTC). The water depth was 150.5 m below sea level.

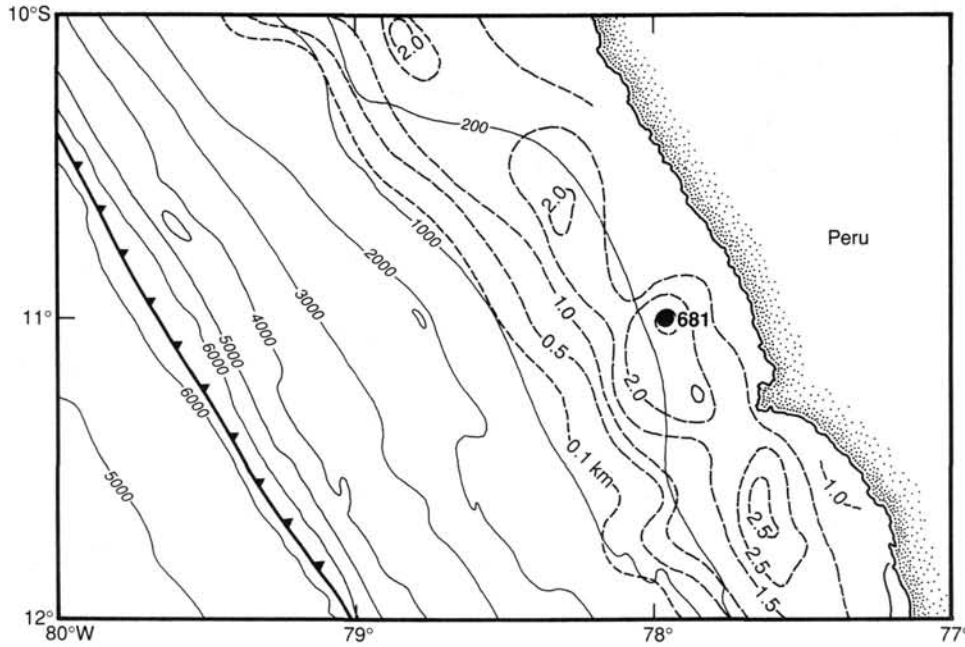

Figure 1. Bathymetry and sediment isopachs along Peru Continental Margin at 11°S; water depths are in intervals of 1000 m, beginning at a water depth of 200 m; sediment isopachs are in increments of 0.5 km. The landward flank of an outer shelf basement high is outlined by the dashed line, where sediment thickness is only 0.1 km. Site 681 is situated above the depositional center of the outer shelf. For an overview of all sites, see Figure 1, Site 679 chapter (this volume).

Hole 681A was drilled to a depth of 101.5 mbsf using HPC coring and had recovery rates of 96%. Recovery was poor in Core 112-681A-6H because of dolomite layers and indurated strata encountered at 54 mbsf. This was the first in a cyclic sequence of numerous gray indurated silts and muds and very soft olive-green muds (Table 1). A second such cycle was encountered with Core 112-681A-12H, which became stuck at 111.0 mbsf and required 130,000 (!) lb of overpull to free it from the sediment. Implemented after the loss of Core 112-680A-10H, the rig's heave compensator (for pulling out stuck core) again functioned well. The drilling personnel performed well during this critical situation. Coring continued with XCB drilling, and recovery remained good until 149 mbsf, when we noted a decrease to <5% for the remaining three cores of Hole 681A (total depth, 187 mbsf). The last core came on deck at 2115 L on 7 November 1986.

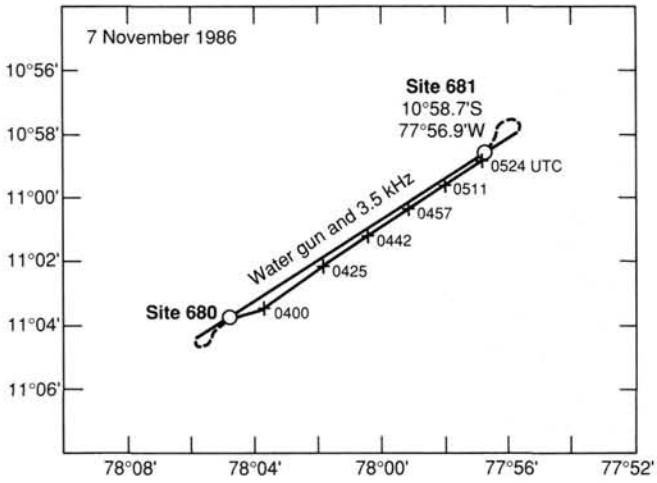

Figure 2. Chart of Site 681 location showing projected and actual approach tracks.

Hole 681B was drilled flawlessly and recovery was excellent using the HPC to a depth of 86.5 mbsf in 10 cores, then we switched to XCB drilling to cut six more cores to a total depth of 143.5 mbsf. At this depth we terminated drilling at 1200 L, 8 November, because core recovery decreased to less than 5% in gray silty muds and sandy muds with indurated dolomite layers. We had previously experienced this same poor recovery at Hole 681A.

At Hole 681C, drilling operations on board *JOIDES Resolution* achieved a record when 10 HPC cores were brought on deck between 1345 and 1541 L. The recovery rate was 94%. Samples from this hole were used to complete the special geomicrobiological sampling and other projects requiring whole-round sample material, which had been cut short at Site 680.

LITHOSTRATIGRAPHY

Lithologic Units

At Site 681, four units were identified on the basis of core description and smear-slide analysis (Fig. 3 and Table 2). Following are descriptions for each unit.

Unit I

Cores 112-681A-1H through 112-681A-5H; depth, 0–35.0 mbsf; age, Pleistocene to Holocene.
Cores 112-681B-1H through 112-681B-4H; depth, 0–34.4 mbsf; age, Pleistocene to Holocene.

Lithologic Unit I consists primarily of dark olive gray diatomaceous mud containing thin laminae of yellow brown diatom ooze. The mud has a high silt content, estimated at between 40% and 60%. Diatoms make up 20% to 40% of the mud but are more concentrated in the thin, yellow-brown laminae. The unit has a distinctive laminated character, although an interval of bioturbated sediment is present between 12 and 15 mbsf. A number of distinctive gray sand beds occur in Unit I. These beds commonly have sharp bases and grade from fine sand to mud. They contain high proportions of lithic clasts, probably of

Table 1. Coring summary for Site 681.

Core/ section	Date (Nov. 1986)	Time (UTC)	Depth (mbsf)	Length cored (m)	Length recovered (m)	Recovery (%)
112-681A-1H	7	0756	0–6.5	6.5	6.51	100.0
2H	7	0810	6.5–16.0	9.5	9.75	102.0
3H	7	0832	16.0–25.5	9.5	9.33	98.2
4H	7	0845	25.5–35.0	9.5	8.21	86.4
5H	7	0855	35.0–44.5	9.5	9.70	102.0
6H	7	0911	44.5–54.0	9.5	0.10	1.1
7H	7	0942	54.0–63.5	9.5	9.19	96.7
8H	7	1112	63.5–73.0	9.5	10.04	105.7
9H	7	1124	73.0–82.5	9.5	9.86	104.0
10H	7	1137	82.5–92.0	9.5	5.71	60.1
11H	7	1206	92.0–101.5	9.5	7.24	76.2
12H	7	1435	101.5–111.0	9.5	9.70	102.0
13X	7	1600	111.0–120.5	9.5	4.43	46.6
14X	7	1637	120.5–130.0	9.5	4.58	48.2
15X	7	1720	130.0–139.5	9.5	5.80	61.0
16X	7	1758	139.5–149.0	9.5	1.51	15.9
17X	7	1845	149.0–158.5	9.5	0.05	0.5
18X	7	1935	158.5–168.0	9.5	0.18	1.9
19X	7	2030	168.0–177.5	9.5	0.19	2.0
20X	7	2115	177.5–187.0	9.5	0.32	3.4
681B-1H	8	0040	0–5.9	5.9	5.94	100.0
2H	8	0058	5.9–15.4	9.5	9.75	102.0
3H	8	0112	15.4–24.9	9.5	9.44	99.3
4H	8	0139	24.9–34.4	9.5	9.43	99.2
5H	8	0201	34.4–43.9	9.5	8.51	89.6
6H	8	0217	43.9–53.4	9.5	3.22	33.9
7H	8	0305	53.4–62.9	9.5	9.58	101.0
8H	8	0438	62.9–72.4	9.5	8.83	92.9
9H	8	0510	72.4–81.9	9.5	2.54	26.7
10H	8	0535	81.9–86.5	4.6	4.60	100.0
11X	8	0700	86.5–96.0	9.5	1.50	15.8
12X	8	0735	96.0–105.5	9.5	6.31	66.4
13X	8	0830	105.5–115.0	9.5	9.28	97.7
14X	8	0900	115.0–124.5	9.5	5.45	57.3
15X	8	1115	124.5–134.0	9.5	2.09	22.0
16X	8	1200	134.0–143.5	9.5	0.83	8.7
681C-1H	8	1345	0–5.9	5.9	5.90	100.0
2H	8	1359	5.9–15.4	9.5	7.95	83.7
3H	8	1409	15.4–24.9	9.5	9.58	101.0
4H	8	1422	24.9–34.4	9.5	9.90	104.0
5H	8	1432	34.4–43.9	9.5	9.82	103.0
6H	8	1445	43.9–53.4	9.5	4.10	43.1
7H	8	1505	53.4–62.9	9.5	9.34	98.3
8H	8	1517	62.9–72.4	9.5	9.92	104.0
9H	8	1529	72.4–81.9	9.5	9.50	100.0
10H	8	1541	81.9–91.4	9.5	10.23	107.7

Note: H = hydraulic piston; X = extended-core barrel; UTC = Universal Time Coordinated.

volcanic origin, making them compositionally distinct from the dark olive gray mud. Volcanic glass is present in small proportions in some beds. Dolomite occurs as small rhombs through most of the unit. Cemented dolomite nodules are present at several zones, with the shallowest occurrence at 4.2 mbsf. Pale yellow, soft nodules of phosphate are also found at shallow depths. Dewatering structures in the form of *en-echelon* subvertical pipes occur below 29 mbsf.

Unit II

Cores 112-681A-6H through 112-681A-11H-4, 51 cm; depth, 35.0–96.0 mbsf; age, Pleistocene.

Cores 112-681B-5H through 112-681B-12X-2, 8 cm; depth, 34.4–97.1 mbsf; age, Pleistocene.

Below 35 mbsf, the diatomaceous mud is interbedded with sequences of terrigenous mud having lower diatom contents (<20%) and a higher degree of bioturbation. Mollusk shells are commonly found both as articulated valves, concentrated in shell beds, and as fragments scattered through both terrigenous and diatomaceous intervals. Sandy and silty beds, commonly graded with sharp bases, form a higher proportion of the sequence in this unit. Light gray beds similar to those described in Unit I are present, but many of the sands have a darker gray color and are massive or poorly graded. These darker sands are generally composed of feldspar and also contain significant proportions of lithic clasts. A sand unit of particular interest is found in Section 112-681B-10H-2. This sand directly overlies a phosphatic gravel lag developed above a partly cemented dolomite bed (Fig. 4). The base of the sand bed probably represents an erosion surface. We did not recognize a phosphatic zone in Hole 681A, although a nodular, calcareous dolomite zone is located in Section 112-681A-10H-1.

A 2-m section in Core 112-681A-7H contains numerous subzonal voids, interpreted as gas-escape structures (Fig. 5). We also noted that this core had a high content of methane gas (see "Organic Geochemistry" section, this chapter). A single dropstone having a diameter of 3 cm and composed of mesocratic diorite was found in Core 112-681A-9H-7.

The base of Unit II is marked by a second distinctive erosional zone where terrigenous muds overlie the olive gray diatomaceous muds of lithologic Unit III. This hiatus is located in Samples 112-681A-11H-4, 51 cm (96.0 mbsf) and 112-681B-12X-2, 10 cm (97.1 mbsf). The erosion surface is characterized by a gravel lag deposit of black phosphate nodules and shell fragments (Fig. 6).

Unit III

Cores 112-681A-11H-4, 51 cm, through 112-681A-15X-4, 83 cm; depth, 96.0–135.3 mbsf; age, Pleistocene.

Cores 112-681B-12X-2, 8 cm, through 112-681B-16X, CC, 12 cm; depth, 97.1–134.5 mbsf; age, Pleistocene.

Lithologic Unit III is characterized by the predominance of olive gray, laminated diatomaceous mud, similar to those sediments of Unit I. Thin, bioturbated, more terrigenous intervals as well as shell fragments are present, but these features are less pronounced than in Unit II. We found a third erosional surface with a phosphate gravel lag deposit in Hole 681A at approximately 110 mbsf (112-681A-12H-7, 28–32 cm), but we could not see this in in Hole 681B because of poor core conditions over the equivalent interval. At this hiatus, olive gray diatomaceous mud overlies dark gray terrigenous mud.

Graded olive gray and gray beds, similar to those found in Units I and II, are found in Unit III, as are graded beds of phosphate-rich sand and fine gravel in Core 112-681B-15X.

Nodular, blocky dolomite zones are common in Unit III. These zones are particularly well developed just below the upper erosion surface. Soft, pale yellow phosphate nodules also are recognized in the diatomaceous muds.

Unit IV

Cores 112-681A-15X-4, 83 cm, through 112-681A-20X, CC; depth, 135.3–177.0 mbsf; age, Pliocene to lower Pleistocene.

Cores 112-681B-16X, CC (12 cm) through 112-681B-16X, CC; depth, 134.5–143.5 mbsf; age, Pliocene to lower Pleistocene.

Lithologic Unit IV was not completely described because of poor core recovery in the deeper part of Hole 681A. The recovered sediment is predominantly very dark gray or black sand, silty sand and sandy silt with thin units of diatomaceous mud to total depth in Section 112-681A-20X, CC. The silt shows parallel and microcross-laminations in Section 112-681A-16X, CC, but generally is badly disturbed or soupy as a result of coring disturbance. These sands and silts have compositions similar to the dark gray sands of lithologic Unit II and contain predominantly quartz, feldspar, and lithic grains, commonly with dolomite rhombs in small proportions. The cores from this unit also contain nodules of cemented dolomite; we found shell fragments in Section 112-681A-19X, CC.

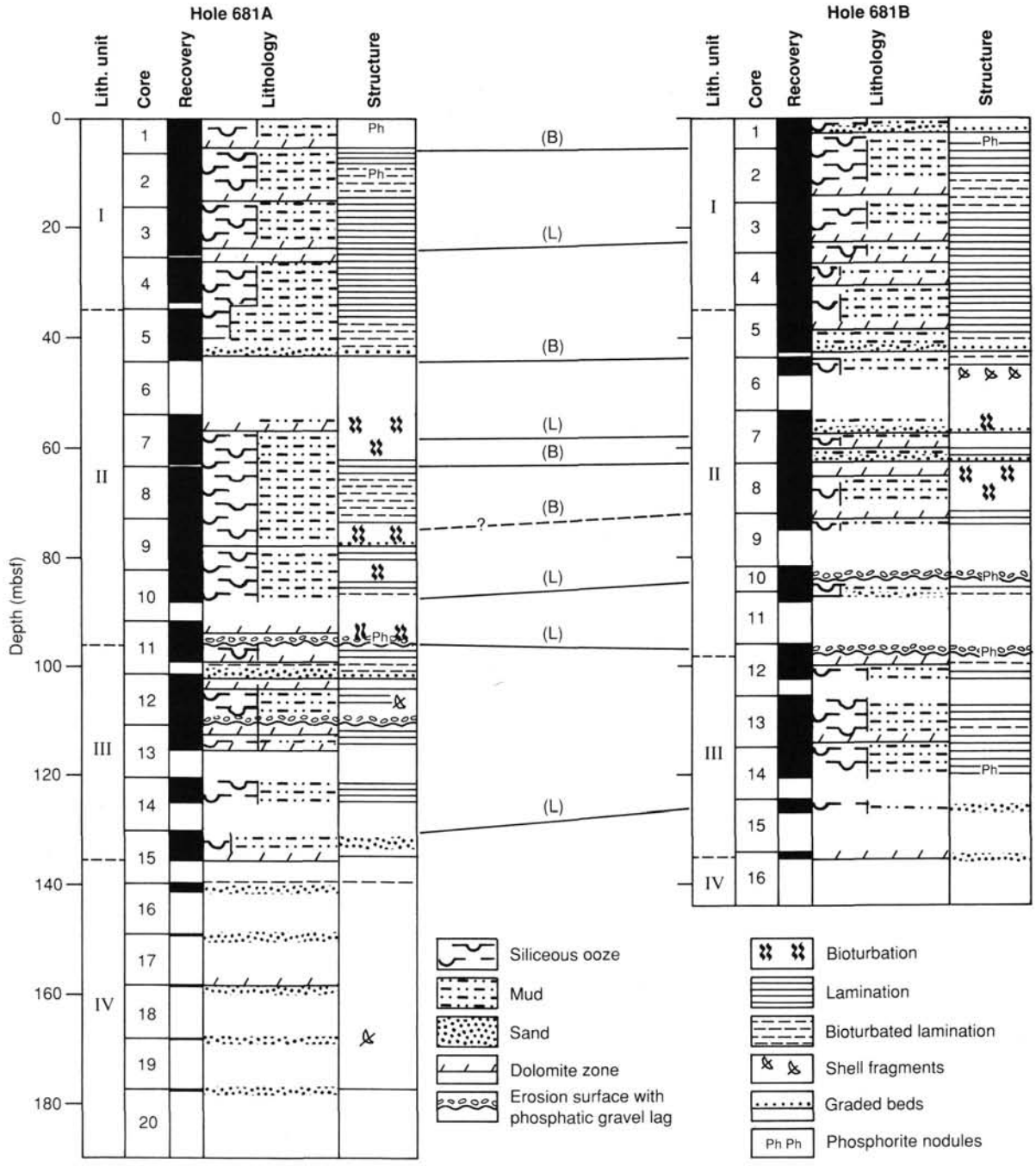

Figure 3. Lithologic units at Site 681. Correlations between holes are based on lithostratigraphic boundaries and biostratigraphic markers. D = dolomite, B = bioturbated, L = laminated.

Table 2. Summary of lithologic units for Site 681.

Lithologic unit	Lithology	Core/section	Depth (mbsf)
I	Laminated diatomaceous mud.	112-681A-1H to 5H 112-681B-1H to 4H	0–35 0–34.4
II	Interbedded terrigenous mud and diatomaceous mud, with common sand and silt beds.	112-681A-6H to 11H-4 112-681B-5H to 12X-2	35–96 34–97.1
III	Laminated diatomaceous mud.	112-681A-11H-4 to 15X-4 112-681B-12X-2 to 16X, CC	96–135 97–134
IV	Sand, silty sand, and sandy silt.	112-681A-15X-4 to 20X, CC 112-681B-16X, CC to 16X, CC	135–177 134–143

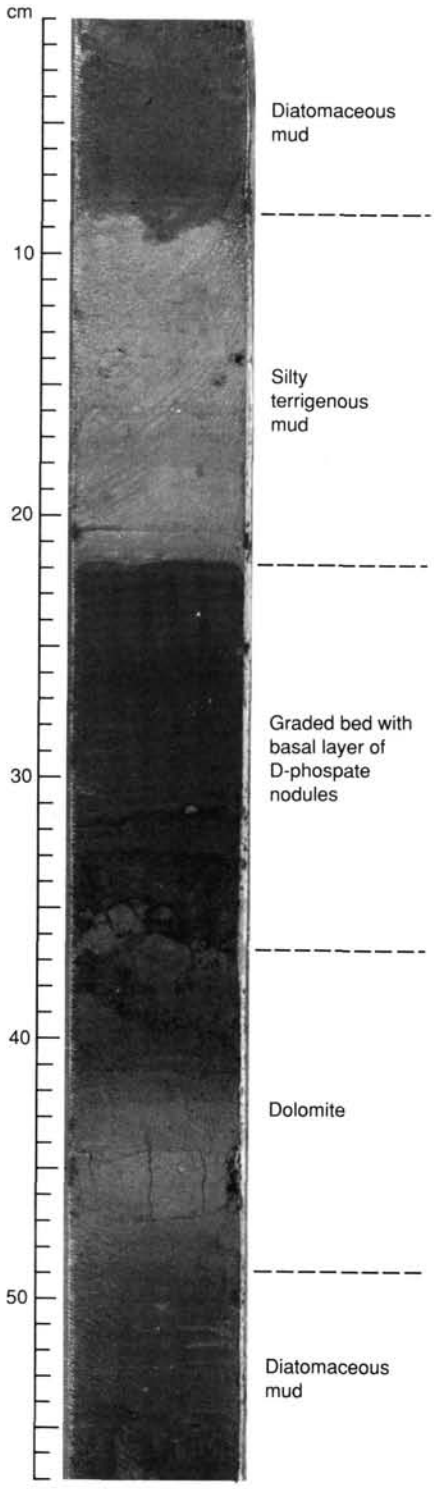

Figure 4. Graded black sand overlying lithified dolomitic zone and phosphate gravel lag, Unit II (Sample 112-681B-10H-2, 1–57 cm).

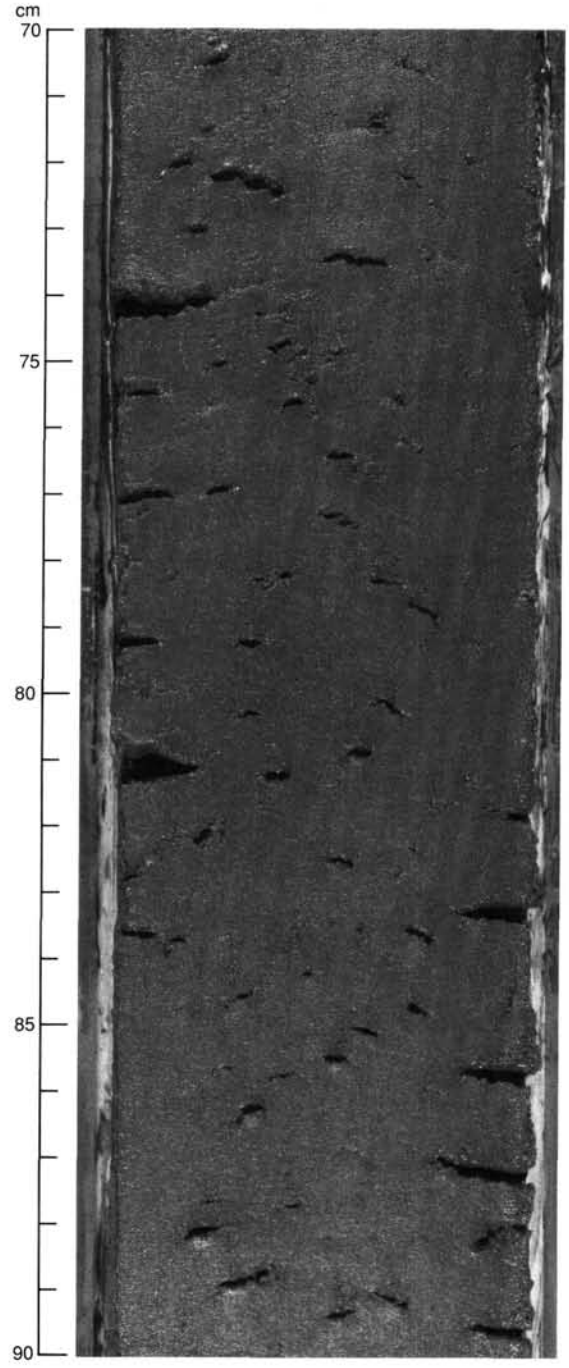

Figure 5. Gas-escape structures, Unit II (Sample 112-681A-7H-4, 70–90 cm). This interval was also characterized by high methane levels (see "Organic Geochemistry" section, this chapter).

Diagenesis

Phosphates

As was the case at Sites 679 and 680, phosphates at Site 681 occur in two major forms: friable, light-colored *F-phosphates* and dense, hard, dark-colored *D-phosphates* (for more complete definitions, see "Lithostratigraphy" section, Site 680 chapter, this volume).

Compared to the two previous sites, F-phosphates are much less abundant at Site 681. These occur as small isolated nodules in laminated to thinly bedded diatomaceous mud of Unit I and, more sparsely, of Unit II (Fig. 7). We did not observe them in Units III and IV. F-phosphates apparently formed during early diagenesis in organic-rich muds. They first appear in both Holes 681A and 681B in the upper 2 m of sediment (112-681A-1H-2, 30 cm, and 112-681B-1H-2, 5 cm). Of particular interest is the occurrence of an F-phosphate nodule containing about 20% fish remains that appear to have acted as nuclei for nodule growth (112-681A-10H-4, 72 cm).

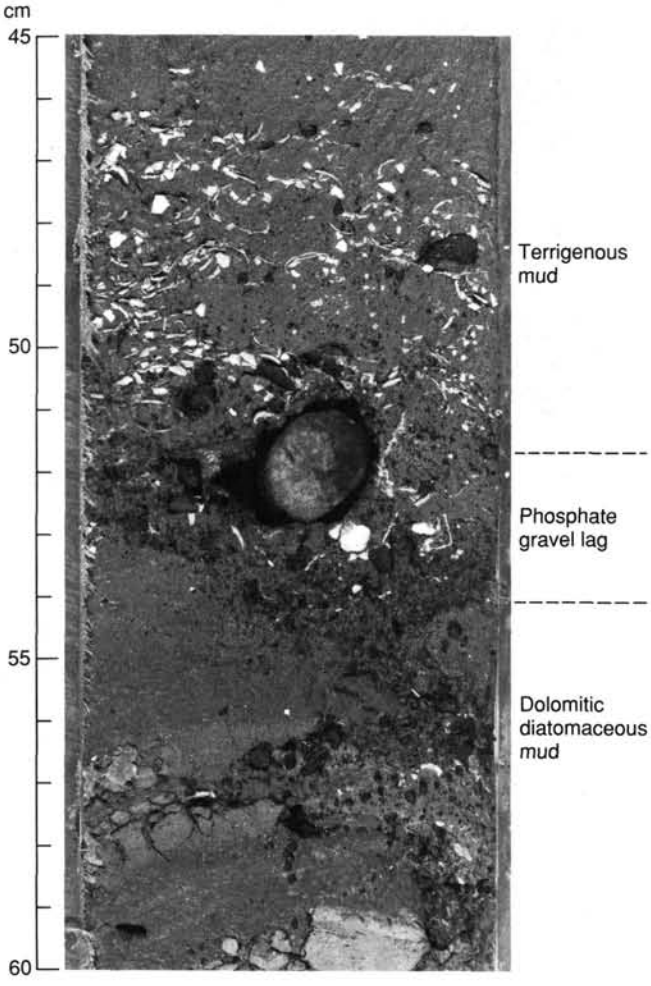

Figure 6. Gravelly phosphatic layer overlying dolomitized sequence of olive gray diatomaceous mud. The gravel is in turn overlain by terrigenous mud containing numerous mollusk shells (Sample 112-681A-11H-4, 45–60 cm). This layer marks the boundary between Units II and III.

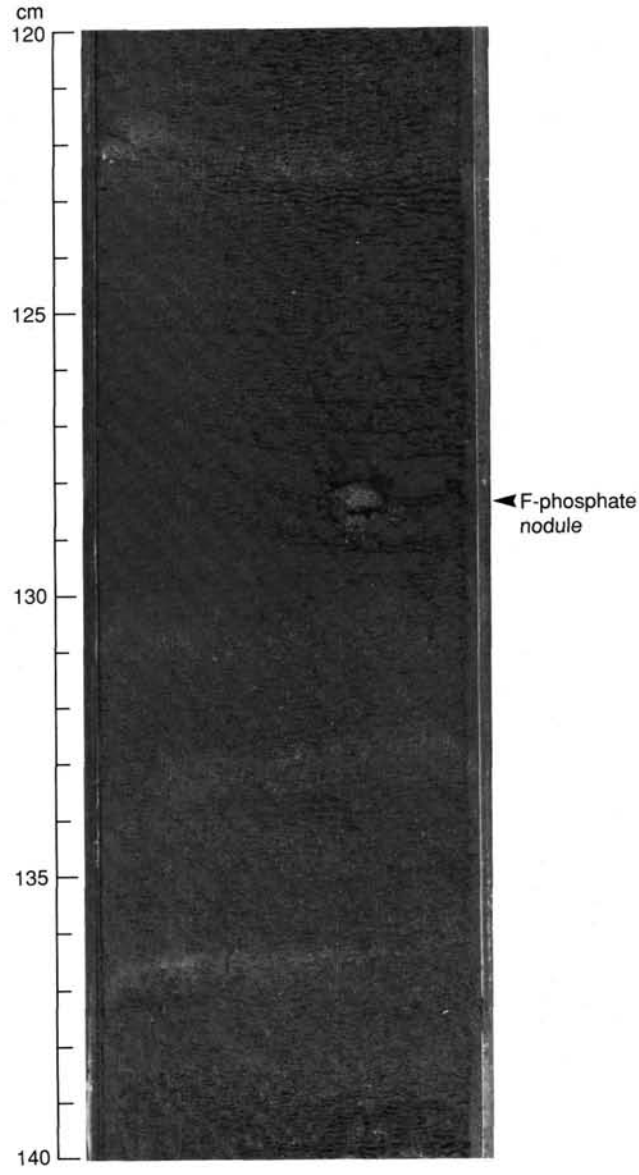

Figure 7. Small F-phosphate nodule in thinly bedded diatomaceous mud, Unit II (Section 112-681A-9H-6).

D-phosphates occur in all four units as nodules in conglomeratic layers and as peloids in thin sandy layers. In most instances, both types of layers are well sorted and appear to have been deposited by currents. However, in a few cases D-phosphate nodules are dispersed in a diatomaceous-mud matrix (e.g., Section 112-681B-1H-3). The most prominent occurrences of D-phosphates are in graded beds that have pebble-sized D-phosphate nodules concentrated at the base; in several instances these beds lie directly above lithified or partly lithified dolomite layers (see Figs. 4 and 6; also Sample 112-681A-12H-7, 28–32 cm). We observed similar sequences at Site 680. At both Sites 680 and 681, erosion prior to deposition of the conglomerate beds appears to have scoured down to the level of dolomites formed earlier. In several of these beds at Site 681, the D-phosphate nodules are piped down into burrows in the underlying dolomitic mud (Fig. 6), indicating that the latter had not become fully lithified. Several beds containing reworked mollusk shells also contain D-phosphate nodules (Fig. 6). Therefore, as at Sites 679 and 680, gravel beds containing D-phosphate nodules appear to mark erosional hiatus surfaces.

In contrast to the phosphatic gravels described above, thin pellets of phosphoritic sands are dispersed throughout Units I, II, and III (Figs. 8 and 9). These sands are well sorted and have a composition dominated by dark, ovoidal grains of phosphate and by foraminifer tests. Like the conglomerates, they appear to have been deposited by currents and perhaps represent less extreme instances of winnowing and reworking.

A comparison of phosphate occurrences at Sites 679, 680, and 681 is instructive. F-phosphates are much more abundant at Sites 679 and 680 than at 681, but for D-phosphates the situation is reversed. Thus, we may surmise that reworking by bottom currents was much more common at Site 681, commensurate with the shallower depth at this site.

Authigenic Carbonates

Dolomite occurs as disseminated rhombs in all four lithologic units at Site 681 in the form of dolomitized but unlithified or only partly lithified layers, and as hard, fully lithified thin beds or nodules; the latter commonly occur as a rubble of broken fragments in core-catcher samples (Fig. 10). We first noted disseminated dolomite rhombs in trace amounts at a depth of about 1 mbsf (112-681A-1H-1, 99 cm). We encountered the shallowest (but fully lithified) dolomites at about 4.2 mbsf in Hole 681A (112-681A-1H-3, 117–121 cm) and at about 14 mbsf in Hole 681B (112-681B-2H-6, 66–77 cm); this difference in sub-

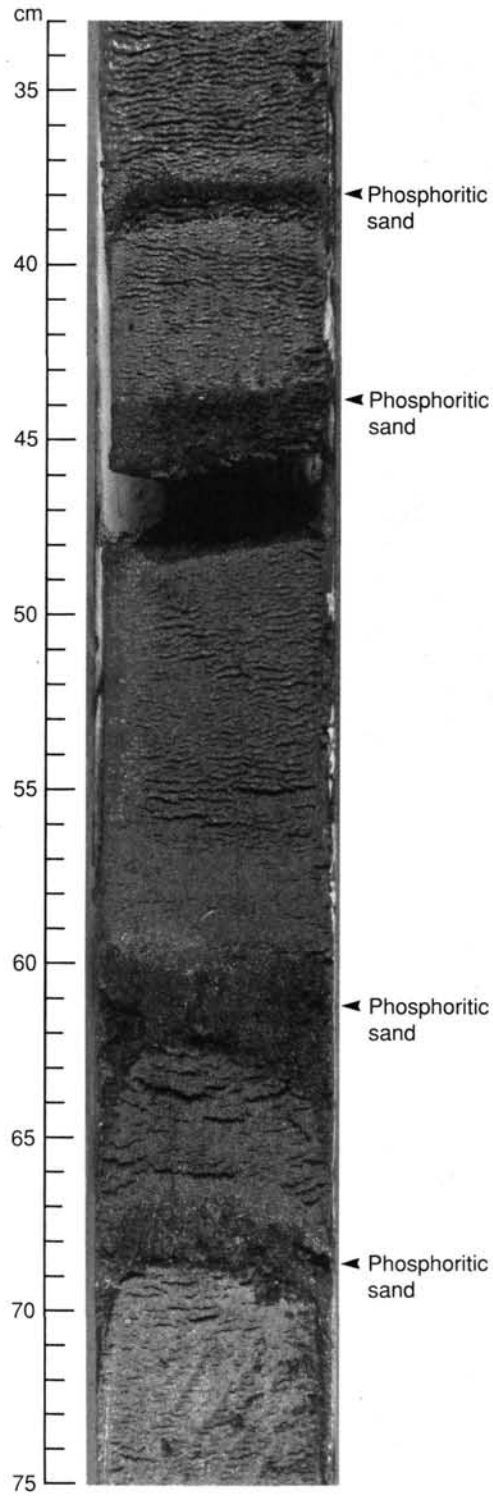

Figure 8. Four thin, pelletal phosphorite layers, interbedded with silty diatomaceous mud; positions are indicated by arrows. Unit III (Section 112-681B-15X-1).

bottom depths may indicate the lenticularity of individual beds. Lithified dolomite beds become common (occurring in nearly every core) at a depth of about 24 mbsf in Hole 681A and at about 14 mbsf in Hole 681B. Therefore, as at Sites 679 and 680, substantial dolomitization occurred at this site near the seafloor during the early stages of diagenesis. Early dolomitization also

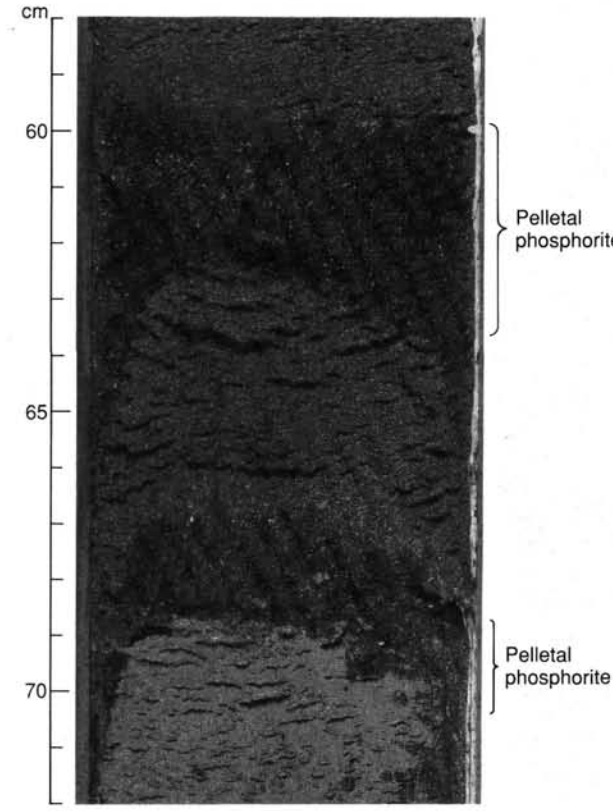

Figure 9. Closeup of two pelletal phosphorite layers shown in previous figure, Unit III (Section 112-681B-15X-1).

is implied by the concentration of D-phosphates along scoured surfaces just above dolomitized layers (Figs. 4 and 6).

Dolomitized layers at Site 681 either replace laminated diatomaceous muds or cement silty and sandy beds. Most dolomitized beds are very hard, but a few appear to be only partly lithified (with a pasty consistency) or unlithified (e.g., 112-681A-10H-4, 6–12 cm) for reasons that are not clear. In many of the lithified beds, dissolved foraminifer tests form a moldic porosity, indicating that dissolution of calcium carbonate either accompanied or followed the formation of dolomite.

Pyrite

Pyrite in small amounts is an ubiquitous component in all units at Site 681, occurring in at least small amounts in nearly every smear slide examined. The most common form is framboidal, with many framboids occurring in foraminifer or diatom tests. Pyrite framboids occur in sediments near the seafloor (e.g., 112-681A-1H-1, 23 cm; 112-681B-1H-1, 21 cm) and therefore must form during the earliest stages of diagenesis.

Evidence for Relative Sea-Level Fluctuations and Cyclic Sedimentation

Erosion Surfaces

In lithologic Units II and III at least three different zones occur where phosphatic gravels overlie sharp breaks in lithology (Fig. 3). Two such zones are illustrated in Figures 4 and 6. Only one of these (Fig. 6) can be correlated between the two holes, which are located only 7 m apart. Lithologic correlation between Holes 681A and 681B indicates that the erosion surfaces may be only locally developed. Similar lateral variability of phosphate zones was observed in the Miocene Monterey Formation

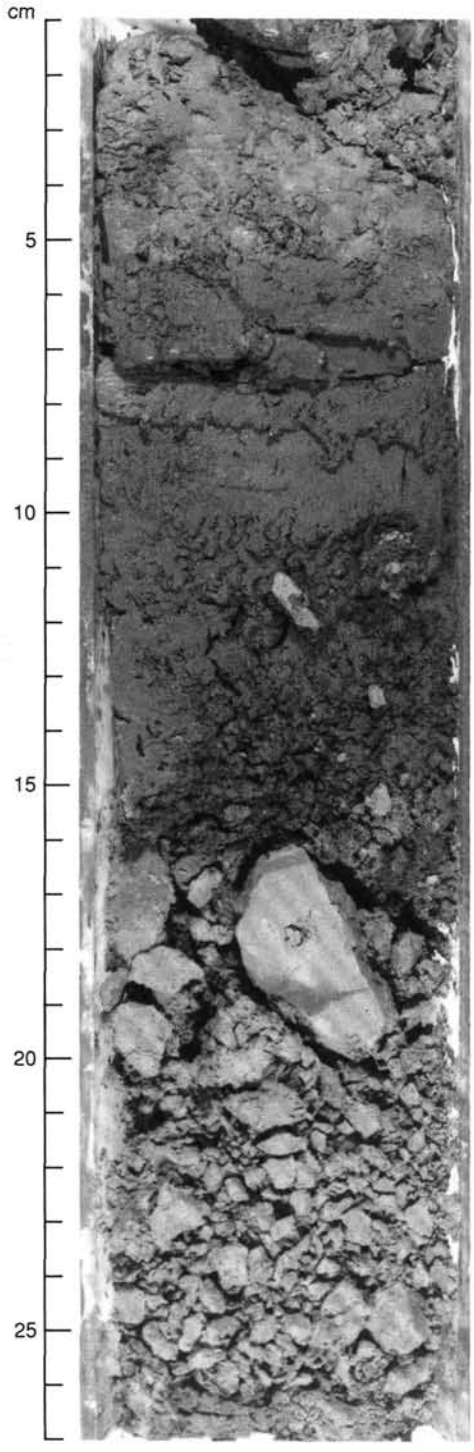

Figure 10. Rubble of dolomite fragments (at bottom) in a drilling breccia, Unit II (Section 112-681B-9H, CC).

of California (Garrison et al., 1987). The presence of gravels and of a graded bed associated with the gravel in Core 112-681B-10 (Fig. 4) nevertheless indicates the periodic development of strong bottom currents, which caused erosion and reworking of the sea bed. Deep burrows on these surfaces indicate that they must have been stable for at least several years. These phenomena may be explained by the development of strong geostrophic contour currents in deep water, or by the development of wind-driven bottom currents, enhanced by a tectonic or glacial lowering of sea levels.

Sedimentation Cycles

In addition to the major lithologic changes indicated by the four units defined above, the sequence also shows a higher frequency of feldspathic silty sand alternating with diatomaceous mud (including laminae of nannofossil and diatom oozes). In general, these two types of sequence alternate. One type is olive gray or dark olive gray (5Y tone), diatomaceous mud having 30% to 40% diatoms; common, pale yellow, diatom ooze laminae; phosphates; and dolomites. The other type is gray (5Y to 5GY tone), bioturbated silty mud (with 10% to 20% diatoms and common shell fragments), silt, and sand. These two sequences normally show relatively sharp contacts with each other.

In the cores of Site 681, we observed several changes between laminated diatomaceous mud and bioturbated silty muds (Fig. 3). In Unit I, laminated diatomaceous muds are predominant but are interbedded with 10-cm- to 1-m-thick bioturbated sequences. In Unit II, coarser and more bioturbated sediments are interrupted by minor laminated sequences of diatomaceous mud up to 5 m thick. Laminated sediments dominate again in lithologic Unit III, while terrigenous sediments are predominant in Unit IV. Below this depth, core recovery is not adequate for discerning lithologic cycles.

Biostratigraphy and paleomagnetostratigraphy at this site (see "Biostratigraphy" and "Paleomagnetics" sections, this chapter) indicate that these cycles were probably deposited during the Quaternary and late Pliocene. Paleomagnetic measurements showed a reversal in polarity at about 85–90 mbsf in Hole 681A, which is taken as the Brunhes/Matuyama boundary (0.73 Ma). The frequency of cycles inferred from preliminary analysis of smear slides and sedimentary structures appears to be of the same order as major glacial/interglacial cycles.

Although these lithologic cycles cannot be related to known sea-level stands (about 6 low stands are reported during the last 0.73 Ma; Shackleton and Opdyke, 1977), the higher frequency cycles may be related to glacial/interglacial changes in sea level.

During glacial periods, sea levels may have dropped 100 m or even more, at which times the water depth at Site 681 may have been only 60 m or less. These silty muds and silts poor in organic matter and rich in terrestrial components probably were deposited during these periods. The low carbon and diatom contents of sediments and the high oxygen contents of the bottom water (signaled by increased bioturbation) indicate that either the production of organic matter and silica was lower at Site 681, or that these sediments were deposited shoreward of the oxygen-minimum zone. Biological production could have been lowered further by a seaward shift of the upwelling cell. This, together with more efficient circulation in the shallower water above Site 681 during glacial times, may alternatively explain the higher oxygen content of the bottom water.

In contrast, the organic-rich, laminated diatomaceous mud may have accumulated during interglacial times when the water depth was greater when the upwelling regime had shifted to Site 681 and when a pronounced oxygen-minimum zone developed at the seafloor. During these periods, the bacterial decomposition of very high amounts of primary produced organic matter may have further diminished low oxygen contents of bottom water, which would have inhibited burrowing organisms so that the lamination of the diatomaceous muds was preserved. Furthermore, the low oxygen environment enhances the accumulation of organic matter.

One puzzling feature of the sequence at Site 681 is that the strongest episodes of reworking took place in the early Pleistocene, before the Brunhes/Matuyama magnetic reversal. These reworking events became less important at Site 681 in the late Pleistocene. This appears to be in contrast to the global oxygen-isotope record, which implies larger-amplitude glacial and sea-level fluctuations in the late Pleistocene. This may be explained by a superimposed tectonic subsidence of Site 681 during the

Pleistocene that maintained water depths at levels where oxygen-depleted conditions predominated, despite major sea-level fluctuations.

Structure

Drilling disturbance was generally low and was notable only for the development of pull-out (concave-upward) structures toward the bottom of some cores (e.g., 112-681A-2H-6 to the core catcher). Little evidence exists for slumping or tectonic disturbance at Site 681. Slumping is confined to one 10-cm zone identified in Samples 112-681A-3H-2, 90–100 cm, and 112-681B-3H-2, 70–80 cm. *En-echelon* mud-filled gashes are relatively rare, compared to Sites 679 and 680. These first appear at Sections 112-681A-4H-3 and 112-681B-5H-5, and are sparsely developed below this level. Extensional faults and broad gashes having mud-filled veins (such as those of Site 679) do not occur. The scarcity of both slump and early tectonic structures is compatible with the location of Site 681 in a stable shelf setting.

BIOSTRATIGRAPHY

Introduction

Three holes were drilled in a water depth of 150.5 m at Site 681 to recover the "near-shore" Quaternary upwelling facies and to establish its facies changes through glacial and interglacial cycles. Two major lithologies were found with greenish/brownish diatomaceous muds alternating with grayish diatom-bearing sands. Diatoms form the major microfossil component, and benthic and planktonic foraminifers are common to 130 mbsf, while radiolarians, calcareous nannofossils, and silicoflagellates are sparse.

Sedimentation rates (Fig. 11) are on the order of 80 m/m.y. for the Jaramillo Normal event to the Holocene. The occurrence of *Rhizosolenia matuyama* associated with the silicoflagellate *Mesocena quadrangula* is the basis for this calculation.

Upwelling and oceanic diatom assemblages alternate in the greenish diatomaceous muds; the sandy sections are characterized by typically well-preserved, neritic and upwelling assemblages. Benthic and heavily silicified, planktonic, neritic diatoms are enriched in the sandy deposits at 44.5–54.0 mbsf, as are benthic-foraminifer species of the *Buccella frigida* Assemblage, which indicates deposition during low sea-level stands of glacial periods.

Whether any of the complex laminations that occur within the diatomaceous muds can be related to seasonal change of runoff and/or productivity, or whether they are related to the El Niño phenomenon (torrential rains are frequently associated with a relaxation of the trade-wind circulation and warming of the coastal waters off Peru, Nials et al., 1979) requires detailed sampling and analysis of complete and composite sections. The presence of a well-preserved, abundant, diatom upwelling assemblage within the sandy diatom-bearing muds seems to exclude the possibility that these are flood deposits.

Pliocene calcareous nannoplankton and diatoms were found in the lowest samples from Site 681A. Because Quaternary species were also present in Section 112-681A-19X, CC, we refrained from placing this sample in the Pliocene.

Diatoms

All core-catcher samples were studied from the three holes drilled; they contained a diversified assemblage that varied from extreme "upwelling" to "oceanic" and a mixture of both. Assemblages are identical to those defined by DeVries and Schrader (1981) and Schuette and Schrader (1979, 1981). Diatom assemblages generally did not vary significantly between the sandy layers and the greenish/brownish mud sections. Sandy layers frequently contained a well-preserved upwelling assemblage but

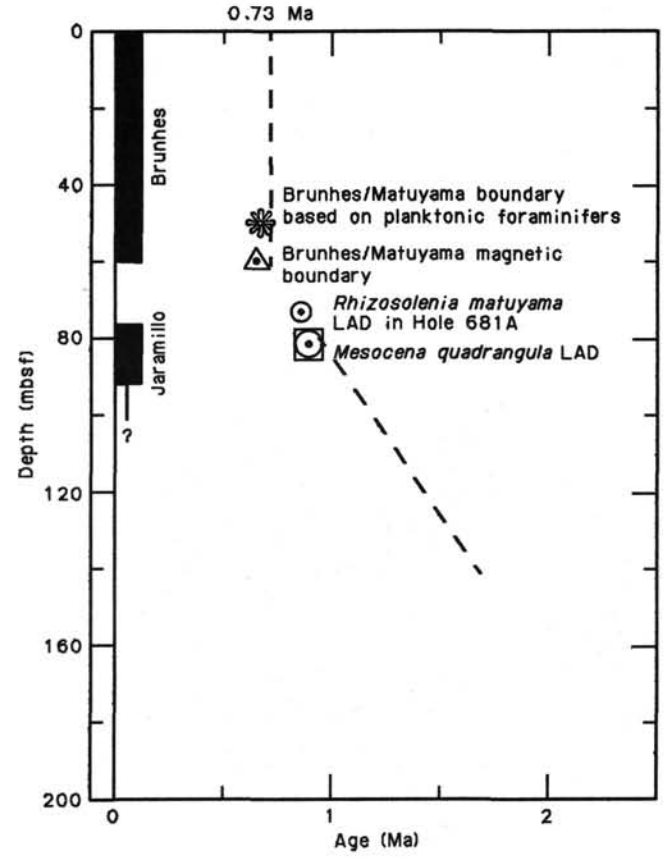

Figure 11. Age vs. depth plot of paleomagnetic reversal stratigraphy and datums of silicoflagellates, planktonic foraminifers, and diatoms.

rarely contained an oceanic assemblage. Neritic nearshore diatoms seemed frequently enriched in the sandy layers. The lighter, distinct laminae intercalated in the greenish/brownish muds contained monospecific diatom assemblages with floods of girdle bands, *Cyclotella striata/stylorum*, and large *Coscinodiscus*. These layers were caused by winnowing, which removed other sized classes of diatoms; they were not the result of massive monospecific diatom blooms.

Correlation among the three holes is illustrated in Figure 12; correlation lines are based on the occurrence of distinct assemblages with *Cyclotella striata/stylorum, Delphineis "ossiformis"* (new species), a barren interval, large *Coscinodiscus*, and the first occurrence of *Distephanus pulchra* (silicoflagellate).

Based on the occurrence of *Rhizosolenia matuyama* Burckle (Burckle et al., 1978) in Sections 112-681C-8H, CC through 112-681C-10H, CC and the correlation as illustrated in Figure 12, a tentative sedimentation rate of 80 m/m.y. for the upper 60 m can be calculated. This site is ideal for studying upwelling variability through time at high resolution. Sediment sections with laminae representing anoxic bottom-water conditions will allow us to study in detail the El Niño phenomenon cyclicity through much of the late Quaternary. Comparisons of interglacial and glacial intervals between Sites 680 and 681 may be especially rewarding.

Distephanus pulchra ranges well through the Brunhes and the upper Matuyama Reversed Magnetic Epoch at this site. We did not find *Mesocena quadrangula*.

Reworked Eocene and Oligocene species were found in Section 112-681A-19X, CC with *Pyxilla* spp., and reworked Pliocene–Miocene species were found in Section 112-681A-15X, CC along with *Denticula hustedtii* and *Actinocyclus oculatus*.

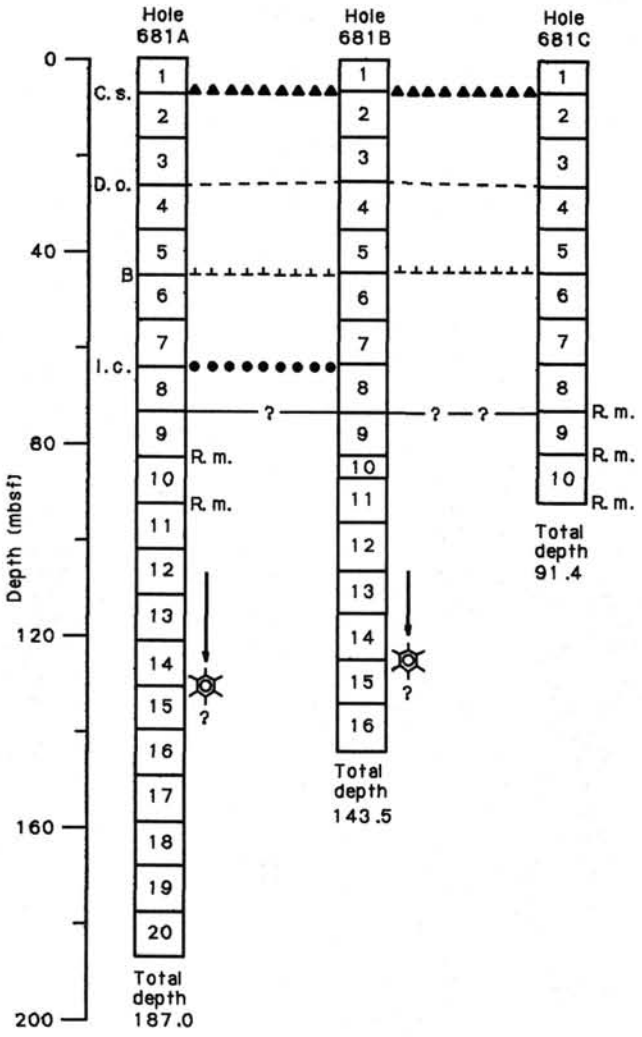

Figure 12. Correlation of Holes 681A, 681B, and 681C, based on occurrence of distinct diatom assemblages (triangles, dashed line, perpendicular line, dots). R.m. = *Rhizosolenia matuyama*. Range of silicoflagellate *Distephanus pulchra*. C.s. = *Cyclotella striata/stylorum*. D.o. = *Delphineis "ossiformis"* [new species]. B = barren in diatoms. l.C. = large *Coscinodiscus* spp.

Freshwater diatoms occurred sporadically in the following samples: Sections 112-681A-11H, CC, 112-681A-10H, CC, 112-681A-8H, CC, 112-681A-6H, CC, as well as Sections 112-681B-16X, CC, 112-681C-8H, CC, and 112-681C-7H, CC.

Shallow-water, benthic marine diatoms occurred in the following samples: Sections 112-681A-19X, CC, 112-681A-15X, CC, 112-681A-11H, CC, 112-681A-10H, CC, 112-681A-8H, CC, 112-681A-6H, CC, 112-681B-16X, CC, 112-681B-14X, CC, 112-681B-13X, CC, 112-681B-12X, CC, 112-681B-10H, CC, 112-681B-5H, CC, 112-681B-4H, CC, 112-681C-10H, CC, and 112-681C-8H, CC. They seem to be enriched in the more sandy layers, which may be intervals of sedimentation during lowered sea-level stands, possibly correlating with glacials.

Silicoflagellates

Preliminary data based solely on core-catcher samples show that silicoflagellates are present throughout the Quaternary at this site and are associated with abundant diatoms, rare sponge spicules, and occasionally with actiniscids. As in the previous sites, specimens of the *Distephanus speculum* group and *Dictyocha messanensis* group were the most common forms observed.

In our preliminary study, the lowest occurrences of *Distephanus bioctonarius bioctonarius* were noted in Sections 112-681A-13X, CC, 112-681B-13X, CC, and 112-681C-9H, CC. We found a co-occurrence of this species with *Mesocena quadrangula* in Sections 112-681B-10H, CC and 112-681C-9H, CC, which supports the assignment of an early Pleistocene age.

Calcareous Nannoplankton

Calcareous nannoplankton were found in meager assemblages at various levels in the Quaternary part of Site 681. The most common species are *Gephyrocapsa aperta, Gephyrocapsa oceanica, Helicosphaera carteri*, and *Cyclococcolithus leptoporus*. The cold-water species *Coccolithus pelagicus* was observed only in Core 112-681A-14X and in Cores 112-681B-12H to 112-681B-15X. Compared with Sites 679 and 680, this species is much more common at the distal Site 679 than at the more proximal Sites 680 and 681.

Minor blooms of *Gephyrocapsa* species, including well-preserved complete cells, were found in Samples 112-681A-1H-4, 125 cm, 112-681A-4H-3, 117 cm, and 112-681B-4H-2, 98–99 cm. Calcareous nannoplankton having low diversity are present only in low individual numbers. As was already noted at Site 680, calcareous nannoplankton may have been further diminished by calcite dissolution and reprecipitation of dolomite.

Cores 112-681A-1H to 112-681A-14X, Cores 112-681B-1H to 112-681B-15X, and all 10 cores of Hole 681C can be placed only generally in the Quaternary because of the low diversity of calcareous nannoplankton. However, some samples yielded further data. Sections 112-681B-9H, CC and 112-681B-10H, CC contained *Pseudoemiliania lacunosa* and thus are not younger than nannoplankton Zone NN19 (*Pseudoemiliania lacunosa* Zone). In Section 112-681B-14X, CC, *Cyclococcolithus macintyrei* was found, indicating that this level is no younger than the lowest part of Zone NN19 (top of subzone NN19a equals the last occurrence of *Cyclococcolithus macintyrei*, 1.45 Ma). This seems in good agreement with the preliminary silicoflagellate data for this hole, since the first occurrence of the silicoflagellate *Distephanus bioctonarius bioctonarius* was noted in Section 112-681B-13X, CC.

Near the bottom of Hole 681A, rare displaced *Reticulofenestra pseudoumbilica, Dictyococcites dictyodus*, and *Cyclococcolithus floridanus* were observed in an otherwise Quaternary nannoplankton assemblage in Section 112-681A-19X, CC. However, the presence of *Reticulofenestra pseudoumbilica* may also indicate that this level represents the early Pliocene with displaced Eocene or Oligocene nannoplankton and with downhole contamination from the Quaternary caused by drilling difficulties.

Radiolarians

Hole 681A

All core-catcher samples from this hole were studied for radiolarians. These are absent in most samples and, when present, are diluted by diatoms and thus appear rare. Preservation is generally good. No precise age assignment was possible because of the scarcity of specimens. Nevertheless, species known from the Quaternary were identified.

Cycladophora davisiana, Theocalyptra bicornis, Carpocanium sp., *Zygocircus* sp., and *Polysenia murrayana* were found in Section 112-681A-1H, CC. *Tetrapyle octacantha*, ?*Phormostichoartus fistula*, and *Dictyoceras wirchowi* were found in Section 112-681A-2H, CC. *Botryostrobus lithobothrys, Siphocampe corbula*, and *Lithostrobus seratus* were found in Section 112-681A-3H, CC; thus, the age is younger than middle Miocene. Usually, radiolarians show a wide diversity of families. Section 112-681A-3H, CC is peculiar in that its radiolarians belong only to two families: the artostrobiids and the spyroids. Such an oc-

currence of two predominant families (orosphaerids and spyroids equals "acanthodesmids") was previously mentioned at Site 573 (Mayer, Thayer, Thomas, E., et al., 1985) just before their disappearance, while they were abundant in upper sections. The existence of two families could represent either the remains of the most robust forms that are resistant to dissolution, or less specialized families able to survive in upwelling regions. The former can be rejected because the morphotypes of these families are far from having the thickest shell walls. Moreover, diatoms (which have thinner walls), are still preserved. These two families likely represent the only two families able to survive in this environment. This hypothesis is supported by another feature: spyroids, which have only a cephalis and some only the cephalic structure, may be considered the most primitive radiolarians and thus the most adaptable.

Hole 681B

Theocalyptra bicornis, Cycladophora davisiana, Theoconus minythorax, and *Theocorytium trachelium* were found in Section 112-681B-1H, CC. These radiolarians are known to occur in the Quaternary. *Pterocanium trilobum, Tholospyris scaphipes*, and *Polysenia murrayana* were found in Section 112-681B-2H, CC. *Lithelius minor, Hexaphimus infabricatus, Hexapyle* sp., *Siphocampe corbula, Polysenia murrayana*, and *Hexacontium encanthum* were found in Section 112-681B-3H, CC; these species indicate an age younger than middle Miocene. The following species were identified in Section 112-681B-4H, CC: *Lamprocyclas maritalis*; Section 112-681B-6H, CC: *Lamprocyclas maritalis* and *Tholospyris scaphipes*; Section 112-682B-8H, CC: *Hexaconthium encanthum*; and Section 112-681B-9H, CC: *Pterocorys zancleus* and *Pterocanium trilobum*; all species are known to occur in the Quaternary. Other samples, from Sections 112-681B-5H, CC through 112-681B-15X, CC were barren.

Planktonic Foraminifers

Hole 681A

Planktonic foraminifers were examined in 18 core-catcher samples. Rare and well-preserved planktonic foraminifers occurred in Sections 112-681A-1H, CC, 682A-2H, CC, 112-681A-3H, CC, 112-681A-5H, CC, 681-6H, CC, 112-681A-7H, CC, 112-681A-8H, CC, 112-681A-10H, CC, and 112-681A-12H, CC.

Globigerina bulloides, G. falconensis, G. quinqueloba, Globigerinoides ruber, Globigerinita glutinata, Neogloboquadrina humerosa, N. incompta, and *N. pachyderma* were present in Section 112-681A-1H, CC. This faunal assemblage is transitional to subtropical (Bé, 1977). The last appearance of *Neogloboquadrina humerosa* is in the Pleistocene Zone N22 (Srinivasan and Kennett, 1981).

Globigerina bulloides, G. calida praecalida, G. falconensis, G. quinqueloba, Globigerinita glutinata, Globorotalia menardii, Globorotaloides hexagona, Neogloboquadrina eggeri, N. dutertrei, N. incompta, N. pachyderma, and *Beella praedigitata* were recognized in Section 112-681A-2H, CC. The stratigraphic range of *Neogloboquadrina dutertrei* is from Zone N21 to the Holocene.

Globigerina bulloides, G. quinqueloba, Globigerinita iota, G. glutinata, G. uvula, and *Neogloboquadrina pachyderma* were recognized in Section 112-681A-3H, CC. This faunal assemblage is known from polar provinces; the specimens are very small.

Globigerina bulloides, G. quinqueloba, Globigerinita uvula, Globorotalia obesa, G. scitula scitula, Neogloboquadrina incompta, and *N. humerosa* were recognized in Section 112-681A-5H, CC; these species occur primarily in cool-water environments. Range of *Neogloboquadrina humerosa* is from Zone N18 to Zone N22 (late Miocene to earliest Pleistocene, Srinivasan and Kennett, 1981).

Globigerina quinqueloba, Globigerinita uvula, Globorotalia obesa, Neogloboquadrina blowi, N. incompta, and *N. pachyderma* were recognized in Section 112-681A-6H, CC. These species occur primarily in cool-water environments. All species are long-ranging and thus not age-specific.

Globigerina quinqueloba, Globigerinita uvula, Neogloboquadrina incompta, and *N. pachyderma* were recognized in Section 112-681A-7H, CC. These species occur primarily in cool-water environments. We could not assign an age for this assemblage.

Globigerina falconensis, G. bulloides, G. quinqueloba, Globigerinoides sacculifer, Globigerinita uvula, Globorotalia obesa, Neogloboquadrina humerosa, and *N. incompta* were recognized in Section 112-681A-8H, CC; these species occur primarily in cool-water environments. The range of *Neogloboquadrina humerosa* is from Zone N18 to Zone N22 (late Miocene to earliest Pleistocene, Srinivasan and Kennett, 1981).

Globigerina bulloides, G. falconensis, G. quinqueloba, Globigerinoides ruber, Globigerinita glutinata, Pulleniatina obliquiloculata, Globorotalia minutissima, and *Neogloboquadrina incompta* were recognized in Section 112-681A-10H, CC. This faunal assemblage is found in transitional to subtropical regions (Bé, 1977). The coiling change of the *Pulleniatina* Assemblage from dextral to sinistral was found between Sections 112-681A-3H, CC and 112-681A-7H, CC. According to Saito (1976), this zone correlates closely with the Brunhes/Matuyama boundary at 0.7 Ma.

Globigerina calida praecalida, Globigerinoides ruber, Globigerinita glutinata, Globorotalia obesa, and *Neogloboquadrina humerosa* were recognized in Section 112-681A-12H, CC. This faunal assemblage is found in transitional regions (Bé, 1977). *Neogloboquadrina humerosa* ranges from Zone N18 to Zone N22 (late Miocene to earliest Pleistocene, Srinivasan and Kennett, 1981).

Hole 681B

All core-catcher samples were examined for planktonic foraminifers. Rare, well-preserved planktonic foraminifers occur throughout this hole. The species associations range from the late Pliocene to Holocene in age. Alternating cool- and warm-water assemblages are present.

Globigerina bulloides, G. quinqueloba, Neogloboquadrina dutertrei, N. eggeri, N. humerosa, and *N. incompta* were found in Section 112-681B-2H, CC, 112-681B-5H, CC, and 112-681B-7H, CC. These species occur in temperate upwelling environments.

Globigerinoides immaturus, G. obliquus obliquus, G. trilobus, G. ruber, G. sacculifer, Pulleniatina obliquiloculata, and *Sphaeroidinella dehiscens* were found in Sections 112-681B-4H, CC, 112-681B-6H, CC, 112-681B-8H, CC, 112-681B-10H, CC, and 112-681B-13X, CC. These species occur in warm-water regions.

Rare specimens of *Globigerina falconensis, Orbulina universa, Globorotalia obesa*, and *Neogloboquadrina humerosa* were recognized in Sections 112-681B-7H, CC, 112-681B-11X, CC, and 112-681B-15X, CC. Other species that occur are *Globigerinita glutinata, G. iota, G. uvula, Globorotalia minutissima, Neogloboquadrina blowi, Hastigerina riedeli*, and *Beella praedigitata*.

Species that are most significant for determining age include *Hastigerina riedeli*, which was found in Section 112-681B-6H, CC and ranges from Zone N22 (Pleistocene) to the Holocene (Poore, 1978). *Globigerinoides obliquus obliquus*, found in Section 112-681-13X, CC, last occurs at about 1.8 Ma (Berggren et al., 1983). *Pulleniatina* changes coiling direction around the

Brunhes/Matuyama boundary at 0.7 Ma. Dextral-coiling *Pulleniatina* was found in Section 112-681B-4H, CC and sinistral-coiling *Pulleniatina* was found in Sections 112-681B-8H, CC, 112-681B-10H, CC, and 112-681B-13X, CC.

Hole 681C

All core-catcher samples were examined for planktonic foraminifers. Rare, well-preserved planktonic foraminifers occur throughout this hole.

Globigerina bulloides, Neogloboquadrina dutertrei, and *N. pachyderma* were found in Sections 112-681C-3H, CC and 112-681C-6H, CC. These species are known to occur in temperate coastal upwelling regions. *Globigerinoides ruber, G. trilobus, Orbulina universa*, and *Pulleniatina primalis* were found in Sections 112-681C-8H, CC and 112-681C-9H, CC. Other species that occur are *Globigerina quinqueloba, Globigerinita glutinata, G. iota, G. uvula, Globorotalia obesa, Neogloboquadrina acostaensis*, and *N. humerosa. Hastigerina riedeli* was recognized in Section 112-681C-1H, CC. The species ranges from Zone N22 to the Holocene. Based on planktonic foraminifers, we placed this section of Hole 681C in Zone N22 (Pleistocene).

Benthic Foraminifers

Hole 681A

With the exception of Sections 112-681A-4H, CC and 112-681A-5H, CC, the core-catcher samples at this site contain abundant to common, well- to moderately well-preserved benthic foraminifers in Sections 112-681A-1H, CC through 112-681A-12H, CC as well as 112-681A-13X, CC and 112-681A-14X, CC. These samples are predominantly diatomaceous mud. Sections 112-681A-15X, CC to 112-681A-20X, CC are sandy and barren of foraminifers.

A single *in-situ* assemblage occurs in the diatomaceous mud, whereas some intercalated sandy layers contain specimens of benthic foraminifers transported from shallower water and/or represent an assemblage of a lower sea-level stand. These assemblages are as follows:

Bolivina seminuda humilis Assemblage. This assemblage occurs in Sections 112-681A-1H, CC to 112-681A-3H, CC (6.3–25.2 mbsf) and Sections 112-681A-7H, CC through 112-681A-14X, CC (63.1–124.8 mbsf). In addition to the nominal species, *Bolivina costata* and *Nonionella* sp. as well as *Buliminella elegantissima* are common to abundant in most samples. *Cassidella glabra* was common to abundant in Sections 112-681A-1H, CC through 112-681A-3H, CC, as well as 112-681A-8H, CC and 112-681A-13X, CC. *Buliminella* cf. *subfusiformis* (large) was common to abundant in Sections 112-681A-8H, CC and 112-681A-11X, CC through 112-681A-14X, CC. *Virgulinella* was rare in Sections 112-681A-8H, CC, 112-681A-10X, CC, 112-681A-12X, CC, and 112-681A-14X, CC.

An outer-shelf, oxygen-minimum environment is indicated by the concurrent high frequencies of *B. seminuda humilis* and *Nonionella* sp. Species diversity is low; the listed species compose more than 90% of the benthic foraminifers.

Nonionella spp. Assemblage. Specimens of this assemblage are sparse and moderately well preserved in Section 112-681A-5H, CC and common and well preserved in Section 112-681A-6H, CC (44.5 mbsf), which has an abundance of shells. In Section 112-681A-6H, CC *Nonionella* spp., *Buccella peruviana*, and *Buliminella elegantissima* are abundant, and *Hanzawaia* sp. as well as *Bulimina pulchella* and *Bolivina seminuda humilis* are sparse. These species are predominantly from shallow inner-shelf environments. Because some of the species also inhabit the outer shelf, the possibility exists that this "assemblage" represents an accumulation of transported tests in which faunal mixing has occurred. Alternatively, these sandy deposits—particularly the shell bed sampled in Section 112-681A-6H, CC—may have been deposited during lower sea levels.

ORGANIC GEOCHEMISTRY

The organic geochemical program at Site 681 is a continuation of the work undertaken at Sites 679 and 680. The three sites constitute an east-west transect across the upwelling deposits of the upper slope and outer shelf of Peru. This program includes measuring hydrocarbon gases and organic carbon, pyrolysis characteristics of organic matter, and collecting samples for geomicrobiological studies. Details of the methods and procedures can be found in the "Organic Geochemistry" section, Site 679 chapter (this volume). Instruments used are described in the "Explanatory Notes" (this volume).

Hydrocarbon Gases

Routine monitoring of hydrocarbon gases was performed at both Holes 681A and 681B to observe concentration profiles with depth. Eight samples from each hole were analyzed by the headspace procedure. We used the Hach-Carle chromatograph (HC) to measure the gaseous components. In addition, one sample from Hole 681C was analyzed by the same method. These results are shown in Table 3, along with the results from the canned-gas procedure applied to six samples from Hole 681B. All data sets show the same general profile of C_1 concentrations with depth, and Figure 13 compares the headspace data at Holes 681A and 681B. Below about 20 mbsf, C_1 increases rapidly to 20,000–26,000 μL/L of wet sediment, ranging in depth from 56 to 72 mbsf. Beginning at about 75 mbsf, values decrease to the general background, as observed at Site 680. The profile of C_1 concentrations with depth correlates inversely with the profile of sulfate values with depth (see "Inorganic Geochemistry" sec-

Table 3. Profile of hydrocarbon gases at Site 681.

Core/section interval (cm)	Depth (mbsf)	C_1 (μL/L)	C_2 (μL/L)	C_3 (μL/L)	C_1/C_2
Hole 681A - Headspace Procedure (HC)					
112-681A-H-4, 0–1	4.5	99	3.7	1.9	27
3H-5, 149–150	23.5	430	4.2	2.6	100
5H-5, 0–1	41.0	11,000	5.0	0.8	2100
7H-5, 149–150	61.5	25,000	6.7	2.0	3700
8H-2, 0–1	65.0	21,000	4.9		4200
1H-3, 149–150	96.5	110	10.0	1.1	11
13X, CC 0–1	120.5	75	3.1		24
15X-2,149–150	133.0	65	8.0		8
Hole 681B - Headspace Procedure (HC)					
112-681B-1H-3, 0–1	3.0	65			
3H-4, 0–1	19.9	19			
5H-3, 149–150	38.9	9500	9.5	2.8	990
7H-3, 0–1	56.4	22,000	8.9	2.1	2400
8H-7, 80–81	72.0	26,000	31.2	2.8	830
9H-2, 0–1	73.9	9900	9.2		1100
12X-4, 0–1	100.5	135	7.9	0.7	17
15X-2, 0–1	126.0	56	3.3	2.6	17
Hole 681B - Canned-Gas Procedure (HC)					
112-681B-1H-2, 145–150	3.0	105		1.0	110
3H-3, 135–140	19.8	446	2.7	0.5	170
7H-2, 135–140	56.3	21,000	3.1		6700
9H-1, 145–150	73.8	13,000	2.3		5500
12X-3,135–140	100.5	87	3.0	0.32	29
15X-1,145–150	126.0	75	2.6	0.24	29
Hole 681C - Both Procedures (HC)					
112-681C-8H-4, 0–1	67.4	25,000	10.6	1.4	2300 Headspace
8H-3, 145–150	67.4	25,000	3.2		7800 Canned-gas

Note: HC = Hach-Carle gas chromatograph.

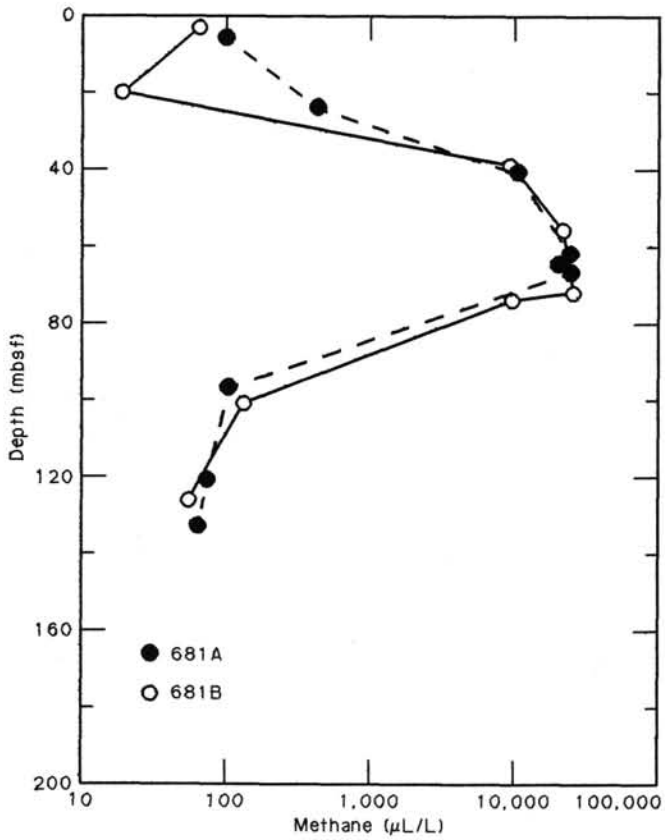

Figure 13. Concentrations of methane with depth at Holes 681A and 681B. Data determined from the headspace procedure and listed in Table 3. Data points at 67 mbsf are from Hole 681C.

tion, this chapter). This correlation strongly suggests that the biological production of C_1 depends inversely on the concentration of sulfate, as was pointed out by Claypool and Kaplan (1974). The concentration of sulfate is sufficiently low to allow high rates of methanogenesis only in the interval from 56 to 72 mbsf. Sulfate appears to be replenished from depth, with the result that below about 75 mbsf methanogenesis is greatly inhibited; C_1 concentrations become very low again as in the more shallow sediments below 56 mbsf.

C_2 and C_3 are present in most samples, and their concentrations show no particular trend with depth. Results for C_2 and C_3, as obtained by the headspace procedure, are not consistent with those obtained by the canned-gas procedure in that more C_2 and C_3 was measured using the headspace method. We also observed this inconsistency at other sites; we tentatively conclude that heating a sample to 70°C during the headspace procedure releases adsorbed C_2 and C_3, which did not evolve during the canned-gas procedure. Also, partitioning effects that occur during the canned-gas procedure were not considered. These procedural differences led to lower values of the C_1/C_2 ratio during the headspace procedure.

Carbon

Samples of "squeezed cakes" from pore-water studies were used to determine carbon and organic-matter characteristics. Organic-carbon and total-organic-carbon (TOC) values are shown in Table 4. In general, these values are significantly lower than those observed at Sites 679 and 680. For example, average organic-carbon and TOC contents in the first 80 m of sediment at the three sites are:

Site	Organic carbon (%)	TOC (%)	Number of samples
679	6.70 ± 2.8	6.46 ± 2.4	10 (Table 7, Site 679 ch.)
680	6.84 ± 2.7	6.66 ± 2.4	5 (Table 7, Site 680 ch.)
681	2.19 ± 1.5	1.97 ± 1.3	6 (Table 4, this chapter)

The overall decrease in the amount of organic carbon at Site 681 may result from the increase in the sediment of silty mud, silt, and fine sand that dilutes the organic-rich diatomaceous mud that is so prevalent at Sites 679 and 680.

At Hole 681B, samples were taken at 56, 74, and 126 mbsf from intervals where the lithology is dominated by silty mud, silt, and fine sand. These intervals have organic-carbon contents of less than 1.2%. Rock-Eval pyrolysis (Tissot and Welte, 1984) characterizes the organic matter in these intervals as type III (Fig. 14) and suggests that the organic matter comes mainly from

Table 4. Organic-carbon and carbonate-carbon data for Hole 681B.

Core/section interval (cm)	Depth (mbsf)	Total carbon (%)	Inorganic carbon (%)	Organic carbon (%)	TOC (%)
112-681B-1H-2, 145–150	3.0	2.35	0.23	2.12	1.87
3H-3, 145–150	19.9	4.70	0.34	4.36	3.97
7H-2, 140–150	56.4	2.04	0.97	1.07	0.99
9H-1, 140–150	73.9	1.57	0.37	1.20	1.05
12X-3, 140–150	100.5	2.91	0.38	2.53	2.07
15X-1, 135–145	126.0	4.63	4.08	0.55	0.83

TOC = total organic carbon from Rock-Eval pyrolysis.

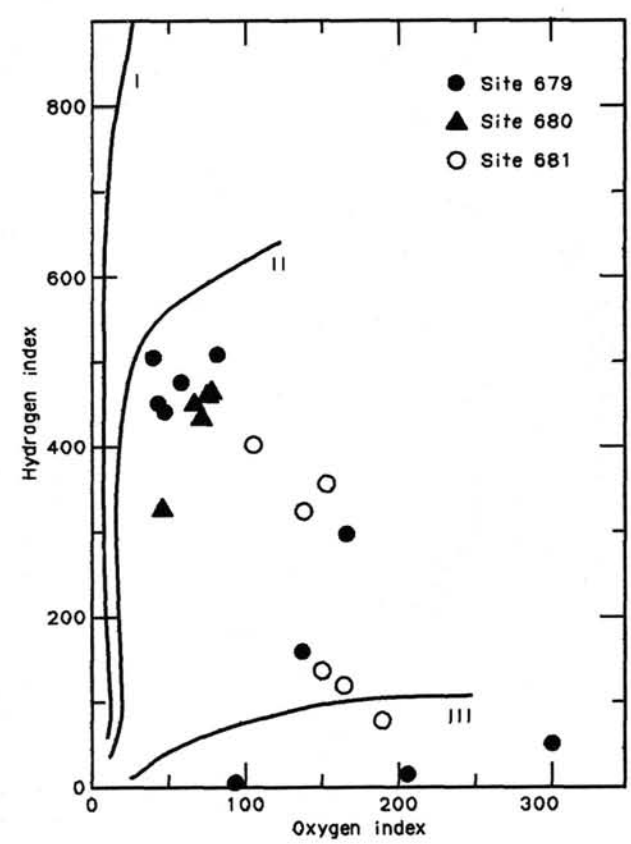

Figure 14. Hydrogen Index (HI) and Oxygen Index (OI) values for organic matter in sediments at Sites 679, 680, and 681, plotted on a van Krevelen-type diagram (Tissot and Welte, 1984).

terrigenous sources, although oxic degradation of marine organic matter in shallow waters could result in a similar type of organic matter (Table 5). Hydrogen Index (HI) and Oxygen Index (OI) values from Sites 679 and 680 are also plotted in Figure 14. This figure shows that the organic matter in most sediments from these two sites is of type II (dominantly of marine origin), whereas at Site 681, the organic matter that is not terrigenous is probably a mixture from both marine and terrigenous sources.

Geomicrobiology

The sampling program for geomicobiology at this site and at the previous ones is described in the "Explanatory Notes" (this volume) and is tabulated in Tables 6 through 8.

INORGANIC GEOCHEMISTRY

Introduction and Operations

A total of 19 interstitial-water samples were obtained from the three holes drilled at Site 681. In Hole 681A, three *in-situ* water samples were recovered at 63.5, 101.5, and 187.5 mbsf; however, no whole-round samples were recovered. In Hole 681B, two *in-situ* samples were recovered at 67.0 and 124.5 mbsf and six whole-round samples were squeezed and analyzed. As at Site 680, only 10 whole-round sediment samples were recovered at Hole 681C. These were squeezed immediately and analyzed. The problems encountered with *in-situ* water samples in Holes 681A and 681B are discussed below.

As at Site 680, major increases in salinity and chloride, sulfate, and Ca^{2+} and Mg^{2+} were observed. For a discussion see "Inorganic Geochemistry" section, Site 680 chapter (this volume). The slopes of the salinity and Cl^- concentration increases are slightly steeper at Site 681 than at Site 680.

Chloride and Salinity

Chloride increases from 557 mmol/L near the sediment/water interface to 989 mmol/L at 126 mbsf (Table 9). At this depth at Site 680, the chloride concentration was 890 mmol/L. The same subsurface brine must be responsible for the diffusion profiles seen in Figure 15.

Alkalinity and Sulfate

Despite the lower TOC contents of between 0.6% and 4.4% (as compared to Site 680), sulfate reduction and alkalinity production are more intense at this site (Fig. 16 and Table 9). At 1.5 mbsf, sulfate concentration is already very low, i.e. 15.5 mmol/L; at Site 680 at 1.3 mbsf, sulfate concentration was considerably higher, i.e., 25.3 mmol/L. Alkalinity at 1.5 mbsf in Sample 112-681C-1H-1, 145–150 cm, is 22.3 mmol/L. At a comparable depth at Site 680 (1.3 mbsf), the value is correspondingly lower, i.e., 16.7 mmol/L.

Sulfate reduction is completed at about 25 mbsf. Between this depth and about 80 mbsf, sulfate concentrations are 0 mmol/L. Below this depth, they increase again by diffusion from the subsurface brine. Unlike Site 680, CH_4 concentrations are high at this site (see "Organic Geochemistry" section, this chapter); methane increases rapidly below the sulfate-reduction zone.

The distinct differences in sedimentation rates in the uppermost 80 m of Sites 680 and 681 influence the observed differences in the extent of sulfate reduction at these two sites. Sedimentation rates are 55 m/m.y. in the top 40 mbsf, and 22–30 m/m.y. between 40 and 120 mbsf at Site 680. At Site 681, however, sedimentation rates are 80 m/m.y. in the uppermost 80 m (see "Lithostratigraphy" section, this chapter). At slower sedimentation rates, as at Site 680, the rate of sulfate diffusion from seawater exceeds the rate of bacterial sulfate reduction; therefore, the sulfate reduction is incomplete at Site 680. At higher sedimentation rates, e.g., Site 681, the rate of sulfate diffusion from seawater is equal to or slightly slower than the rate of bacterial sulfate reduction. Hence, a rather thick sulfate-free zone developed at Site 681. At both sites, the diffusional communication of sulfate with the subsurface brine is similar. The maximum alkalinity occurs at a slightly shallower depth than the sulfate minimum. For discussion of this observation and the effect of sulfate diffusion from the subsurface brine, see the "Inorganic Geochemistry" section, Site 680 chapter (this volume).

Ammonia, Phosphate, Silica, Calcium, and Magnesium

These profiles are similar to those encountered at Site 680 (Figs. 17 and 18; Table 9). Discussions appear in the "Inorganic Geochemistry" section, Site 680 chapter (this volume), as well as for the identical behaviors of Ca^{2+} and Mg^{2+} at both sites (Fig. 18).

Comments About *In-Situ* Water Samples, Sites 680 and 681

Two water samples from the high salinity zones in Holes 681A and 681B (*in-situ* sample 2 in both holes, at 101.5 and 124.5 mbsf, respectively) were recovered from the stainless steel and copper coils. In both samples, light blue crystals (copper sulfate) precipitated in the laboratory. Therefore, chemical data from these samples are not included with the data of the interstitial-water samples obtained by squeezing. For the other *in-situ* water samples analyzed, only the stainless-steel coil fraction was used.

In all *in-situ* samples, silica concentrations are lower than in adjacent squeezed-mud water samples. The known temperature effect on dissolved silica in interstitial waters is enhanced in diatomaceous sediments. For example, in *in-situ* sample 1 (Hole 680B at 61.5 mbsf), the observed silica value is 992 μmol/L; on the basis of the silica profile (Fig. 22, Site 680), the expected value from a squeezed sample at this depth is approximately 1100 μmol/L.

The correspondence between chemical data from *in-situ* samples listed next and from squeezed-mud samples from the same holes generally is excellent (Table 9).

Table 5. Rock-Eval summary for Hole 681B.

Core/section interval (cm)	Depth (mbsf)	Temp. (°C)	S_1	S_2	S_3	PI	PC	TOC (%)	HI	OI
112-681B-1H-2, 145–150	3.0	400	1.43	6.60	2.43	0.18	0.66	1.87	352	129
3H-1, 145–150	19.9	393	3.03	15.93	3.20	0.16	1.58	3.97	401	80
7H-2, 140–150	56.4	386	0.37	1.26	1.55	0.23	0.13	0.99	127	156
9H-1, 140–150	73.9	386	0.31	1.42	1.47	0.18	0.14	1.05	135	140
12X-3, 140–150	100.5	388	1.61	6.73	2.50	0.19	0.69	2.07	325	120
15X-1, 135–140	126.0	373	0.25	0.66	1.57	0.28	0.07	0.83	79	189

Note: Rock-Eval parameters are defined in "Organic Geochemistry" section, Site 679 chapter.

Table 6. Geomicrobiology data from whole-round core sections at Hole 679C.

Core-section interval (cm)	Depth (mbsf)	Comment
112-679C-1-1, 130-140	1.30	
1-2, 10-20	1.60	
1-2, 70-79	2.20	Quaternary, olive-gray
1-4, 130-140	5.80	diatomaceous,
2-2, 119-128	11.69	foraminiferous
3-1, 121-130	19.71	mud.
4-1, 131-140	29.31	
4-5, 131-140	35.31	
6-3, 125-135	51.25	Pliocene, olive-black
8-6, 131-140	74.81	diatomaceous mud.

Note: Depths are for the top of the interval sampled. Lithological descriptions are drawn from those of the other cores at this site. Direct correlation will be aided by visual inspection when cores are sectioned at Texas A&M University and by comparison of GRAPE data.

Table 7. Geomicrobiology samples (whole-round core sections), Hole 680C.

Core/section interval (cm)	Depth (mbsf)	Comment
112-680C-1-1, 120-130	1.20	Late Quaternary
1-2, 20-30	1.70	thinly laminated
1-2, 50-60	2.00	dark olive-green
1-2, 100-110	2.50	foraminifer
1-4, 30-40	4.80	diatomaceous muds
2-3, 30-4	9.10	and sandy silts.

Table 8. Geomicrobiology samples (whole-round core sections), Hole 681C.

Core/section interval (cm) Comment	Depth (mbsf)	
112-681C-1-2, 0-10	1.50	Quaternary
1-2, 20-30	1.70	dark olive-gray
1-2, 50-60	2.00	laminated
1-2, 100-110	2.50	diatomaceous mud.
1-3, 30-40	3.30	
1-4, 30-40	4.80	
1-2, 30-40	7.70	
4-2, 30-40	26.70	
5-3, 30-40	36.20	Interbedded
7-2, 30-40	55.20	terrigenous and
8-2, 30-40	64.70	diatomaceous muds,
9-6, 30-40	80.20	sand-silt beds.

However, *in-situ* water samples 1 (680A, 93.9 mbsf) and 3 (681A, 187.5 mbsf) are contaminated because of dilution from drill-hole seawater. For example, note the following observations:

Sample			Cl^- (mmol/L)	Salinity (g/kg)
1	680A	observed	616.89	37.7
1	680A	expected	~775	~47
3	681A	observed	857.70	52.5
3	681A	expected	~1400	>70

PALEOMAGNETICS

Introduction

At Site 681, the upper 60 m of each core had a strong magnetic signal that was easy to measure with the shipboard spinner magnetometer. As at earlier sites, the rest of the sediments were characterized by weak magnetic moments (<0.05 mA/m). Therefore, we feel it is important to state that the results from samples collected at >60 mbsf should be considered preliminary until shore-based studies with a cryogenic magnetometer can be conducted. Although we started working on samples from Hole 681B, the weak remanent magnetization within these samples led us to abandon these measurements. Instead, we decided to complete measurements of this second hole with shore-based investigations.

Results

Figures 19 and 20 show the declination, inclination, and intensity values vs. depth for the samples measured. The value selected and reported in the plots is a 150-Oe demagnetization value and was selected on the basis of the vector plots and low circular standard deviations. For samples that occur below 60 m, the intensity of magnetization decreased below the background noise level of the shipboard magnetometer. Next, we summarize the results from the two holes. These descriptions refer to downhole plots (Figs. 19 and 20).

Hole 681A

With one noticeable exception (discussed next), all samples collected from this hole are normal (negative inclination in the Southern Hemisphere) down to between 82 and 84 mbsf. The Brunhes-Matuyama boundary is believed to occur at this depth. As stated previously, samples recovered from below 82 mbsf do show both polarities (Fig. 19); Thus, these results should be considered preliminary. An examination of the right column of Figure 19 shows that below 60 m the intensity of magnetization is extremely weak (less than 0.5 mA/m) and is not easily distinguishable from the background noise level of the Molspin. Although one can obtain inclination values from these measurements, one must be careful because these values are somewhat questionable. Although the measurements show reliable angular standard deviations, vector plots of these low-intensity samples do not show the straight line decay of the magnetic directional vectors characteristic of a stable single component of magnetization (Fig. 20). Two of the critical cores (112-681-6H and 112-681-7H) are incomplete. This abrupt change in the magnetic character of these samples is discussed in detail in the Site 680 chapter (this volume).

The one exception to the normal polarity in the upper part of 681A is one section of reversed polarity at 18 mbsf. A similar result was obtained at approximately the same depth in Hole 681B. We believe that this reversal in polarity is real and represents a minor event in the Brunhes Normal Epoch. Because of its relative position in the core, we have tentatively assumed that this reversed polarity is the Blake event.

One other point of interest in the magnetic behavior of Hole 681A is the plot of intensity of magnetization (at 150-Oe level of demagnetization) vs. depth. From this plot one can see that two (perhaps four) local maxima occur.

Hole 681B

Figure 21 shows a plot of declination, inclination, and intensity of Site 681B vs. depth. Although the inclination vs. age suggests a reversal at approximately 40 mbsf, the samples were mixed up and these values are highly suspect. We will resample the entire hole for shore-based studies. A period of reversed polarity was also observed in the upper 18 m of this hole (as in Hole 681A).

PHYSICAL PROPERTIES

Physical-property measurements were performed on split cores in Holes 681A and 681B. Samples also were taken from

Table 9. Interstitial-water analyses for Site 681.

Core-section interval (cm)	Depth (mbsf)	pH	Alkalinity (mmol/L)	SO_4^{2-} (mmol/L)	PO_4^{2-} (μmol/L)	NH_4^+ (mmol/L)	SiO_2 (μmol/L)	Salinity (g/kg)	Cl^- (mmol/L)	Ca^{2+} (mmol/L)	Ma^{2+} (mmol/L)	Mg^{2+}/Ca^{2+}
112-681C-1H-1, 145-150	1.5	7.5	22.28	15.51	24.97	2.62	992	34.2	557.11	9.58	52.25	5.45
681B-1H-2, 145-150	3.0	7.9	21.82	17.23	16.73	2.18	938	36.0	563.73	8.85	50.90	5.75
681C-1H-3, 145-150	4.5	7.8	17.74	15.03	i	1.74	968	34.5	558.05	8.29	50.66	6.11
2H-1, 140-150	7.4	7.8	15.95	15.33	i	2.15	1007	34.8	562.79	8.77	50.34	5.74
2H-4, 145-150	11.9	7.7	14.87	12.84	i	1.59	1031	34.9	574.16	8.70	48.90	5.62
681B-3H-3, 145-150	19.8	7.5	16.66	—	13.61	2.51	999	35.8	608.27	8.04	46.77	5.82
681C-4H-2, 142-150	27.9	7.7	19.50	1.18	i	3.16	1072	36.5	630.06	8.02	45.74	5.70
4H-5, 142-150	32.4	7.7	18.74	0	i	3.51	1055	37.0	646.17	8.06	45.86	5.69
5H-3, 142-150	38.9	7.6	18.05	0	i	3.81	1118	38.0	655.64	8.82	46.61	5.29
7H-2, 140-150	56.3	7.6	16.84	0	5.97	4.72	1075	43.8	731.44	11.30	54.02	4.78
681B-7H-2, 140-150	56.3	7.4	16.72	3.73	6.78	4.88	1062	42.8	746.60	11.24	53.78	4.79
681A *In-situ* 1	63.5	7.3	*17.28	*1.71	—	*4.45	*1046	*43.8	*758.03	*12.24	*55.75	*4.72
681C-8H-2, 140-150	65.8	7.4	16.44	0.0	6.58	5.02	1081	45.2	766.49	12.49	57.15	4.58
681B *In-situ* 1	67.0	7.5	*17.63	*1.26	*1.26	*4.94	*1068	*43.7	*757.02	*12.08	*56.85	*4.71
681B-9H-1, 140-150	73.8	7.4	15.73	0	5.07	5.50	1081	46.0	794.92	13.22	60.04	4.54
681C-9H-2, 140-150	75.3	7.6	15.93	0	5.37	4.48	1062	51.5	786.39	13.81	60.32	4.37
681B-12X-3, 140-150	98.9	7.3	13.99	2.72	6.78	4.56	1142	52.3	914.30	18.31	73.23	4.00
15X-1, 135-145	126.0	7.3	10.99	10.67	5.07	4.56	1001	57.8	989.15	23.70	83.49	3.52
681A *In-situ* 3	187.5	7.8	*5.16	*34.04	*4.57	*2.06	*643	*52.5	*857.70	*25.35	*81.95	*3.23

i = color interference from H_2S. * = *in-situ* samples. Results of two additional *in-situ* interstitial-water, samples, taken in Hole 681A at 101.5 mbsf and 681B at 124.5 mbsf, are not reported here because light blue crystals precipitated in laboratory before analyses.

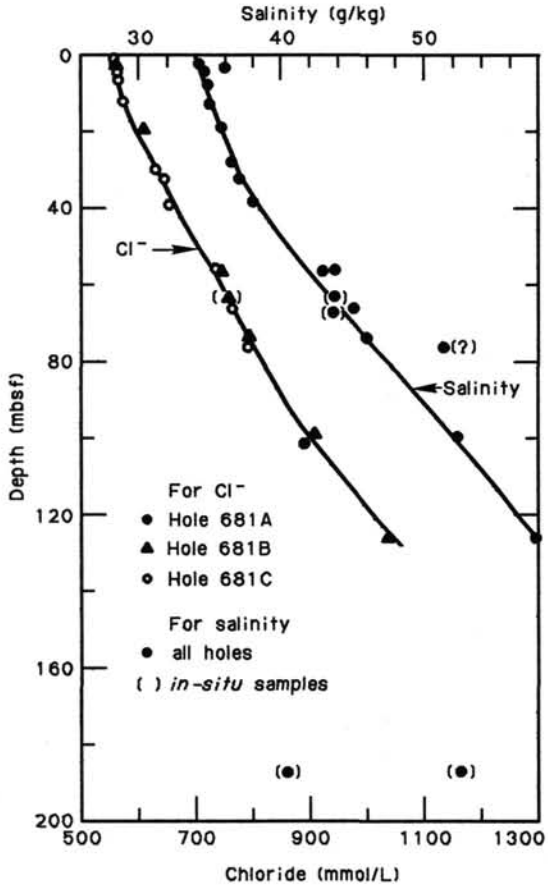

Figure 15. Profiles of chloride and salinity at Site 681.

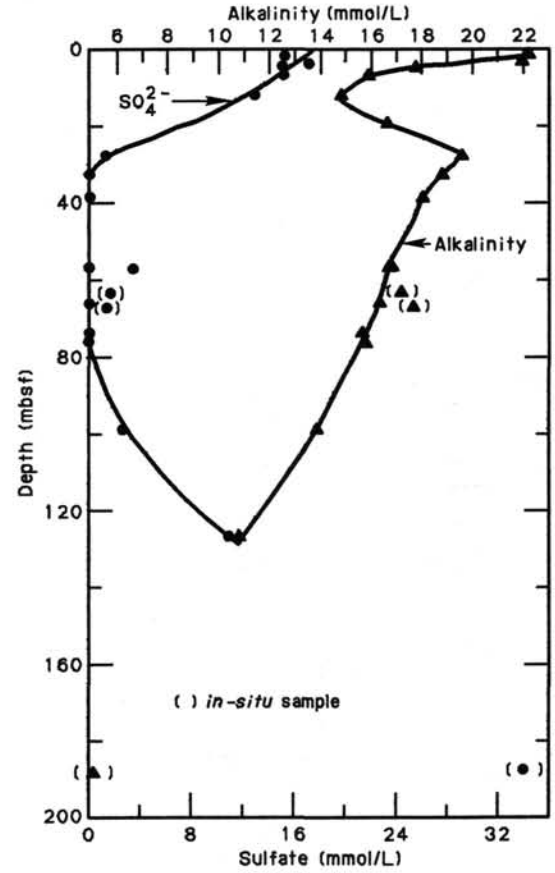

Figure 16. Profiles of sulfate and alkalinity at Site 681.

the split core of Hole 681A for shore-based analysis of the Atterberg Limits. Whole-round samples were taken from Hole 681C for shore-based triaxial, creep, and consolidation tests.

Data presented in this section include index properties, compressional-wave velocity, undrained vane shear strength, and thermal conductivity. Samples were taken from good quality APC cores, with a few samples obtained from XCB cores if the "biscuits" appeared intact and at their natural water content.

Index Properties

The index properties measured at Site 681 included water content (presented as a percentage of dry sample weight), porosity, bulk density, and grain density. These data are presented in Table 10. The methods used to measure index properties at Site 681 were the same as those specified in the "Explanatory Notes" (this volume). Usually, salinity is assumed to be 35‰ when calculating index properties. At Site 681, the salinity increased

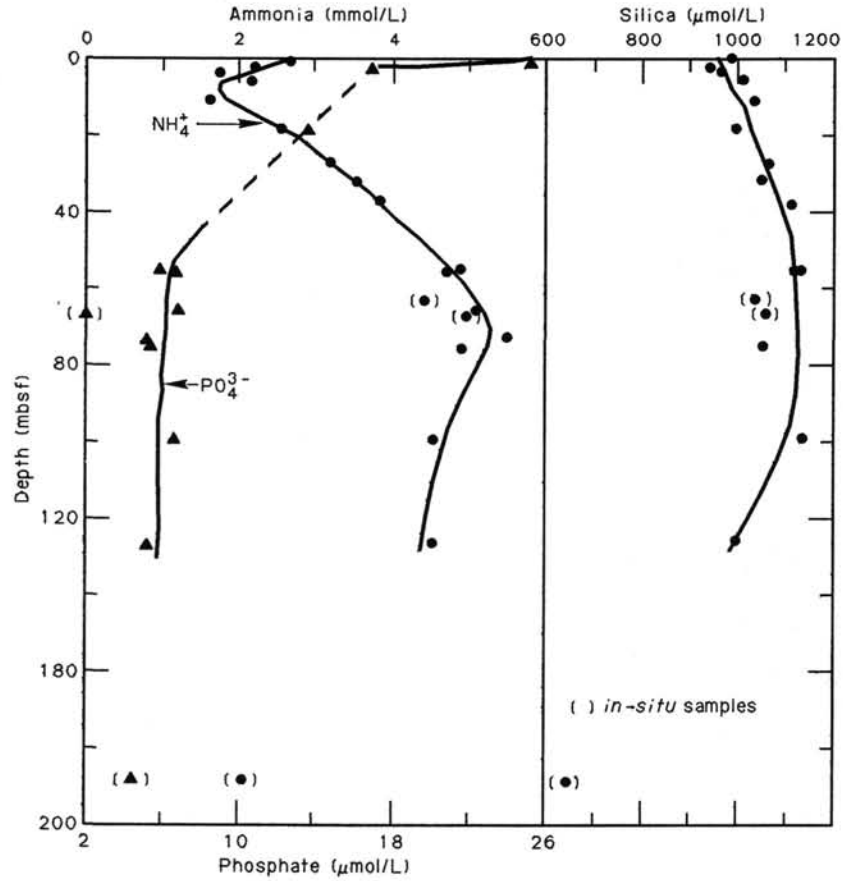

Figure 17. Profiles of ammonia, silica, and phosphate at Site 681.

with depth below seafloor to almost 60‰ at 120 mbsf (see "Inorganic Geochemistry" section, this chapter). Therefore, index properties were calculated using the interpolated salinity for the sample depth.

Figure 22 illustrates the downhole trends in water content and porosity with depth and the lithology for Holes 681A and 681B. Figure 23 shows the GRAPE and selected sample bulk-density data for Site 681. At least one section of each core was analyzed using the GRAPE (more sections were run if time allowed). In general, the values obtained from the GRAPE data agreed closely with the bulk-density values obtained from the index-property samples. The peaks that occur in the GRAPE data probably result from the cemented dolomite nodules that occur in this variable lithology. We expected the values obtained for bulk density using the GRAPE to be lower for the XCB cores because of drilling slurry and sediment disturbance.

The water-content values for the sediments at Site 681 decrease rapidly from a high of 271% at 2 mbsf to 66% at 74 mbsf. Different water contents were superimposed on the data from frequent alternations of sandy silts and diatomaceous muds in lithologic Units I, II, and III. The samples at 12 and 14 mbsf and again between 50 and 78 mbsf are from such sandy intervals. The porosity data also generally follow a linearly decreasing trend, with a high of 87% at 2 mbsf and a value of 65% at 74 mbsf. Again, the values obtained for the sandy layers superimpose an oscillation on this trend, with lower porosities of 68% and 50%. The boundary between lithologic Units I and II cannot be distinguished based on the index-property data.

At approximately 80 mbsf, in the lower section of Unit II, the water content increases to values of 140% to 186%, and an increase in porosity to values of 80% to 86% results from the diatomaceous muds that dominate lithologic Unit III. The water-content values obtained for samples taken in XCB cores appear to increase dramatically.

Compressional-Wave Velocity

Velocities were measured using the Hamilton Frame, following the procedures described in the "Explanatory Notes" (this volume). The Hamilton Frame data are presented in Table 11 and shown in Figure 24. The velocity values appear to be fairly consistant. They increase linearly from 1.53 km/s at the top of Unit I to 1.55 km/s a few meters below the top of Unit II. The values then stay fairly constant with depth at approximately 1.55 km/s through the remainder of lithologic Unit II. Only four measurements were performed on samples taken from Unit III, but the results show an increase in the velocity to approximately 1.58 km/s. These generally low velocity values reflect the high water contents of the sediments.

The *P*-wave logger was operated in conjunction with the GRAPE. Velocity data from the *P*-wave logger were inspected from shipboard printouts. In general, the *P*-wave data gave similar values as the Hamilton Frame data.

Vane Shear Strength

The undrained vane shear strength for Site 681 was measured with the Wykham Farrance vane apparatus. Values obtained for peak undrained vane shear strength are presented in Table 12 and are shown vs. depth below seafloor in Figure 25. According to the data plots, the boundaries between the lithologic units are not indicated by changes in vane shear strength. Although there is some scatter, the trend is of slightly increasing strength with depth, from a value of 95 kPa just below the seafloor to approx-

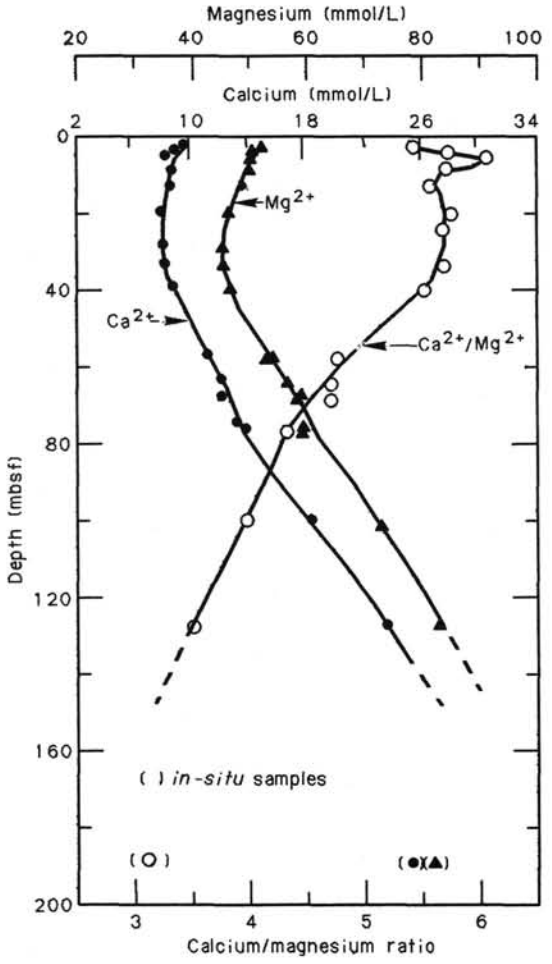

Figure 18. Profiles of calcium and magnesium at Site 681.

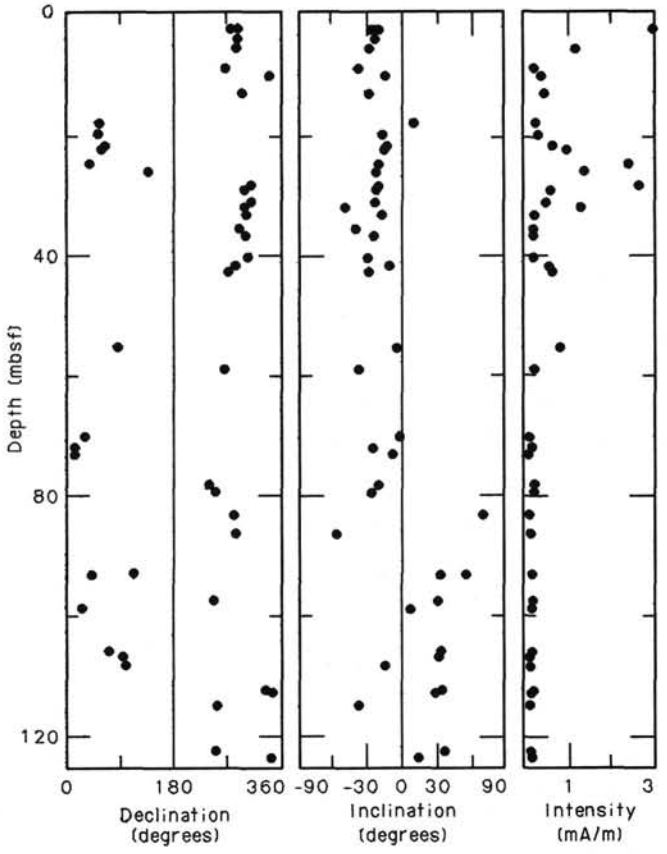

Figure 19. Declination, inclination, and intensity plots vs. depth below seafloor. The Brunhes-Matuyama boundary is clearly noted at around 82 mbsf. Note that the intensity of magnetization shows a cyclicity that perhaps reflects cyclic sedimentary input into the basin. A small magnetic reversed event is seen at 18 mbsf.

imately 103 kPa at 120 mbsf. The scattered data probably result from the highly varied lithology at this site owing to cyclic sedimentation controlled by climate and fluctuations in sea level (see "Lithostratigraphy" section, this chapter).

Thermal Conductivity

Thermal conductivity was measured by the needle-probe method mainly on samples from Hole 681C, where whole-round core sampling was conducted. As we planned to drill to only 100 mbsf at Hole 681C, we tried to measure deeper sediments at Hole 681B. Cores that were obviously disturbed were not tested, and some of the obtained values were discarded when we saw drilling disturbance after splitting the cores.

The data from both holes are listed in Table 13 and plotted in Figure 26. In lithologic Units I and II, the thermal conductivity generally increases with depth from about 0.8 W/m·K near the seafloor to about 1.0 W/m·K at around 100 mbsf. The large data scatter is probably caused by cyclic variation in lithology similar to that in samples from Holes 681A and 681B, although we did not split cores from Hole 681C. Thus, we could not examine the correlation between thermal conductivity and lithology. The thermal conductivity is relatively low, about 0.8 W/m·K, near 120 mbsf.

Such variation in thermal conductivity seems to correlate well with the variation in water content. Water content decreases with depth from the seafloor to 74 mbsf and is high near 120 mbsf (Fig. 22). Therefore, the variation in thermal conductivity is probably dominated by the variation in water content, which in turn reflects texture, lithology, and organic-matter content.

Summary

The boundary between Units I and II is not indicated by changes in index properties or vane shear strengths. This Unit I/II boundary results in a change in index properties with depth, but no change in undrained vane shear strength occurs across the boundary. The oscillatory nature of the data is the result of the frequent facies changes within each unit, which is caused by cyclic sedimentation.

As was the case at Sites 679 and 680, the extremely high water-content, porosity, and shear-strength values are the result of the high organic carbon contents of the sediments, while the low velocities reflect the high water content of the sediments.

GEOPHYSICS

Seismic Records

Site 681 was positioned on the eastern end of the drilling transect across the seaward flank of a lens-shaped sediment sequence underlying coastal upwelling. Drilling at this site completed a transect from the distal part of the lens (Site 679) (where upwelling sediment could not be resolved in our seismic data) to the 0.17-s reflective sequence at the most landward site (Site 681). Seismic record YALOC 74-03-20 provided the prime geophysical data for this site (Fig. 27). Beneath the site, the reflective sequence is regular and lacks any distinctive features corresponding to changes in the lithology. The agreement in depth between the base of lithologic Unit III (136 mbsf) and the base of the lens in the seismic record (128 m) is good. The dif-

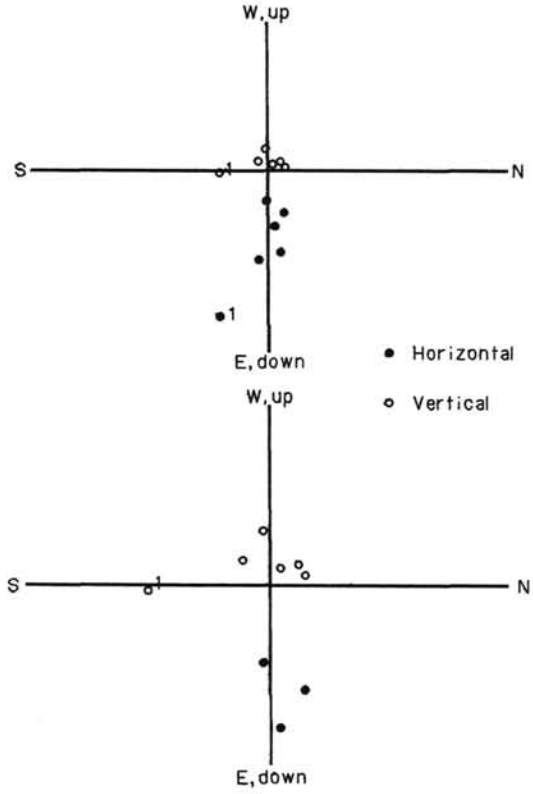

Figure 20. Two plots of samples collected from Core 112-681A-7H. These diagrams show that we were unable to isolate a single component of magnetization. This is characteristic of lower sections at this site; thus, these data should be regarded as suspect.

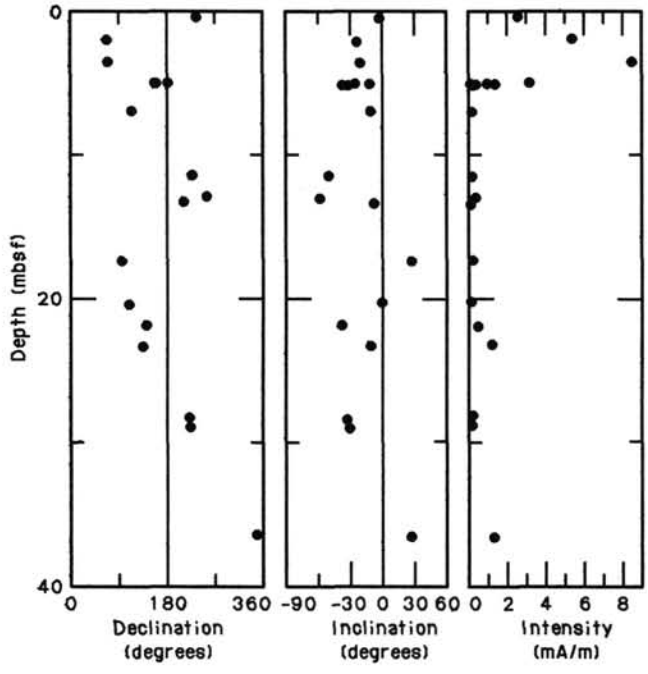

Figure 21. Declination, inclination, and intensity plots vs. depth below seafloor. We regard these data as suspect because of a mix-up of samples for Core 112-681B-5H. Hole 681B also shows the small magnetic reversed event at 18 mbsf.

Table 10. Summary of index properties data for Site 681.

Core/section interval (cm)	Depth (mbsf)	Water content (dry wt%)	Porosity (%)	Bulk density (g/cm^3)	Grain density (g/cm^3)
112-681A-1H-3, 67	3.67	183.50	81.92	1.30	2.39
2H-3, 78	10.28	151.01	81.07	1.38	2.76
3H-4, 77	21.27	130.37	75.26	1.36	2.32
4H-5, 65	32.15	183.76	80.59	1.27	2.25
5H-4, 45	39.95	100.70	71.82	1.47	2.56
8H-4, 69	68.69	68.98	66.56	1.67	2.75
9H-5, 75	79.75	144.26	80.45	1.40	2.37
11H-2, 68	94.18	55.75	61.86	1.77	2.75
12H-6, 82	109.82	114.05	74.07	1.42	2.27
13X-2, 71	113.21	163.62	80.94	1.34	2.20
112-681-B1H-2, 67	2.17	270.36	87.25	1.22	2.43
2H-2, 56	7.96	202.15	85.56	1.31	2.37
2H-4, 91	11.31	70.87	65.82	1.63	2.65
2H-6, 51	13.91	38.16	50.34	1.87	2.56
3H-2, 99	17.89	125.13	78.02	1.44	2.44
3H-4, 78	20.68	143.62	81.05	1.41	2.56
3H-6, 53	23.43	181.41	81.83	1.30	2.32
4H-2, 73	27.13	216.63	83.86	1.26	2.19
4H-4, 35	29.75	118.60	75.77	1.43	2.43
5H-4, 78	39.68	142.56	79.49	1.39	2.44
7H-2, 68	55.58	61.30	62.83	1.69	2.57
7H-4, 91	58.81	99.99	72.76	1.49	2.39
8H-3, 20	65.83	79.04	69.44	1.61	2.61
8H-6, 75	69.37	67.55	66.97	1.70	2.65
9H-2, 43	74.33	68.22	65.98	1.67	2.66
10H-2, 63	84.03	194.27	86.82	1.35	2.65
12X-3, 54	99.54	133.09	79.42	1.42	2.46
14X-2, 79	117.29	262.82	88.43	1.25	2.25
14X-3, 110	119.10	212.61	86.37	1.30	2.37

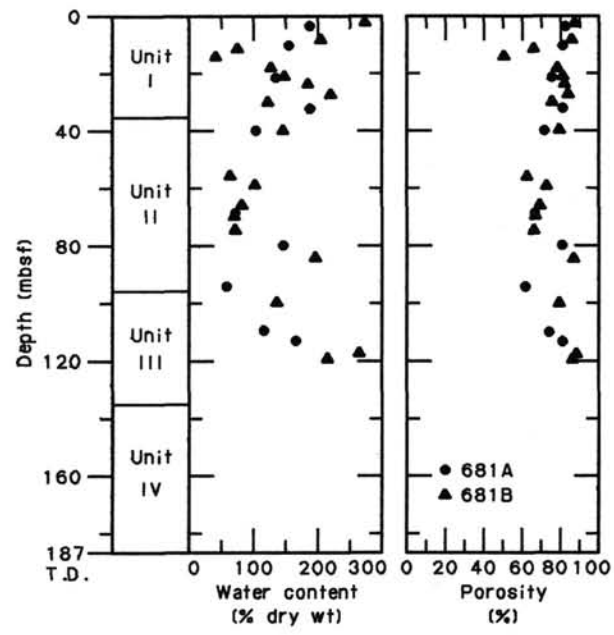

Figure 22. Water-content and porosity profiles for Site 681; lithologic units also are shown schematically.

ference is attributed to an imprecise measurement of traveltime from the small scale of the record (Fig. 27). The water-gun record made on board the *Resolution* told us very little while the 3.5-kHz record does show several reflections. However, none of them correlate with distinct lithologic-unit boundaries. A broad perspective of the transect is shown on multichannel line 2800

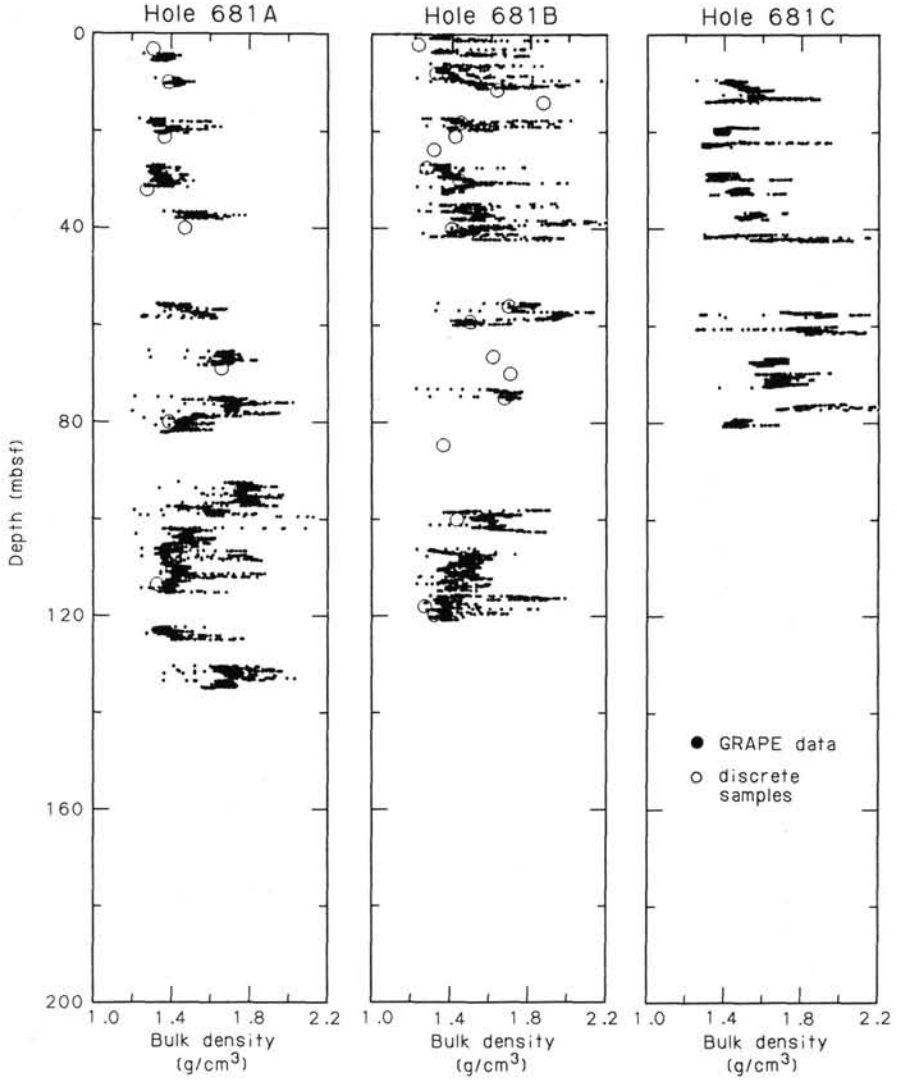

Figure 23. GRAPE and bulk-density data from discrete samples for Site 681.

(Thornburg, 1985), which parallels the YALOC 74-03-20 record (Fig. 28). The center of upwelling at Site 681 is also the depositional and structural center of the Neogene Salaverry Basin, and the distal edge at Site 679 coincides with the edge of that basin. The present lens of upwelling deposits represents only a thin layer at the top of this section.

Heat Flow

Temperature Measurements

Hole 681A

In combination with the APC tool, the T-probe was deployed three times. The data obtained during the first and second runs could not be used because of a problem with electronics. Another electronics package was used for the third run, but the temperatures recorded were too high even for the laboratory and thus were discarded.

When used with the pore-water sampler (see "Explanatory Notes," this volume), the APC tool tends to give lower temperatures than the true formation temperature. Therefore, the temperature recorded just before pull-out can be treated as the lower limit of the true temperature at this hole.

Hole 681B

We performed the first measurement at Hole 681B with the APC tool while collecting Core 112-681B-5H, but the preset recording time ran out 5 min after penetration. It is difficult to estimate the equilibrium temperature as various theoretical decay curves can fit the 5-min record. However, we concluded that the equilibrium temperature should be lower than 15°C.

After this measurement, the APC tool was run in combination with the T-probe twice. Again, the T-probe produced anomalously high temperatures similar to those at Hole 681A, probably from a defect in the temperature sensor. The APC tool gave two minimum formation-temperature values.

Discussion

The temperature data obtained with the APC tool at Site 681 are summarized in Table 14 and plotted in Figure 29. The arrows in Figure 29 indicate that these values are the minimum or maximum estimates of the true formation temperatures.

If all the temperature data are reliable, the geothermal gradient at Site 681 should be extremely high. Records obtained after those for Cores 112-681A-7H and 112-681A-11H, however, show oscillatory variation of temperature with a large amplitude, which suggests that the pore-water sampler was not stable in the

Table 11. Compressional-wave velocity for Holes 681A and 681B.

Depth (mbsf)	Vertical velocity (km/s)	Horizontal velocity (km/s)
Hole 681A		
3.67	1.54	1.50
10.28	1.54	1.53
21.27	1.55	1.54
32.15	1.56	1.54
39.95	1.55	1.54
68.69	1.53	1.52
79.75	1.54	1.55
94.18	1.55	1.54
109.82		1.56
Hole 681B		
2.17	1.53	1.46
7.96	1.54	1.53
11.31	1.55	1.53
17.89	1.54	1.53
23.43	1.56	1.54
27.13	1.56	1.56
39.68	1.56	1.55
55.58	1.55	1.52
58.81		1.61
66.10	1.55	1.55
71.15	1.55	1.57
74.33	1.57	
117.29	1.58	1.60
119.10	1.57	

Table 12. Vane shear strength data for Holes 681A and 681B.

Depth (mbsf)	Undrained peak vane shear strength (kPa)
Hole 681A	
3.71	90.95
10.32	96.79
21.32	94.46
37.20	162.09
39.99	93.29
68.67	93.29
79.73	156.26
94.15	97.96
109.89	216.90
113.18	102.62
Hole 681B	
2.22	48.53
8.01	61.96
14.90	55.99
11.29	87.46
17.88	93.29
20.66	114.28
23.47	132.94
27.17	94.46
29.79	97.96
39.73	104.95
55.64	86.30
58.85	121.28
66.08	90.96
71.14	100.29
74.32	97.96
117.35	94.46
119.27	113.70

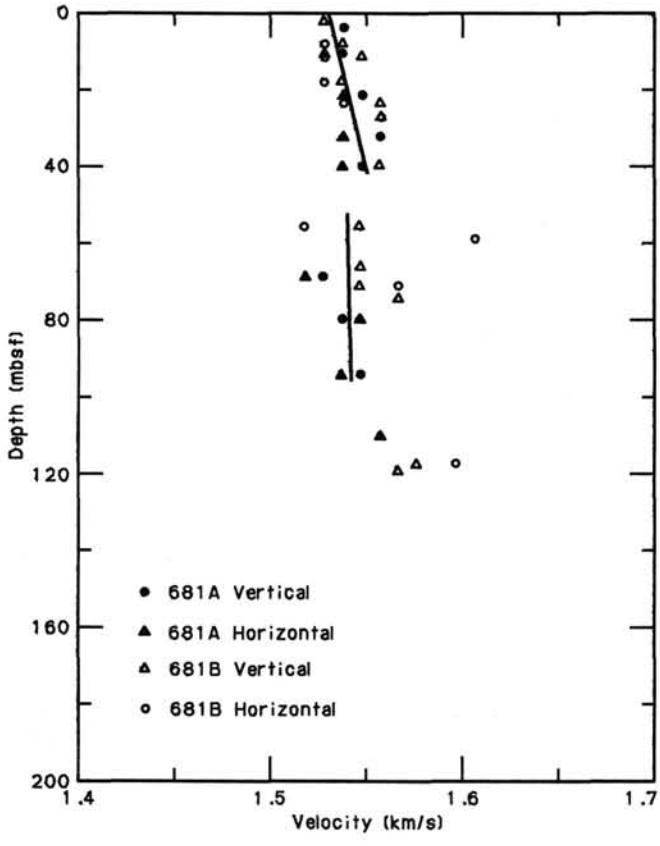

Figure 24. Hamilton Frame velocity data for Site 681.

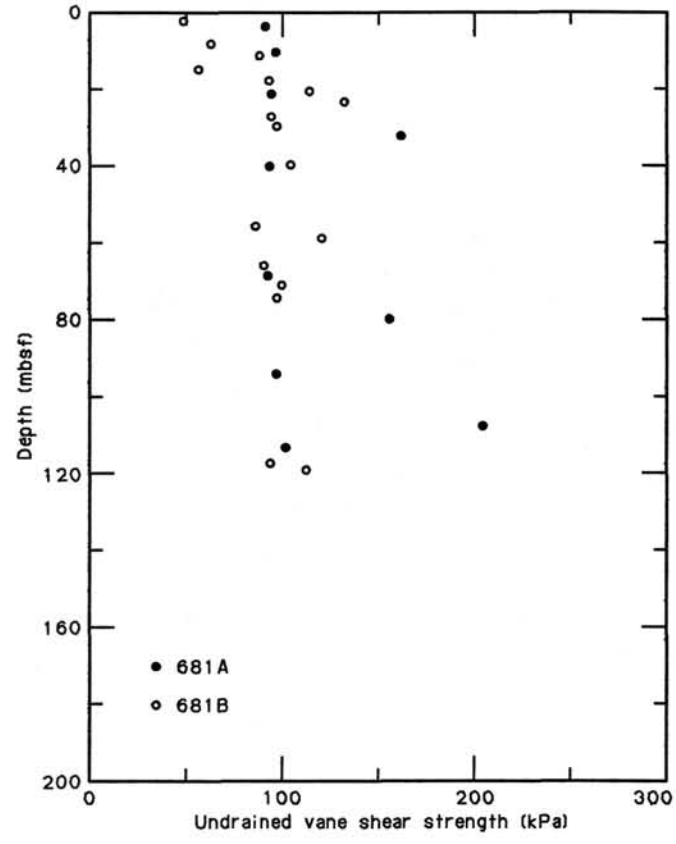

Figure 25. Profile of undrained vane shear strength for Site 681.

Table 13. Profile of thermal conductivity for Holes 681B and 681C.

Core/section interval (cm)	Depth (mbsf)	Thermal conductivity (W/m·K)
112-681B-12X-3, 50	99.50	0.964
12X-4, 40	100.90	0.924
12X-4, 110	101.60	1.128
13X-6, 70	113.70	0.764
13X-6, 130	114.30	0.849
14X-1, 70	115.70	0.765
14X-2, 30	116.80	0.745
14X-2, 120	117.70	0.748
14X-3, 40	118.40	0.780
14X-3, 120	119.20	0.796
14X-4, 30	119.80	0.820
112-681C-2H-3, 10	9.0	0.784
2H-3, 128	10.18	0.884
2H-4, 11	10.51	0.913
2H-4, 74	11.14	0.877
3H-2, 10	17.00	0.781
3H-2, 140	18.30	0.937
3H-5, 20	21.60	0.696
3H-5, 110	22.50	0.673
4H-3, 20	28.10	0.722
4H-3, 130	29.20	0.845
4H-5, 20	31.10	0.868
4H-5, 115	32.05	0.935
5H-2, 20	37.60	0.905
5H-2, 130	38.70	0.840
5H-5, 20	40.60	0.820
5H-5, 130	41.70	1.002
8H-3, 20	66.10	0.921
8H-3, 145	67.35	0.869
8H-6, 20	70.60	1.041
8H-6, 130	71.70	1.007
9H-2, 20	74.10	1.065
9H-2, 139	75.29	1.227
9H-5, 20	78.60	0.838
9H-5, 130	79.70	0.883

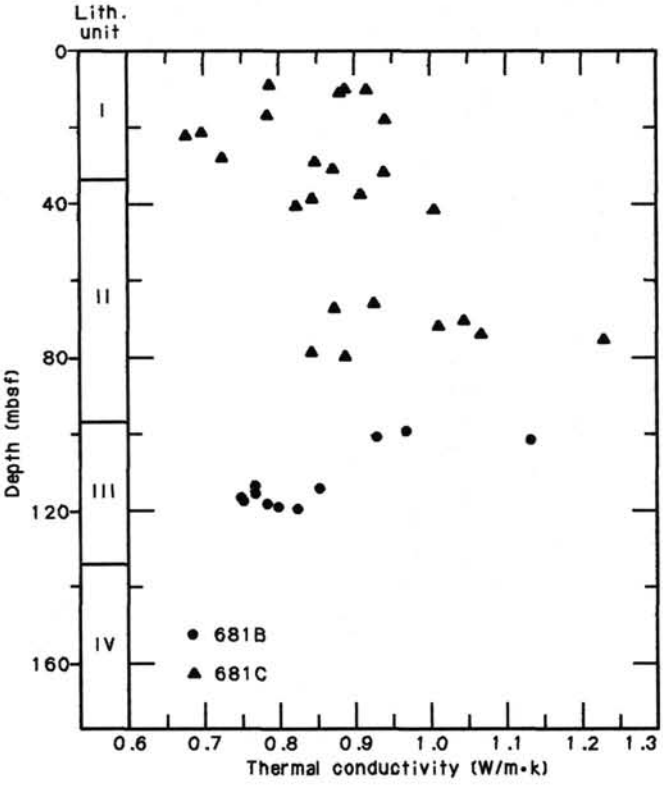

Figure 26. Thermal conductivity vs. depth below seafloor for Holes 681B and 681C.

sediment or that the data recorder did not work properly. Thus, these records may not be reliable. Excluding these two data points (indicated by triangles in Fig. 29), the minimum geothermal gradient between 43.9 and 187.0 mbsf can be estimated as 34×10^{-3} K/m (as shown by the broken line in Fig. 29).

At Site 681, we measured thermal conductivity only down to 120 mbsf (see "Physical Properties" section, this chapter). If one assumes that the mean *in-situ* thermal conductivity between 43.9 and 187.0 mbsf is 0.9 to 1.0 W/m·K, which seems reasonable considering the data above 120 mbsf, the heat flow at Site 681 should be higher than about 30 mW/m^2. This is consistent with the reliable heat-flow values obtained at the other shelf sites (Sites 686 and 687).

SUMMARY AND CONCLUSIONS

Site 681 is the shallowest and most landward target along the east-west transect crossing the upwelling deposits of the Peruvian shelf and upper slope. Of the three sites (679, 680, and 681) along the transect, Site 681 is located nearest the origin of coastal upwelling centers around the headlands near 11°S. The water depth of 150.5 m nearly coincides with the top of the oxygen-minimum zone. Because of the high sedimentation rates, drilling at Site 681 recovered an expanded Quaternary record for studying temporal changes in the upwelling character. At this site, interest focused on the effect of fluctuations in the upper boundary of the oxygen-minimum zone impinging on the shelf. The base of the most recent upwelling deposits is located at approximately 130 m in the seismic records, which indicates that the thickness of the Holocene to late Quaternary sequence here is about twice that encountered at Site 680. Three holes were drilled through this sequence. Hole 681A penetrated to 187.0 mbsf and Hole 681B to 143.5 mbsf. In both holes >90% of the sediment record was recovered to the contact at 135 mbsf between the prograding beds and the underlying continuous strata.

The sections in the upper interval consisted of repeated sequences of dark olive gray diatomaceous mud with laminae of diatom ooze (Units I and III) and massive dark gray terrigenous muds with some degree of bioturbation (Unit II). In both holes magnetic reversals (?Blake event at 18 mbsf), the Brunhes/Matuyama paleomagnetic boundary (at 83 mbsf), and numerous diatom and coccolith markers facilitate correlation within the hole. Evidence exists in these units for relative fluctuations in sea level and cyclic sedimentation based on the presence of erosion surfaces, phosphatic lag deposits, and repeated intervals of increased influx of terrigenous clastics.

The organic-carbon content is about 3 wt%, which is about one-half that measured at Site 680. As the sedimentation rate at Site 681 has increased two-fold, accumulations of organic carbon and preservation rates are similar at both sites. This indicates a complete organic-carbon record, which is important for estimating paleo-bioproduction from these sediments underlying the trail of the upwelling plumes. Well-preserved and abundant diatom floras of "oceanic" and "upwelling" character alternate within Units I and III. Unit III contains more heavily silicified upwelling assemblages, indicating deposition during glacial periods. The same climatic and/or sea-level trends are indicated by the planktonic foraminifer assemblages containing well-known upwelling species.

In Unit IV, below 139.5 mbsf to the bottom of Hole 681A at 187.0 mbsf, dark gray silty sand having sparse intervals of diatomaceous mud and occasionally cemented dolomite nodules was sampled. Unit IV appears similar to the lithofacies encountered at Sites 679 and 680, represented by the continuous reflective sequence of Pliocene strata. The deposition environment is one of near-shore affinities well outside the coastal upwelling influence.

At Hole 681C, 86.4 m of core was recovered, and the materials were frozen to complete sampling later for geomicrobiology,

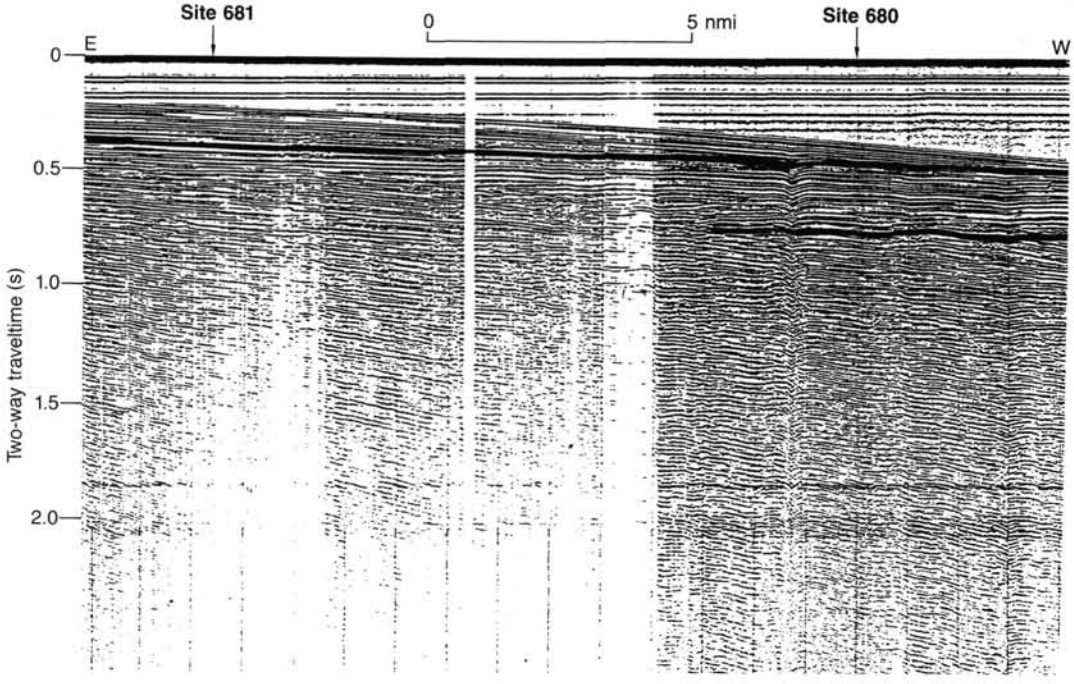

Figure 27. Single-channel seismic record (YALOC 74-03-20) showing location of Sites 680 and 681.

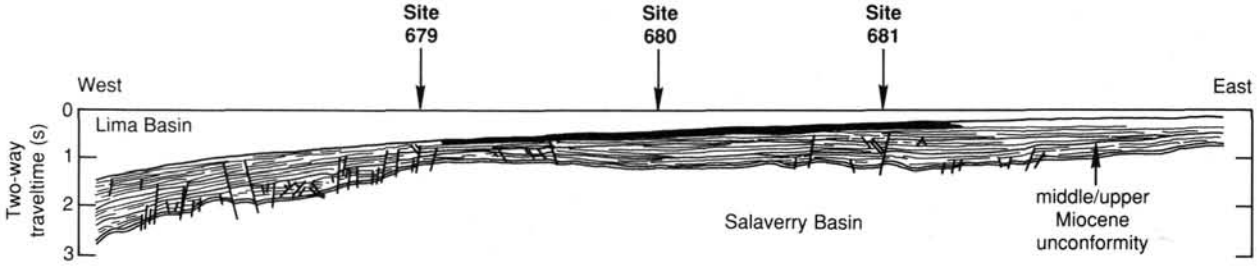

Figure 28. Line drawing of multichannel seismic record 2800 showing location of sites on the transect across the upwelling deposits. Upwelling deposits shown by solid area at the seafloor. The middle to upper Miocene unconformity is indicated. Vertical scale is in seconds, and the distance between sites is about 12 nmi (after Thornburg, 1985).

Table 14. Temperature data at Site 681.

Hole	Core	Depth (mbsf)	Temperature (°C)
112-681A	after 7H	63.5	(>18.3)
112-681A	after 11H	101.5	(>21.0)
112-681A	after 20X	187.0	>19.9
112-681B	5H	43.9	<15.0
112-681B	after 7H	62.9	>15.6
112-681B	after 14X	124.5	>16.8

organic-geochemistry, and physical-properties projects, which we had cut short at the previous site.

At Site 681, the sediment and its pore-water and dissolved-gas chemistries reveal extensive early diagenetic processes. Throughout the section, organic matter is mineralized by microbial sulfate reduction. Authigenic dolomite (found as rhombs, nodular and blocky zones, and as thinly bedded layers) is one product of diagenesis in the upwelling facies. Phosphorites are another product. Friable, yellowish, phosphatic material and dark, nodular phosphorites attest to *in-situ* formation and reworking as the principal mechanisms for concentrating carbonate fluorapatite at certain stratigraphic zones. Moreover, early diagenetic reactions are affected by highly saline pore fluids similar to those discovered at Site 680. The percentage of chloride and other dissolved major ions at the bottom of Hole 681B increased to concentrations of twice those of seawater. The distinctly higher rate of sedimentation of 80 m/m.y. at Site 681, as compared with 55 m/m.y. at Site 680, indicates complete microbial sulfate reduction at only 25 mbsf. Below this depth, a zone of methanogenesis develops between 25 and 85 mbsf. At deeper levels, methane formation again is inhibited by sulfate replenished from the subsurface brine. The dolomites forming in this lower zone of sulfate reduction should record a distinct "brine" signature in their stable isotopic composition.

The high magnesium content of the pore waters indicates that the brine is not generated by merely dissolving underlying evaporites. Such a process would increase dissolved sodium, chloride, calcium, and sulfate, but would not increase magnesium. On the other hand, residual brines from sabkhas or playas have high levels of magnesium along with the other ions. Therefore, the existence of fossil residual brines in the subsurface or the in-

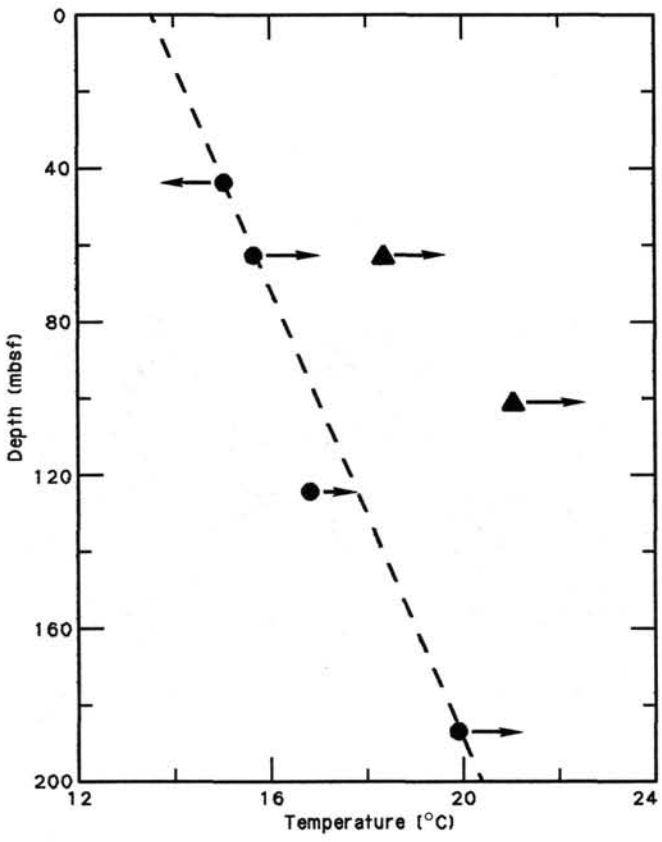

Figure 29. Temperature data plotted vs. depth below seafloor. At Site 681. Triangles indicate less reliable data. Arrows indicate that these values are the minimum or maximum estimates of the formation temperature. Broken line represents the minimum geothermal gradient.

flux of such brines from recent evaporite systems on land must be considered possible sources.

Preliminary shipboard studies of Site 681 sediments indicate deposition of a high-resolution Quaternary to late Pleistocene record of the Peru coastal upwelling regime. This oceanographic process is reflected in well-preserved and abundant diatom floras that occur in laminated muds alternating with bioturbated silty muds. Synchronous alternations in amount and type of organic matter appear similar in frequency to those of major glacial/interglacial cycles. The large amplitudes of Pleistocene sea-level fluctuations have not erased the upwelling record at Site 681 because tectonic subsidence during deposition apparently maintained the optimal water depth for its preservation.

REFERENCES

Bé, A.W.H., 1977. An ecological, zoogeographic and taxonomic review of Recent planktonic foraminifera. *In* Ramsay, A.T.S. (Ed.), *Oceanic Micropaleontol.*, 1:1-100.

Berggren, W. A., Aubry, M. P., and Hamilton, N., 1983. Neogene magnetobiostratigraphy of DSDP Site 516 (Rio Grande Rise, south Atlantic). *In* Barker, P., Johnson, D., et al., *Init. Repts. DSDP*, 72: Washington (U.S. Govt. Printing Office), 675-706.

Burckle, L. H., Hammond, S. R., Seyb, S. M., 1978. A stratigraphically important new diatom from the Pleistocene of the north Pacific. *Pacific Science,* 32:209-214.

Bullard, E. C., 1954. The flow of heat through the floor of the Atlantic Ocean. *Proc. Roy. Soc. London*, A222:408-429.

Claypool, G. E., and Kaplan, I. R., 1974. The origin and distribution of methane in marine sediments. *In* Kaplan, I. R. (Ed.), *Natural Gases in Marine Sediments*: New York (Plenum), 94-129.

DeVries, T., and Schrader, H., 1981. Variation of upwelling/oceanic conditions during the latest Pleistocene through Holocene off the central Peruvian coast: a diatom record. *Mar. Micropaleontol.*, 6: 157-167.

Garrison, R. E., Kastner, M., and Kolodny, Y., 1987. Phosphorites and phosphatic rocks in the Monterey Formation and related Miocene units, coastal California. *In* Ingersoll, R. V., and Ernst, W. G. (Eds.), *Cenozoic Basin Development in Coastal California*, Rubey volumes: Englewood Cliffs, NJ (Prentice Hall), 6:348-381.

Mayer, L., Thayer, F., Thomas, E., et al., 1985. Site 573, *Init. Repts. DSDP*, 85: Washington (U.S. Govt. Printing Office), 137-223.

Nials, F. L., Deeds, E. E., Moseley, M. E., Pozorski, S. G., Feldman, R. F., 1979. Catastrophic flooding of coastal Peru. *Field Museum of Natural History*, (Chicago), *Bull.* 50:4-14.

Poore, R. Z., 1978. Oligocene through Quaternary planktonic foraminiferal biostratigraphy of the north Atlantic: DSDP Leg 49. *In* Luyendyk, B. P., Cann, J. R., et al., *Init. Repts. DSDP*, 49: Washington (U.S. Govt. Printing Office), 447-517.

Saito, T., 1976. Geologic significance of coiling direction in the planktonic foraminifer "Pulleniatina." *Geology*, 4:305-309.

Schuette, G., and Schrader, H., 1979. Diatom taphocoenosis in the coastal upwelling area off western South America. *Nova Hedwigia, Beihefte,* 64:359-378.

Schuette, G., and Schrader, H., 1981. Diatoms in surface sediments: a reflection of coastal upwelling. *In* Richard, F. A. (Ed.), *Coastal upwelling*: Washington (Am. Geophys. Union), 372-380.

Shackleton, N. J., and Opdyke, N. D., 1977. Oxygen isotope and palaeomagnetic evidence for early Northern Hemisphere glaciation. *Nature*, 270:216-219.

Srinivasan, M. S., and Kennett, J. P., 1981. A review of Neogene planktonic foraminiferal biostratigraphy: Equatorial to subantarctic, South Pacific. *Mar. Micropaleontol.*, 6:499-534.

Thornburg, T. M., 1985. Seismic stratigraphy of Peru forearc basins. *In* Hussong, D. M., et al. (Eds.), *Atlas of the Ocean Margin Drilling Program, Peru Continental Margin, Region VI*: Woods Hole (Marine Science International).

Tissot, B. P., and Welte, D. H., 1984. *Petroleum Formation and Occurrence*: San Francisco (W. H. Freeman).

Ms 112A-112

SITE 681 HOLE A CORE 1H CORED INTERVAL 152.0-158.5 mbsl; 0-6.5 mbsf

TIME-ROCK UNIT	BIOSTRAT. ZONE/ FOSSIL CHARACTER: FORAMINIFERS	NANNOFOSSILS	RADIOLARIANS	DIATOMS	PALEOMAGNETICS	PHYS. PROPERTIES	CHEMISTRY	SECTION	METERS	GRAPHIC LITHOLOGY	DRILLING DISTURB.	SED. STRUCTURES	SAMPLES
QUATERNARY	* N 23	* insignificant	* insignificant	* *Pseudoeunotia doliolus* Zone		γ=1.29, φ=81.92		1, 2, 3, 4, 5, CC	0.5, 1.0			D	*

LITHOLOGIC DESCRIPTION

DIATOMACEOUS MUD

Major lithology: diatomaceous mud, dark olive gray to black (5Y 3/2, 5Y 2.5/2, 5Y 4/3). Laminated and homogeneous.

Minor lithologies:
1. diatom ooze, yellow brown (10YR 6/6), thin laminae.
2. silt and sand, gray (5Y 5/1), sharp-based and graded.
3. dolomite, olive (5Y 4/3), nodules.

SMEAR SLIDE SUMMARY (%):

	1, 28 D	2, 30 M	2, 110 M	4, 125 M
TEXTURE:				
Sand	—	10	90	—
Silt	60	60	10	35
Clay	40	30	—	65
COMPOSITION:				
Quartz	—	10	35	5
Feldspar	—	—	35	—
Rock fragments	—	—	20	5
Clay	43	30	—	65
Calcite/dolomite	—	—	Tr	—
Accessory minerals	—	—	Tr	Tr
Pyrite	—	Tr	Tr	—
Hornblende	—	—	10	—
Foraminifers	5	Tr	—	—
Nannofossils	2	—	—	5
Diatoms	50	30	—	20
Sponge spicules	Tr	—	—	—
Silicoflagellates	Tr	Tr	—	—
Phosphorite	—	30	—	—

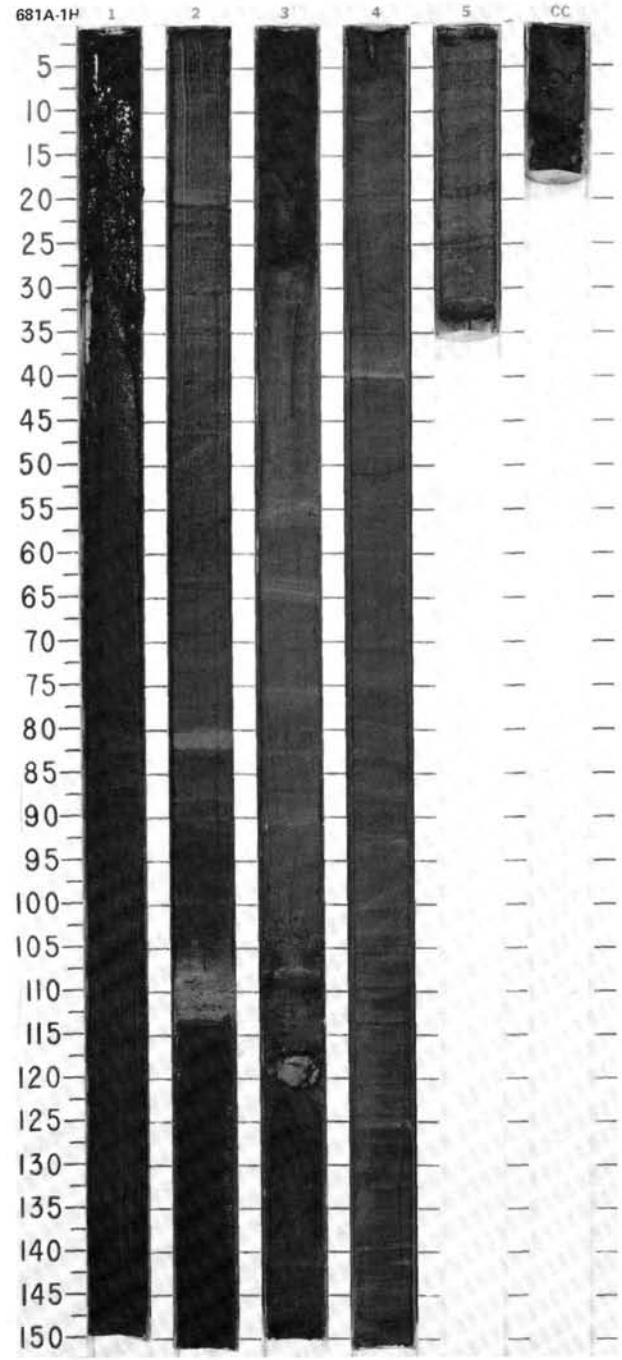

SITE 681 HOLE A CORE 2H CORED INTERVAL 158.5-168.0 mbsl; 6.5-16.0 mbsf

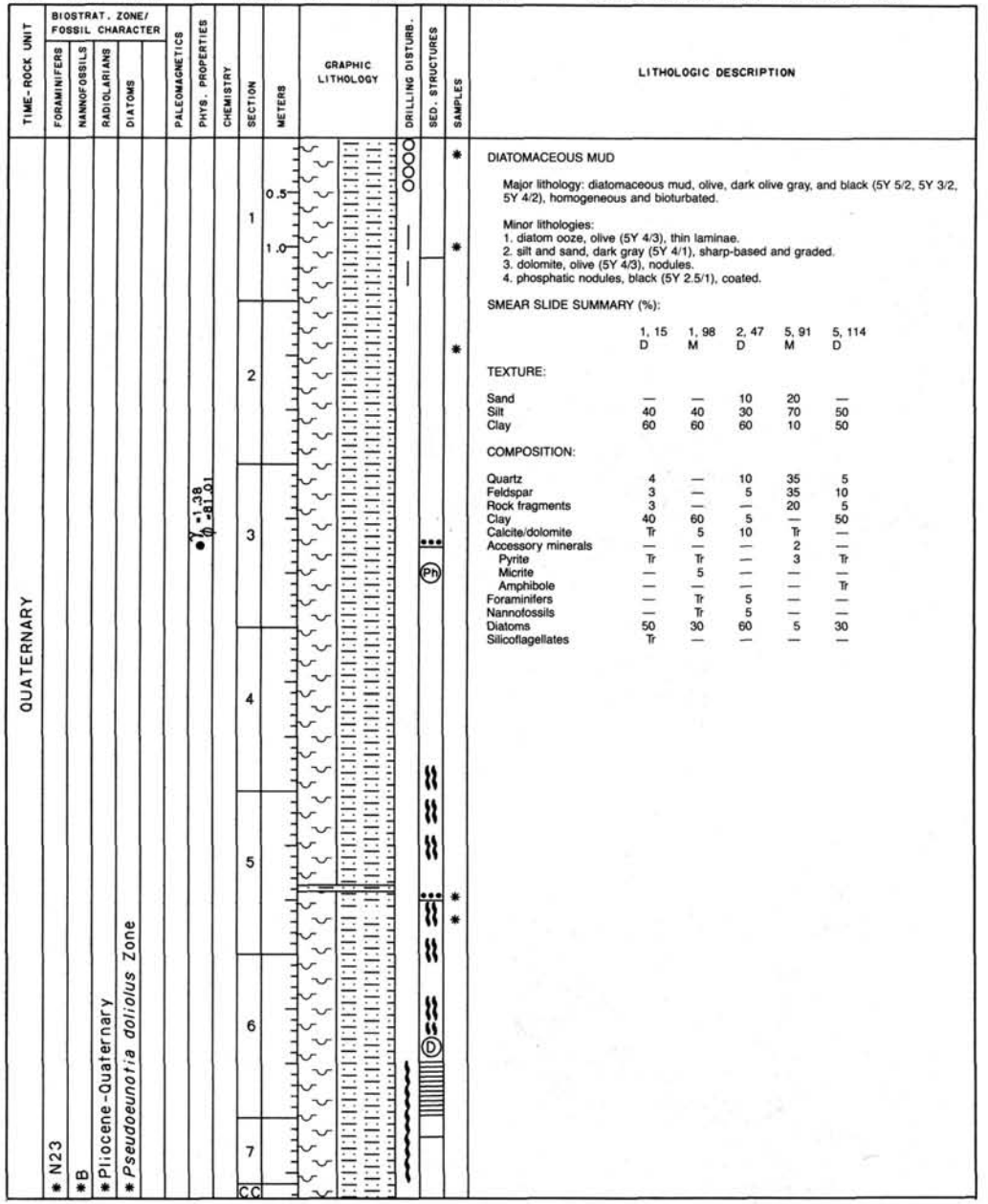

LITHOLOGIC DESCRIPTION

DIATOMACEOUS MUD

Major lithology: diatomaceous mud, olive, dark olive gray, and black (5Y 5/2, 5Y 3/2, 5Y 4/2), homogeneous and bioturbated.

Minor lithologies:
1. diatom ooze, olive (5Y 4/3), thin laminae.
2. silt and sand, dark gray (5Y 4/1), sharp-based and graded.
3. dolomite, olive (5Y 4/3), nodules.
4. phosphatic nodules, black (5Y 2.5/1), coated.

SMEAR SLIDE SUMMARY (%):

	1, 15 D	1, 98 M	2, 47 D	5, 91 M	5, 114 D
TEXTURE:					
Sand	—	—	10	20	—
Silt	40	40	30	70	50
Clay	60	60	60	10	50
COMPOSITION:					
Quartz	4	—	10	35	5
Feldspar	3	—	5	35	10
Rock fragments	3	—	—	20	5
Clay	40	60	5	—	50
Calcite/dolomite	Tr	5	10	Tr	—
Accessory minerals	—	—	—	2	—
Pyrite	Tr	Tr	—	3	Tr
Micrite	—	5	—	—	—
Amphibole	—	—	—	—	Tr
Foraminifers	—	Tr	5	—	—
Nannofossils	—	Tr	5	—	—
Diatoms	50	30	60	5	30
Silicoflagellates	Tr	—	—	—	—

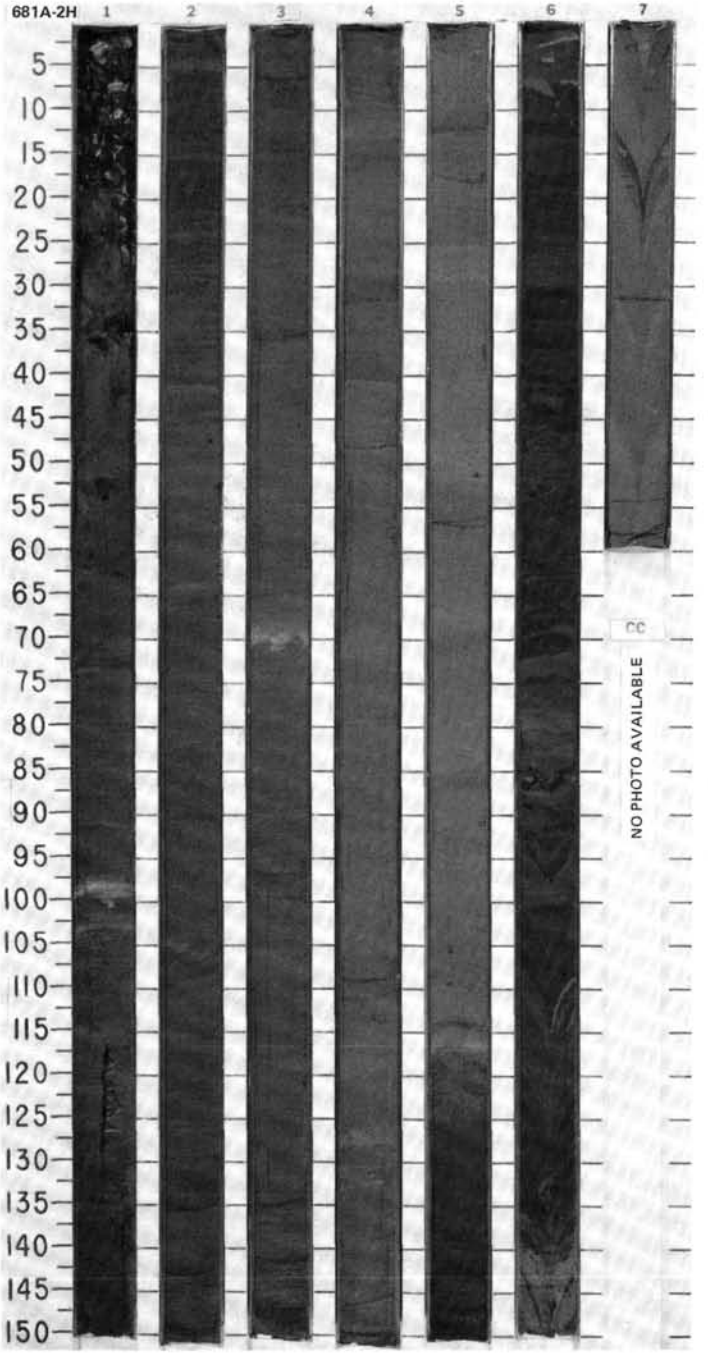

SITE 681 HOLE A CORE 3H CORED INTERVAL 168.0-177.5 mbsl; 16.0-25.5 mbsf

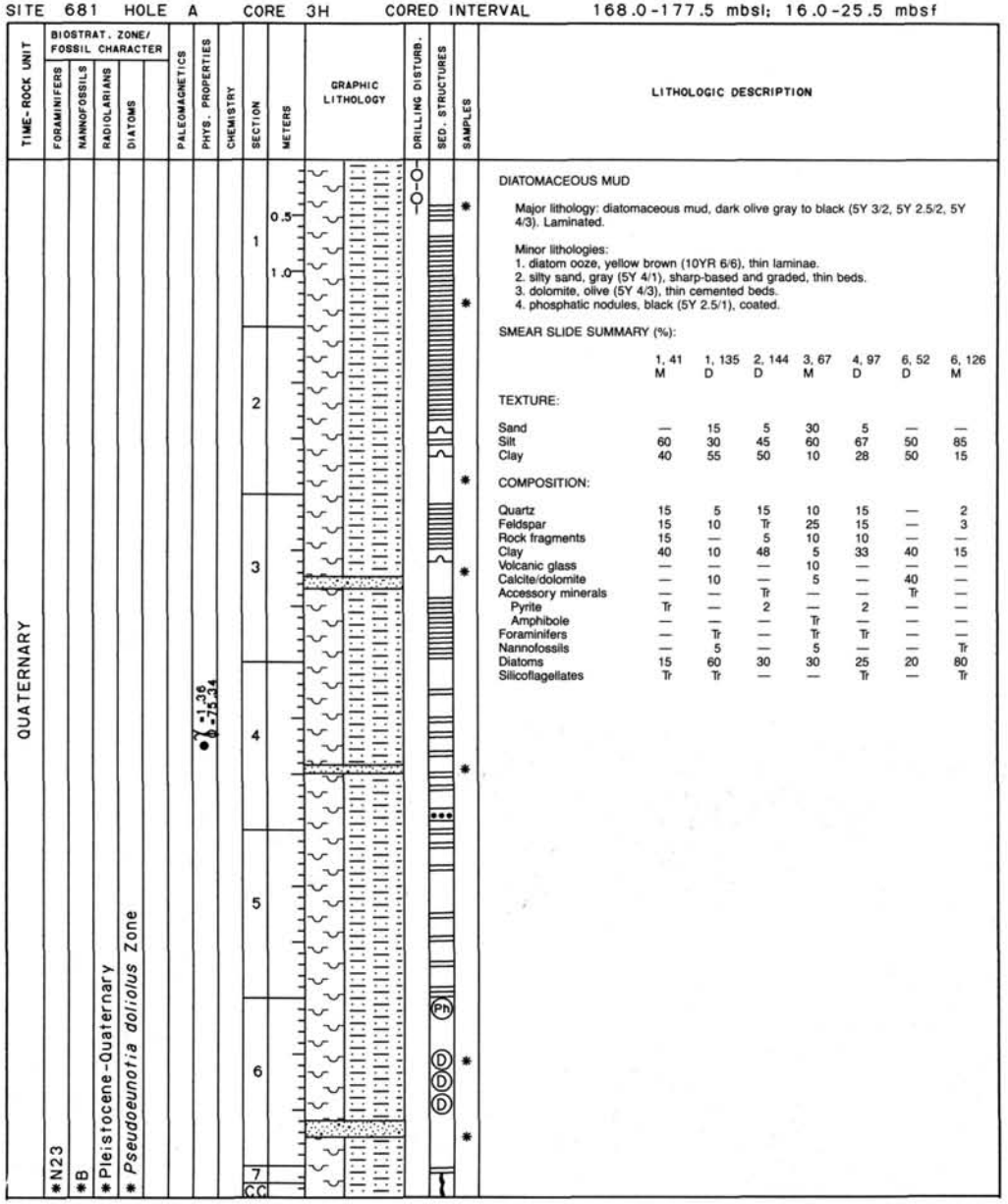

LITHOLOGIC DESCRIPTION

DIATOMACEOUS MUD

Major lithology: diatomaceous mud, dark olive gray to black (5Y 3/2, 5Y 2.5/2, 5Y 4/3). Laminated.

Minor lithologies:
1. diatom ooze, yellow brown (10YR 6/6), thin laminae.
2. silty sand, gray (5Y 4/1), sharp-based and graded, thin beds.
3. dolomite, olive (5Y 4/3), thin cemented beds.
4. phosphatic nodules, black (5Y 2.5/1), coated.

SMEAR SLIDE SUMMARY (%):

	1, 41 M	1, 135 D	2, 144 D	3, 67 M	4, 97 D	6, 52 D	6, 126 M
TEXTURE:							
Sand	—	15	5	30	5	—	—
Silt	60	30	45	60	67	50	85
Clay	40	55	50	10	28	50	15
COMPOSITION:							
Quartz	15	5	15	10	15	—	2
Feldspar	15	10	Tr	25	15	—	3
Rock fragments	15	—	5	10	10	—	—
Clay	40	10	48	5	33	40	15
Volcanic glass	—	—	—	10	—	—	—
Calcite/dolomite	—	10	—	5	—	40	—
Accessory minerals	—	—	Tr	—	—	Tr	—
Pyrite	Tr	—	2	—	2	—	—
Amphibole	—	—	—	Tr	—	—	—
Foraminifers	—	Tr	—	Tr	Tr	—	—
Nannofossils	—	5	—	5	—	—	Tr
Diatoms	15	60	30	30	25	20	80
Silicoflagellates	Tr	Tr	—	—	Tr	—	Tr

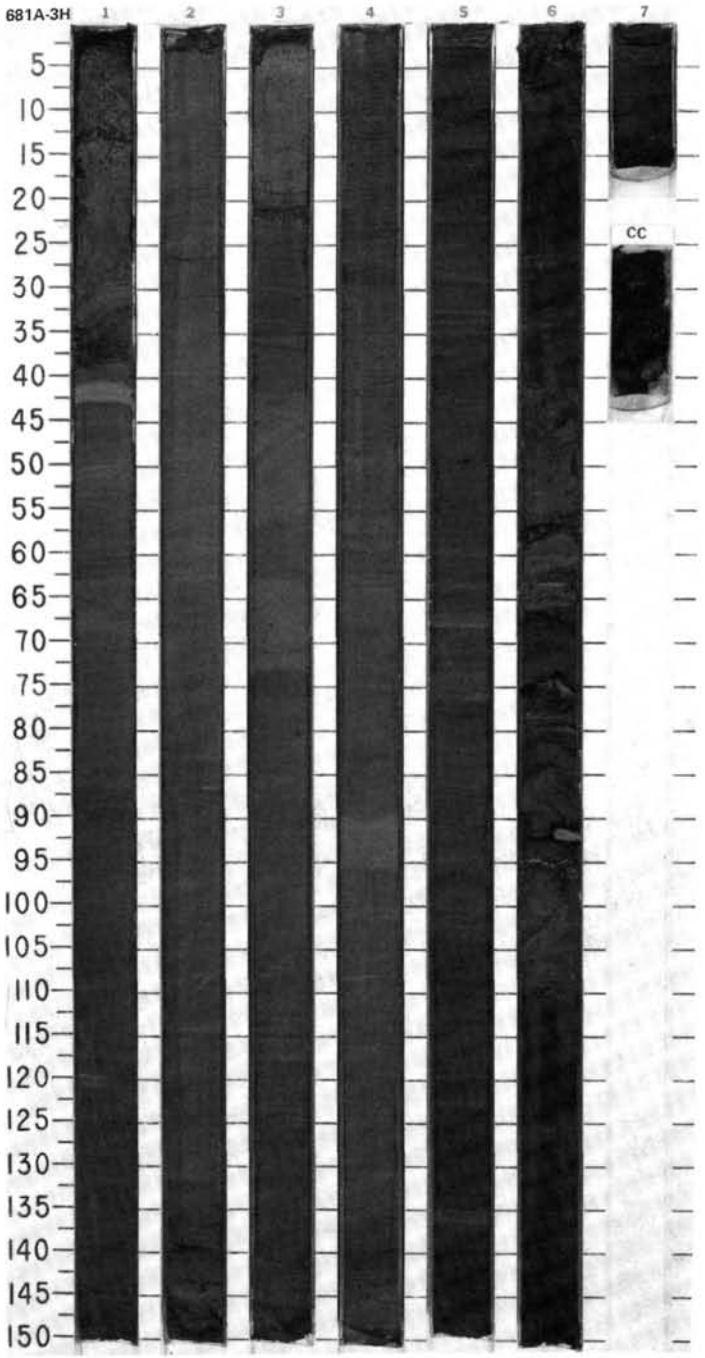

SITE 681 HOLE A CORE 4H CORED INTERVAL 177.5-187.0 mbsl; 25.5-35.0 mbsf

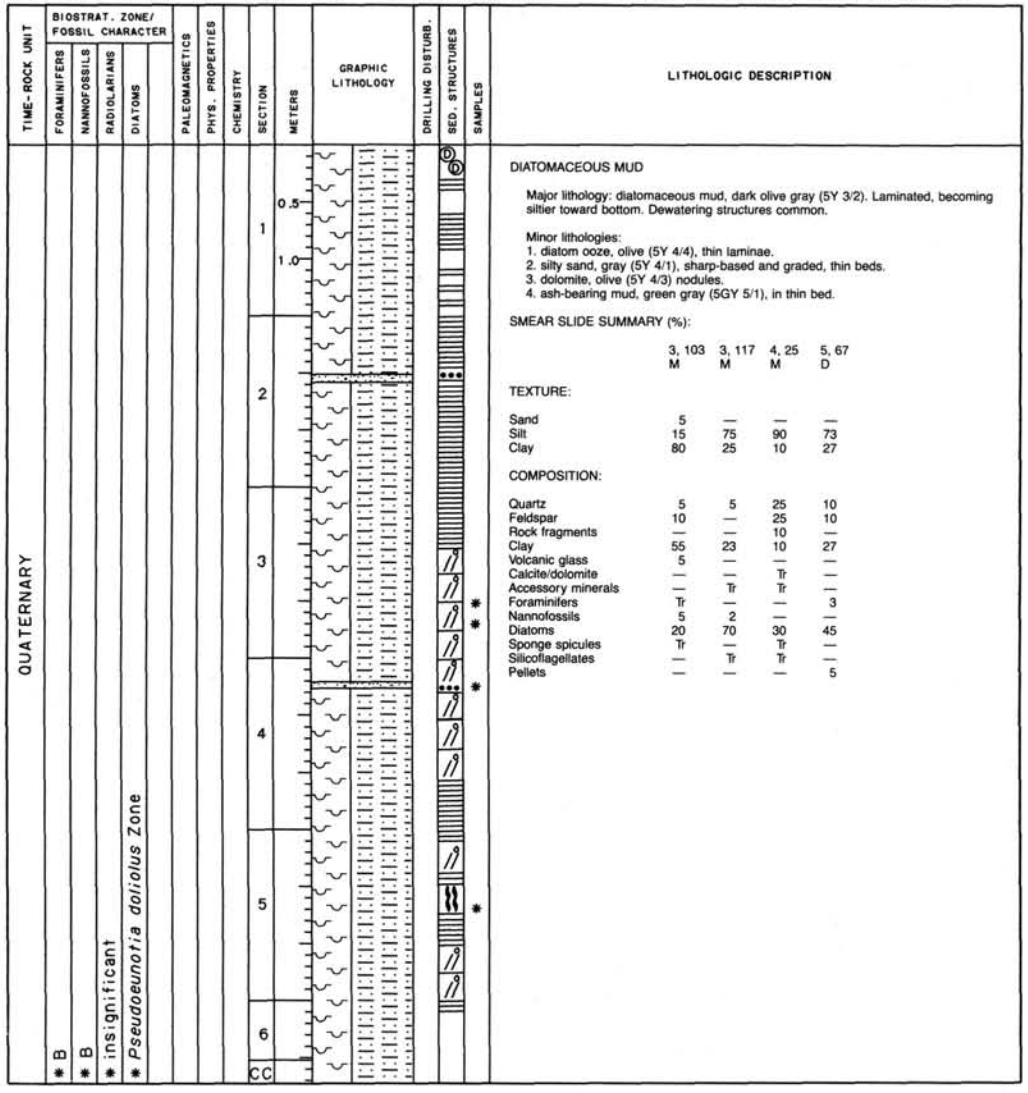

LITHOLOGIC DESCRIPTION

DIATOMACEOUS MUD

Major lithology: diatomaceous mud, dark olive gray (5Y 3/2). Laminated, becoming siltier toward bottom. Dewatering structures common.

Minor lithologies:
1. diatom ooze, olive (5Y 4/4), thin laminae.
2. silty sand, gray (5Y 4/1), sharp-based and graded, thin beds.
3. dolomite, olive (5Y 4/3) nodules.
4. ash-bearing mud, green gray (5GY 5/1), in thin bed.

SMEAR SLIDE SUMMARY (%):

	3, 103 M	3, 117 M	4, 25 M	5, 67 D
TEXTURE:				
Sand	5	—	—	—
Silt	15	75	90	73
Clay	80	25	10	27
COMPOSITION:				
Quartz	5	5	25	10
Feldspar	10	—	25	10
Rock fragments	—	—	10	—
Clay	55	23	10	27
Volcanic glass	5	—	—	—
Calcite/dolomite	—	—	Tr	—
Accessory minerals	—	Tr	Tr	—
Foraminifers	Tr	—	—	3
Nannofossils	5	2	—	—
Diatoms	20	70	30	45
Sponge spicules	Tr	—	Tr	—
Silicoflagellates	—	Tr	Tr	—
Pellets	—	—	—	5

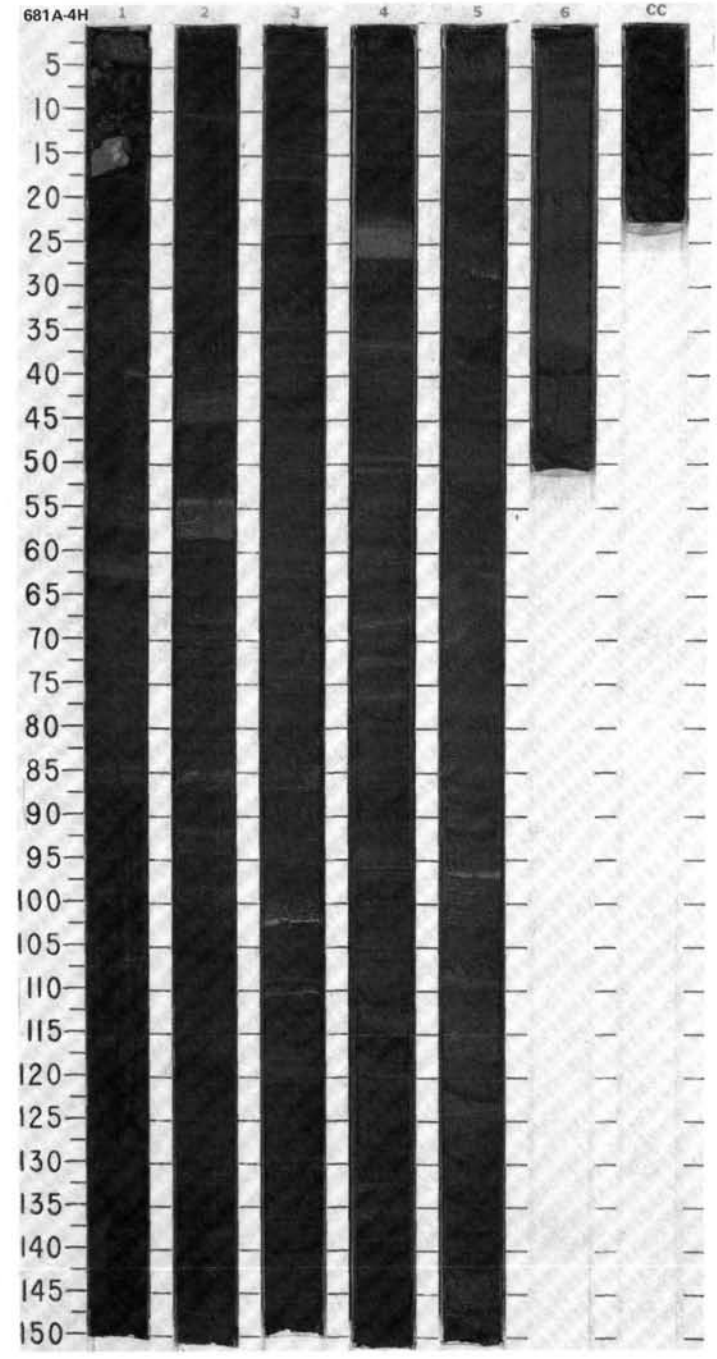

SITE 681 HOLE A CORE 5H CORED INTERVAL 187.0-196.5 mbsl; 35.0-44.5 mbsf

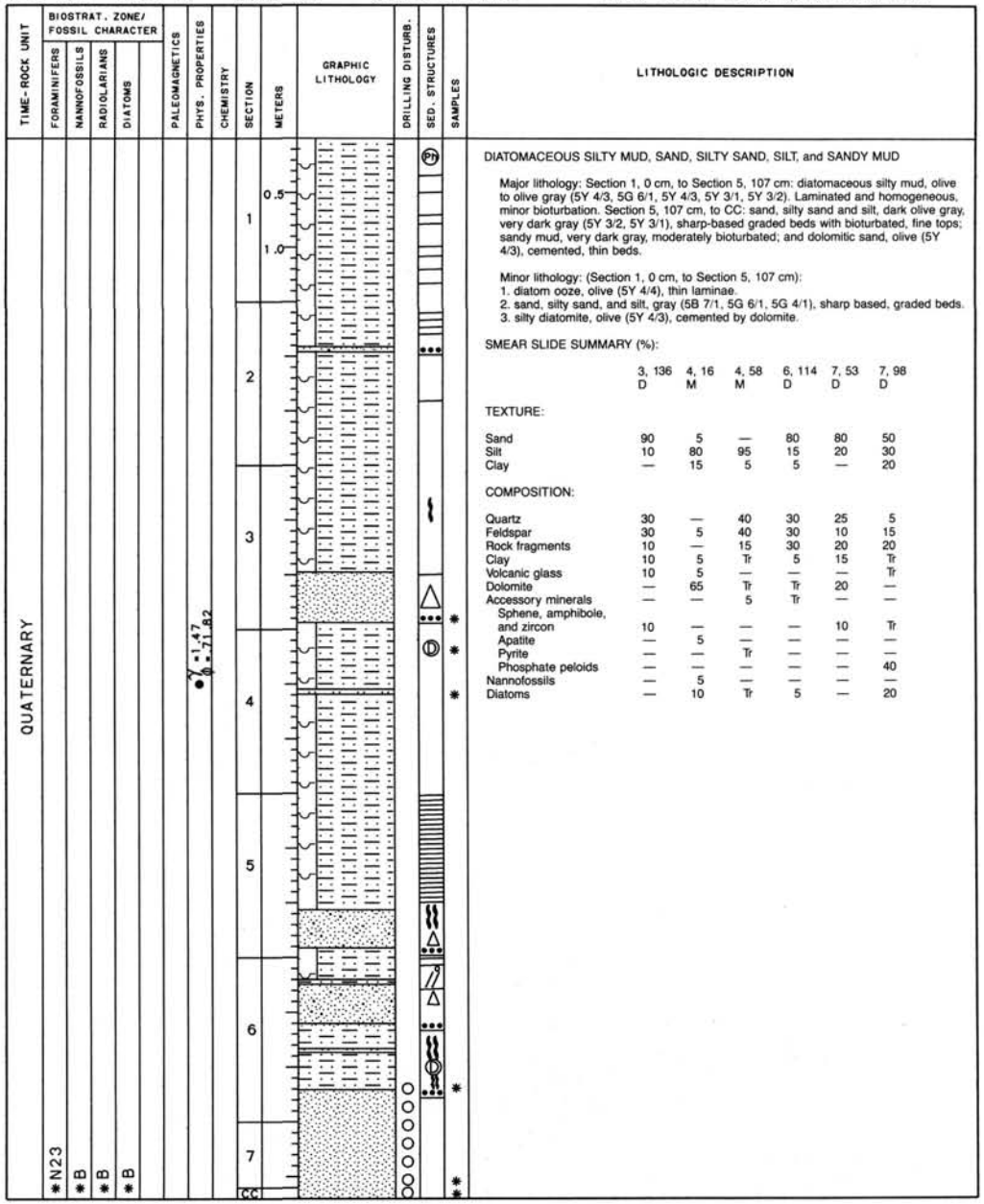

LITHOLOGIC DESCRIPTION

DIATOMACEOUS SILTY MUD, SAND, SILTY SAND, SILT, and SANDY MUD

Major lithology: Section 1, 0 cm, to Section 5, 107 cm: diatomaceous silty mud, olive to olive gray (5Y 4/3, 5G 6/1, 5Y 4/3, 5Y 3/1, 5Y 3/2). Laminated and homogeneous, minor bioturbation. Section 5, 107 cm, to CC: sand, silty sand and silt, dark olive gray, very dark gray (5Y 3/2, 5Y 3/1), sharp-based graded beds with bioturbated, fine tops; sandy mud, very dark gray, moderately bioturbated; and dolomitic sand, olive (5Y 4/3), cemented, thin beds.

Minor lithology: (Section 1, 0 cm, to Section 5, 107 cm):
1. diatom ooze, olive (5Y 4/4), thin laminae.
2. sand, silty sand, and silt, gray (5B 7/1, 5G 6/1, 5G 4/1), sharp based, graded beds.
3. silty diatomite, olive (5Y 4/3), cemented by dolomite.

SMEAR SLIDE SUMMARY (%):

	3, 136 D	4, 16 M	4, 58 M	6, 114 D	7, 53 D	7, 98 D
TEXTURE:						
Sand	90	5	—	80	80	50
Silt	10	80	95	15	20	30
Clay	—	15	5	5	—	20
COMPOSITION:						
Quartz	30	—	40	30	25	5
Feldspar	30	5	40	30	10	15
Rock fragments	10	—	15	30	20	20
Clay	10	5	Tr	5	15	Tr
Volcanic glass	10	5	—	—	—	Tr
Dolomite	—	65	Tr	Tr	20	—
Accessory minerals	—	—	5	Tr	—	—
Sphene, amphibole, and zircon	10	—	—	—	10	Tr
Apatite	—	5	—	—	—	—
Pyrite	—	—	Tr	—	—	—
Phosphate peloids	—	—	—	—	—	40
Nannofossils	—	5	—	—	—	—
Diatoms	—	10	Tr	5	—	20

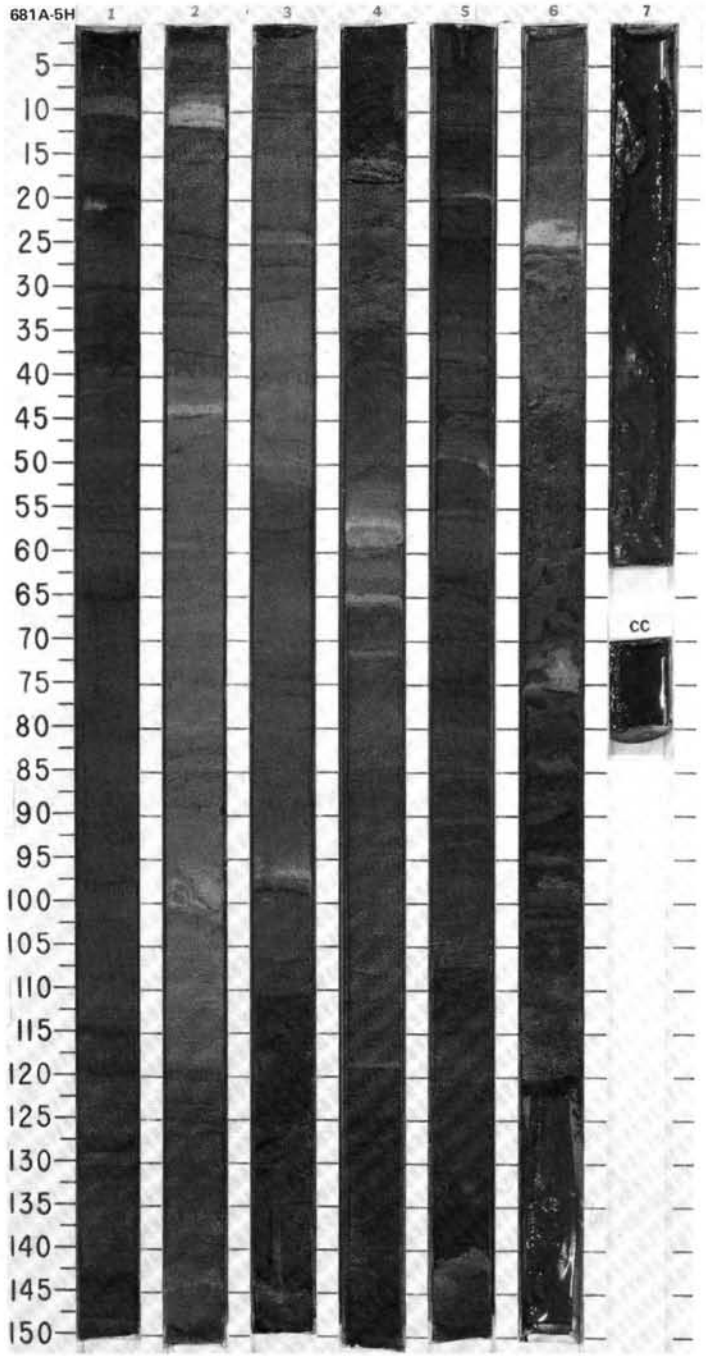

SITE 681 HOLE A CORE 6H CORED INTERVAL 196.5-206.0 mbsl; 44.5-54.0 mbsf

TIME-ROCK UNIT	BIOSTRAT. ZONE/ FOSSIL CHARACTER: FORAMINIFERS	NANNOFOSSILS	RADIOLARIANS	DIATOMS	PALEOMAGNETICS	PHYS. PROPERTIES	CHEMISTRY	SECTION	METERS	GRAPHIC LITHOLOGY	DRILLING DISTURB.	SED. STRUCTURES	SAMPLES	LITHOLOGIC DESCRIPTION
QUATERNARY	N22 *	B *	? (non diagnostic) *					CC					*	PHOSPHATIC MUDDY SAND

Major lithology: phosphatic muddy sand, black (5Y 3/1).

SMEAR SLIDE SUMMARY (%):

	CC, 5 D
TEXTURE:	
Sand	55
Silt	25
Clay	20
COMPOSITION:	
Quartz	5
Feldspar	20
Rock fragments	25
Clay	5
Volcanic glass	Tr
Dolomite	Tr
Accessory minerals	
Phosphate peloids	30
Hornblende	Tr
Diatoms	15

681A-6H CC

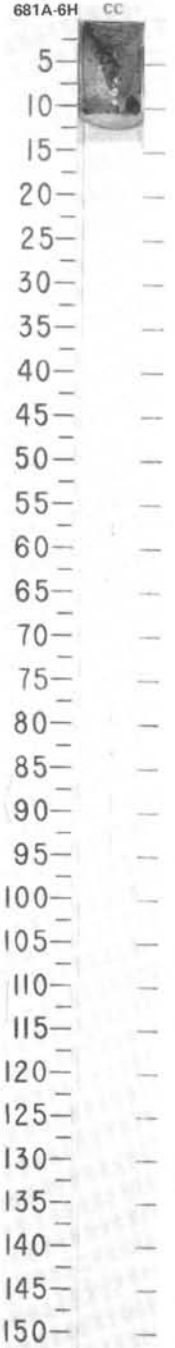

SITE 681 HOLE A CORE 7H CORED INTERVAL 206.0-215.5 mbsl; 54.0-63.5 mbsf

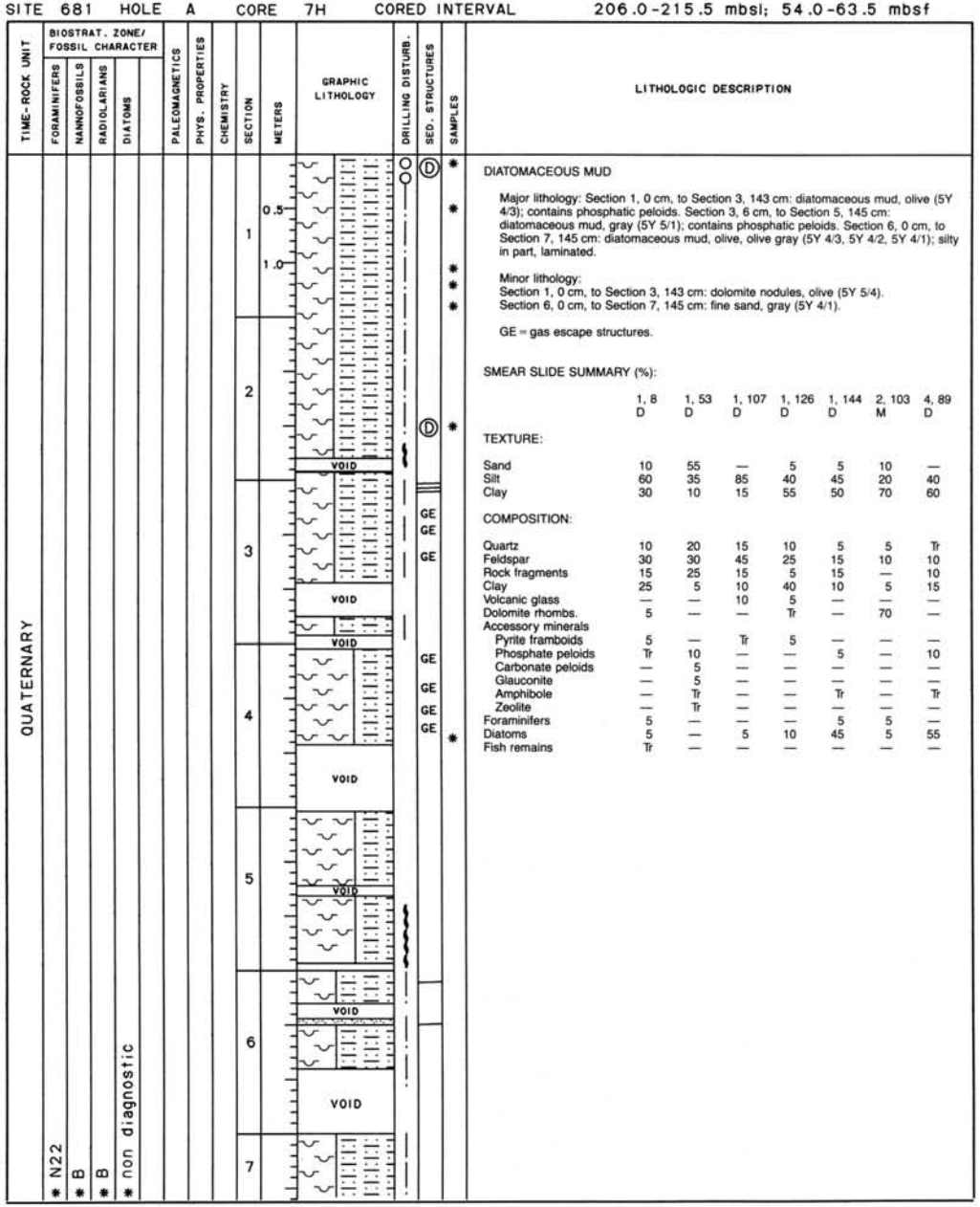

LITHOLOGIC DESCRIPTION

DIATOMACEOUS MUD

Major lithology: Section 1, 0 cm, to Section 3, 143 cm: diatomaceous mud, olive (5Y 4/3); contains phosphatic peloids. Section 3, 6 cm, to Section 5, 145 cm: diatomaceous mud, gray (5Y 5/1); contains phosphatic peloids. Section 6, 0 cm, to Section 7, 145 cm: diatomaceous mud, olive, olive gray (5Y 4/3, 5Y 4/2, 5Y 4/1); silty in part, laminated.

Minor lithology:
Section 1, 0 cm, to Section 3, 143 cm: dolomite nodules, olive (5Y 5/4).
Section 6, 0 cm, to Section 7, 145 cm: fine sand, gray (5Y 4/1).

GE = gas escape structures.

SMEAR SLIDE SUMMARY (%):

	1, 8 D	1, 53 D	1, 107 D	1, 126 D	1, 144 D	2, 103 M	4, 89 D
TEXTURE:							
Sand	10	55	—	5	5	10	—
Silt	60	35	85	40	45	20	40
Clay	30	10	15	55	50	70	60
COMPOSITION:							
Quartz	10	20	15	10	5	5	Tr
Feldspar	30	30	45	25	15	10	10
Rock fragments	15	25	15	5	15	—	10
Clay	25	5	10	40	10	5	15
Volcanic glass	—	—	10	5	—	—	—
Dolomite rhombs.	5	—	—	Tr	—	70	—
Accessory minerals							
Pyrite framboids	5	—	Tr	5	—	—	—
Phosphate peloids	Tr	10	—	—	5	—	10
Carbonate peloids	—	5	—	—	—	—	—
Glauconite	—	5	—	—	—	—	—
Amphibole	—	Tr	—	—	Tr	—	Tr
Zeolite	—	Tr	—	—	—	—	—
Foraminifers	5	—	—	—	5	5	—
Diatoms	5	—	5	10	45	5	55
Fish remains	Tr	—	—	—	—	—	—

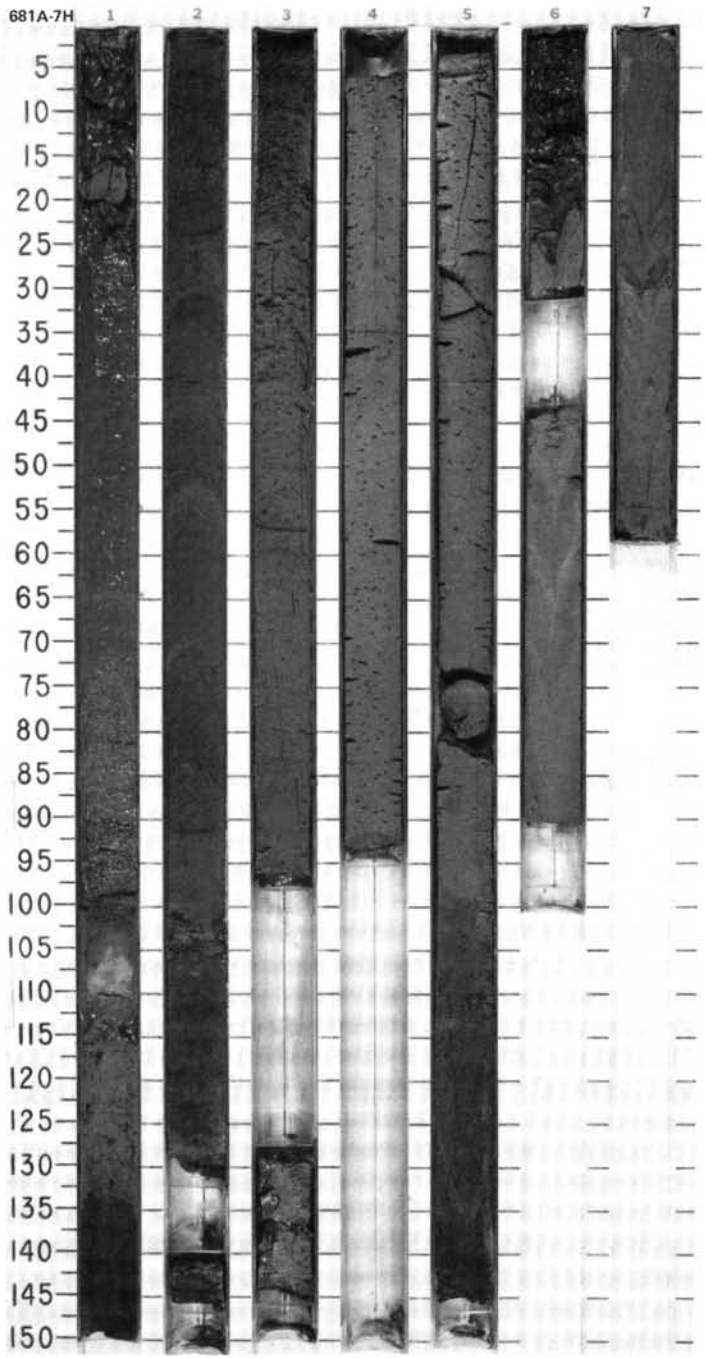

SITE 681 HOLE A CORE 8H CORED INTERVAL 215.5-225.0 mbsl; 63.5-73.0 mbsf

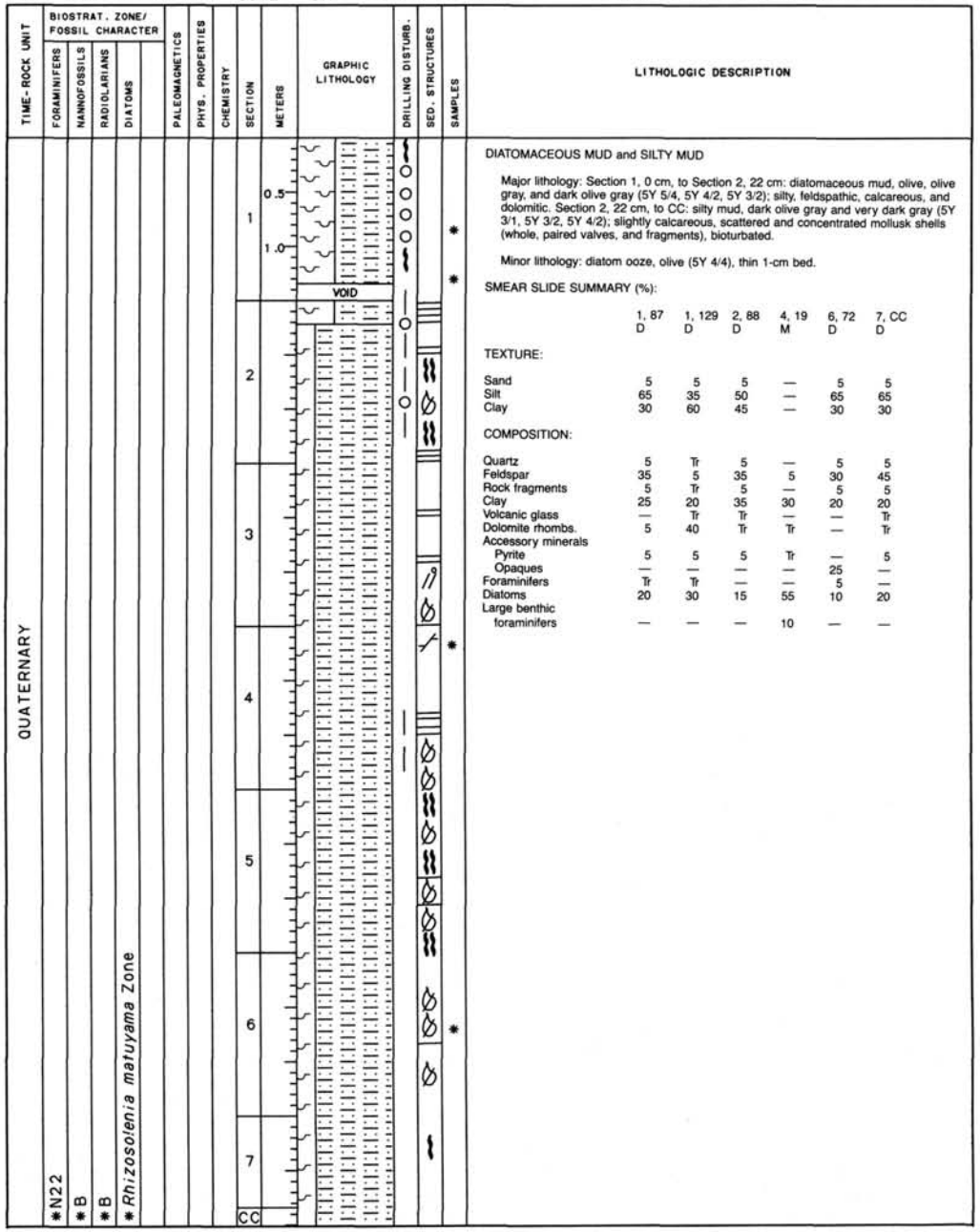

LITHOLOGIC DESCRIPTION

DIATOMACEOUS MUD and SILTY MUD

Major lithology: Section 1, 0 cm, to Section 2, 22 cm: diatomaceous mud, olive, olive gray, and dark olive gray (5Y 5/4, 5Y 4/2, 5Y 3/2); silty, feldspathic, calcareous, and dolomitic. Section 2, 22 cm, to CC: silty mud, dark olive gray and very dark gray (5Y 3/1, 5Y 3/2, 5Y 4/2); slightly calcareous, scattered and concentrated mollusk shells (whole, paired valves, and fragments), bioturbated.

Minor lithology: diatom ooze, olive (5Y 4/4), thin 1-cm bed.

SMEAR SLIDE SUMMARY (%):

	1, 87 D	1, 129 D	2, 88 D	4, 19 M	6, 72 D	7, CC D
TEXTURE:						
Sand	5	5	5	—	5	5
Silt	65	35	50	—	65	65
Clay	30	60	45	—	30	30
COMPOSITION:						
Quartz	5	Tr	5	—	5	5
Feldspar	35	5	35	5	30	45
Rock fragments	5	Tr	5	—	5	5
Clay	25	20	35	30	20	20
Volcanic glass	—	Tr	Tr	—	—	Tr
Dolomite rhombs.	5	40	Tr	Tr	—	Tr
Accessory minerals						
Pyrite	5	5	5	Tr	—	5
Opaques	—	—	—	—	25	—
Foraminifers	Tr	Tr	—	—	5	—
Diatoms	20	30	15	55	10	20
Large benthic foraminifers	—	—	—	10	—	—

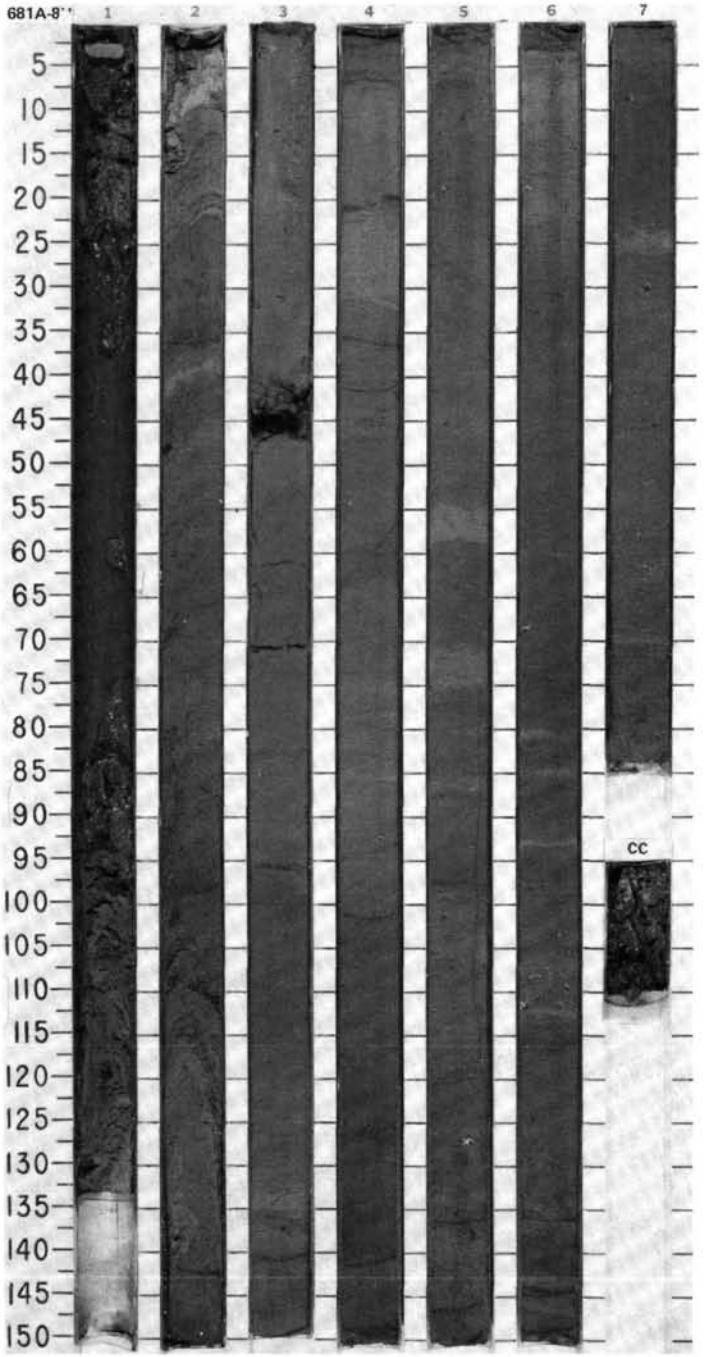

SITE 681 HOLE A CORE 9H CORED INTERVAL 225.0-234.5 mbsl; 73.0-82.5 mbsf

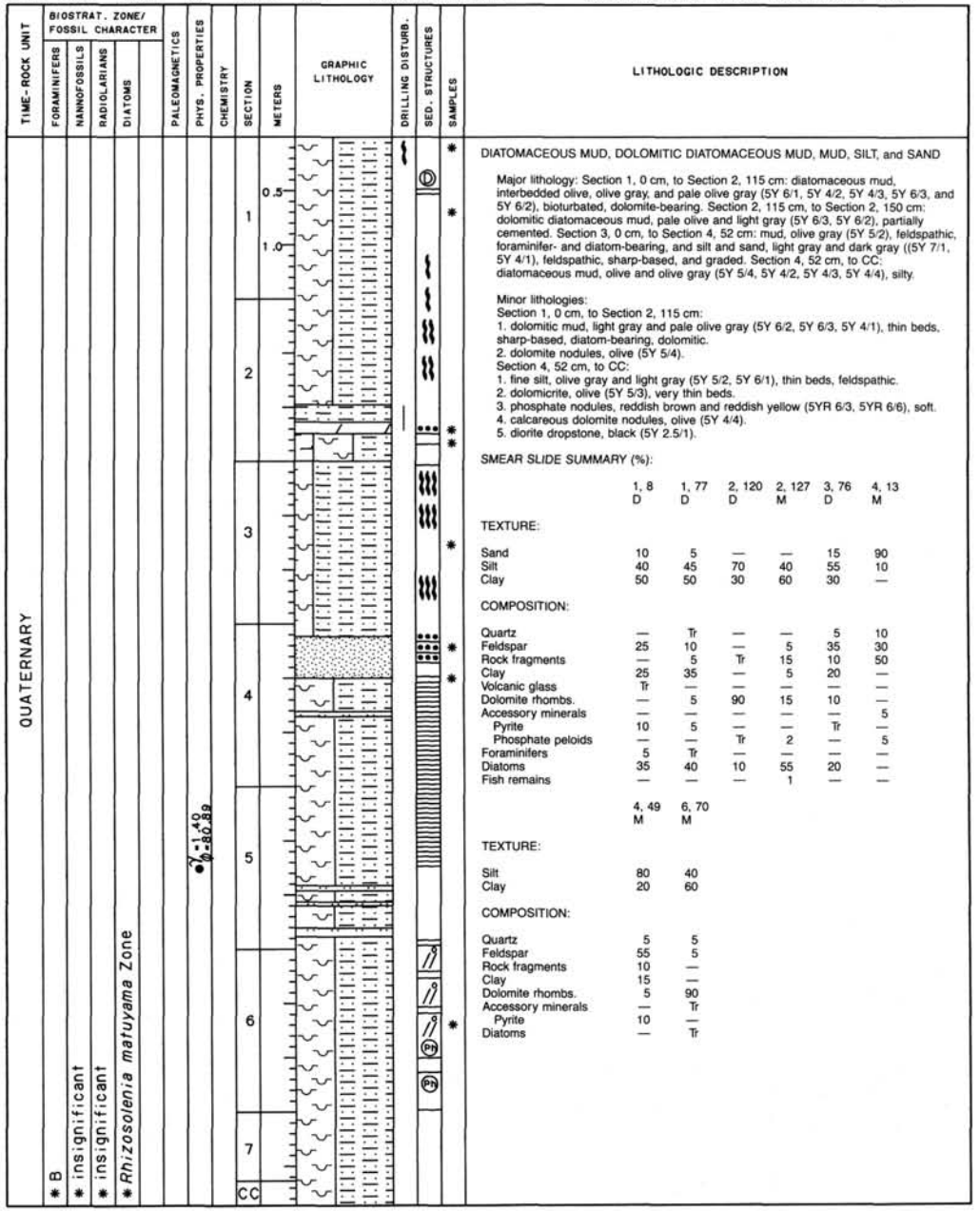

LITHOLOGIC DESCRIPTION

DIATOMACEOUS MUD, DOLOMITIC DIATOMACEOUS MUD, MUD, SILT, and SAND

Major lithology: Section 1, 0 cm, to Section 2, 115 cm: diatomaceous mud, interbedded olive, olive gray, and pale olive gray (5Y 6/1, 5Y 4/2, 5Y 4/3, 5Y 6/3, and 5Y 6/2), bioturbated, dolomite-bearing. Section 2, 115 cm, to Section 2, 150 cm: dolomitic diatomaceous mud, pale olive and light gray (5Y 6/3, 5Y 6/2), partially cemented. Section 3, 0 cm, to Section 4, 52 cm: mud, olive gray (5Y 5/2), feldspathic, foraminifer- and diatom-bearing, and silt and sand, light gray and dark gray ((5Y 7/1, 5Y 4/1), feldspathic, sharp-based, and graded. Section 4, 52 cm, to CC: diatomaceous mud, olive and olive gray (5Y 5/4, 5Y 4/2, 5Y 4/3, 5Y 4/4), silty.

Minor lithologies:
Section 1, 0 cm, to Section 2, 115 cm:
1. dolomitic mud, light gray and pale olive gray (5Y 6/2, 5Y 6/3, 5Y 4/1), thin beds, sharp-based, diatom-bearing, dolomitic.
2. dolomite nodules, olive (5Y 5/4).
Section 4, 52 cm, to CC:
1. fine silt, olive gray and light gray (5Y 5/2, 5Y 6/1), thin beds, feldspathic.
2. dolomicrite, olive (5Y 5/3), very thin beds.
3. phosphate nodules, reddish brown and reddish yellow (5YR 6/3, 5YR 6/6), soft.
4. calcareous dolomite nodules, olive (5Y 4/4).
5. diorite dropstone, black (5Y 2.5/1).

SMEAR SLIDE SUMMARY (%):

	1, 8 D	1, 77 D	2, 120 D	2, 127 M	3, 76 D	4, 13 M
TEXTURE:						
Sand	10	5	—	—	15	90
Silt	40	45	70	40	55	10
Clay	50	50	30	60	30	—
COMPOSITION:						
Quartz	—	Tr	—	—	5	10
Feldspar	25	10	—	5	35	30
Rock fragments	—	5	Tr	15	10	50
Clay	25	35	—	5	20	—
Volcanic glass	Tr	—	—	—	—	—
Dolomite rhombs.	—	5	90	15	10	—
Accessory minerals	—	—	—	—	—	5
Pyrite	10	5	—	—	Tr	—
Phosphate peloids	—	—	Tr	2	—	5
Foraminifers	5	Tr	—	—	—	—
Diatoms	35	40	10	55	20	—
Fish remains	—	—	—	1	—	—

	4, 49 M	6, 70 M
TEXTURE:		
Silt	80	40
Clay	20	60
COMPOSITION:		
Quartz	5	5
Feldspar	55	5
Rock fragments	10	—
Clay	15	—
Dolomite rhombs.	5	90
Accessory minerals	—	Tr
Pyrite	10	—
Diatoms	—	Tr

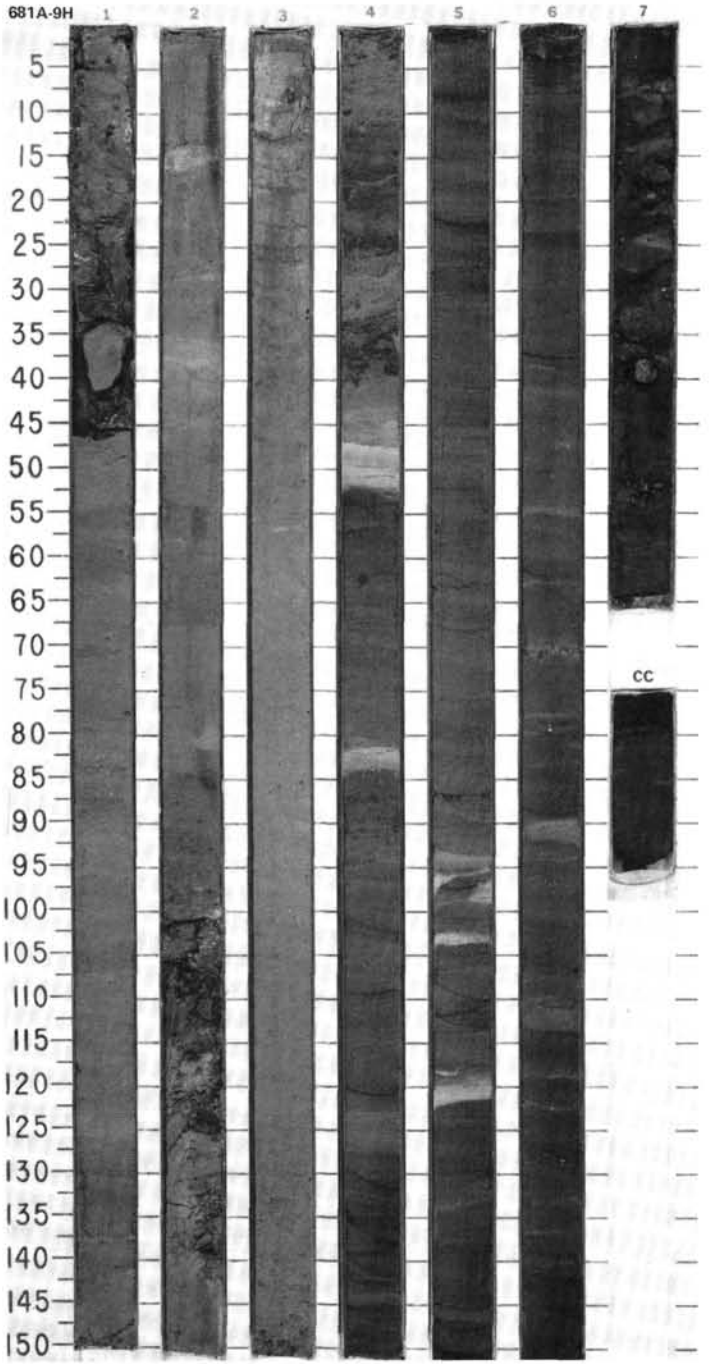

SITE 681 HOLE A CORE 10H CORED INTERVAL 234.5-244.0 mbsl; 82.5-92.0 mbsf

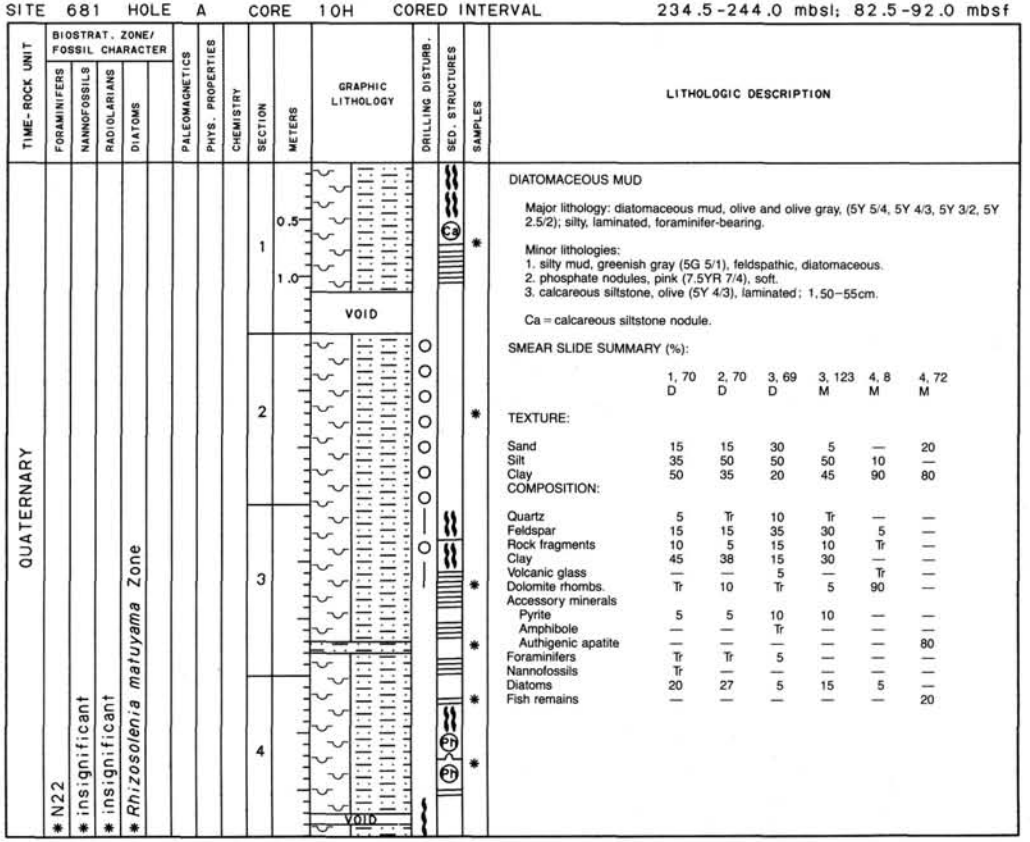

LITHOLOGIC DESCRIPTION

DIATOMACEOUS MUD

Major lithology: diatomaceous mud, olive and olive gray, (5Y 5/4, 5Y 4/3, 5Y 3/2, 5Y 2.5/2); silty, laminated, foraminifer-bearing.

Minor lithologies:
1. silty mud, greenish gray (5G 5/1), feldspathic, diatomaceous.
2. phosphate nodules, pink (7.5YR 7/4), soft.
3. calcareous siltstone, olive (5Y 4/3), laminated; 1,50–55cm.

Ca = calcareous siltstone nodule.

SMEAR SLIDE SUMMARY (%):

	1, 70 D	2, 70 D	3, 69 D	3, 123 M	4, 8 M	4, 72 M
TEXTURE:						
Sand	15	15	30	5	—	20
Silt	35	50	50	50	10	—
Clay	50	35	20	45	90	80
COMPOSITION:						
Quartz	5	Tr	10	Tr	—	—
Feldspar	15	15	35	30	5	—
Rock fragments	10	5	15	10	Tr	—
Clay	45	38	15	30	—	—
Volcanic glass	—	—	5	—	Tr	—
Dolomite rhombs.	Tr	10	Tr	5	90	—
Accessory minerals						
Pyrite	5	5	10	10	—	—
Amphibole	—	—	Tr	—	—	—
Authigenic apatite	—	—	—	—	—	80
Foraminifers	Tr	Tr	5	—	—	—
Nannofossils	Tr	—	—	—	—	—
Diatoms	20	27	5	15	5	—
Fish remains	—	—	—	—	—	20

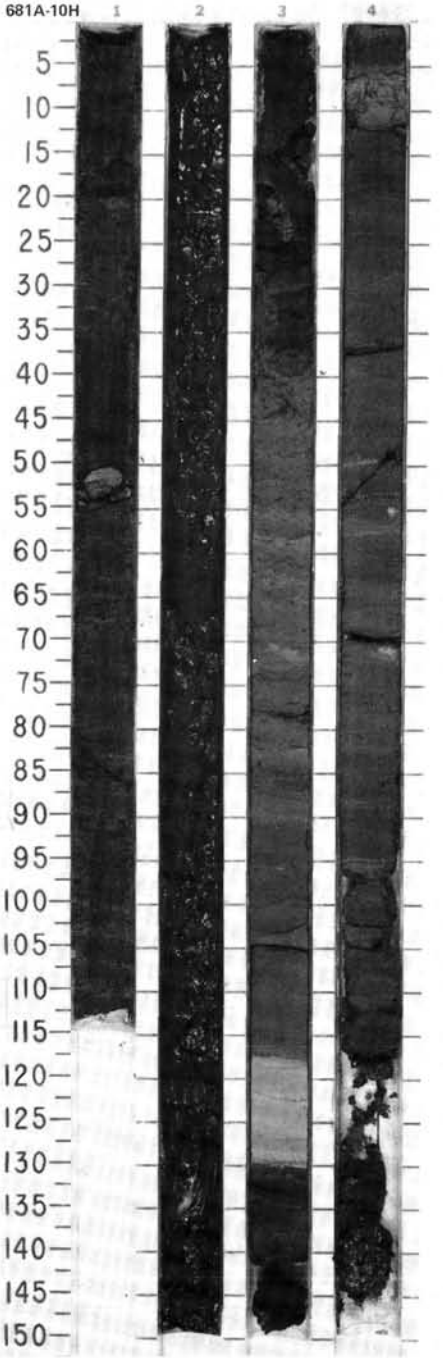

SITE 681 HOLE A CORE 11H CORED INTERVAL 244.0-253.5 mbsl; 92.0-101.5 mbsf

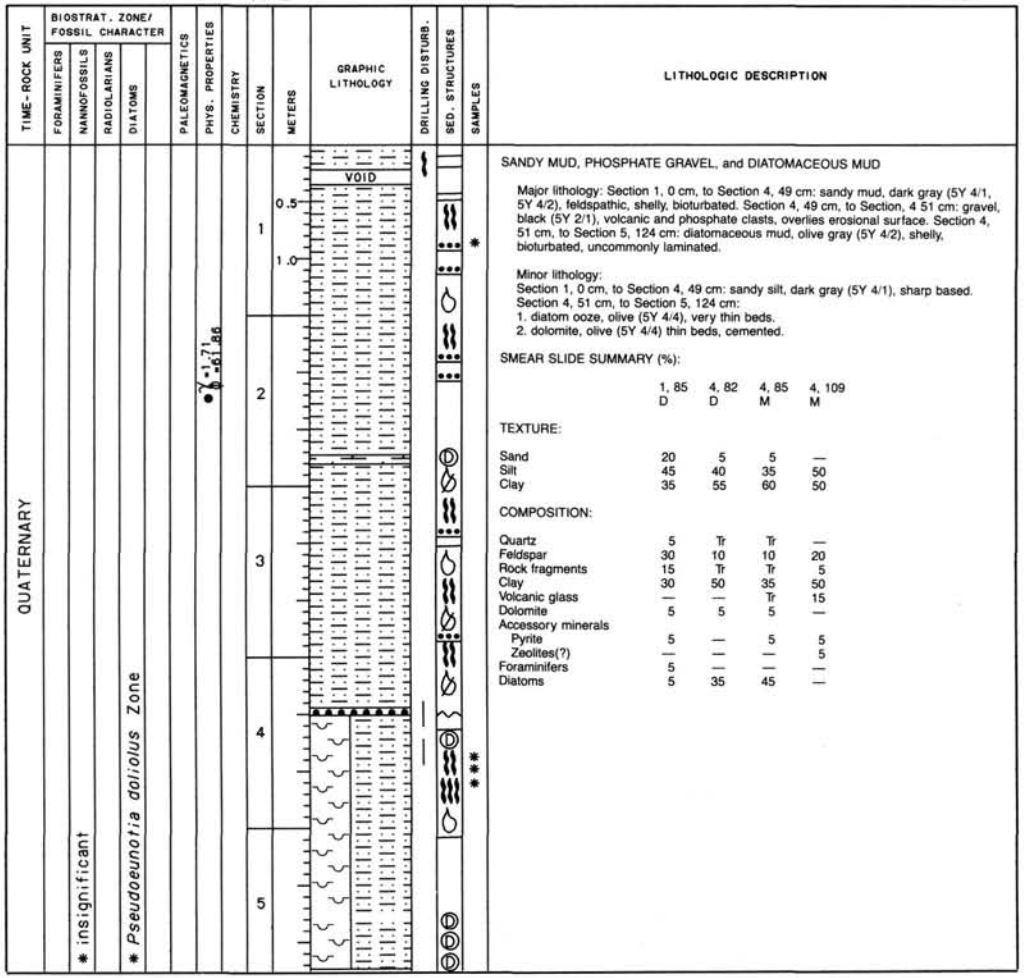

LITHOLOGIC DESCRIPTION

SANDY MUD, PHOSPHATE GRAVEL, and DIATOMACEOUS MUD

Major lithology: Section 1, 0 cm, to Section 4, 49 cm: sandy mud, dark gray (5Y 4/1, 5Y 4/2), feldspathic, shelly, bioturbated. Section 4, 49 cm, to Section, 4 51 cm: gravel, black (5Y 2/1), volcanic and phosphate clasts, overlies erosional surface. Section 4, 51 cm, to Section 5, 124 cm: diatomaceous mud, olive gray (5Y 4/2), shelly, bioturbated, uncommonly laminated.

Minor lithology:
Section 1, 0 cm, to Section 4, 49 cm: sandy silt, dark gray (5Y 4/1), sharp based.
Section 4, 51 cm, to Section 5, 124 cm:
1. diatom ooze, olive (5Y 4/4), very thin beds.
2. dolomite, olive (5Y 4/4) thin beds, cemented.

SMEAR SLIDE SUMMARY (%):

	1, 85 D	4, 82 D	4, 85 M	4, 109 M
TEXTURE:				
Sand	20	5	5	—
Silt	45	40	35	50
Clay	35	55	60	50
COMPOSITION:				
Quartz	5	Tr	Tr	—
Feldspar	30	10	10	20
Rock fragments	15	Tr	Tr	5
Clay	30	50	35	50
Volcanic glass	—	—	Tr	15
Dolomite	5	5	5	—
Accessory minerals				
Pyrite	5	—	5	5
Zeolites(?)	—	—	—	5
Foraminifers	5	—	—	—
Diatoms	5	35	45	—

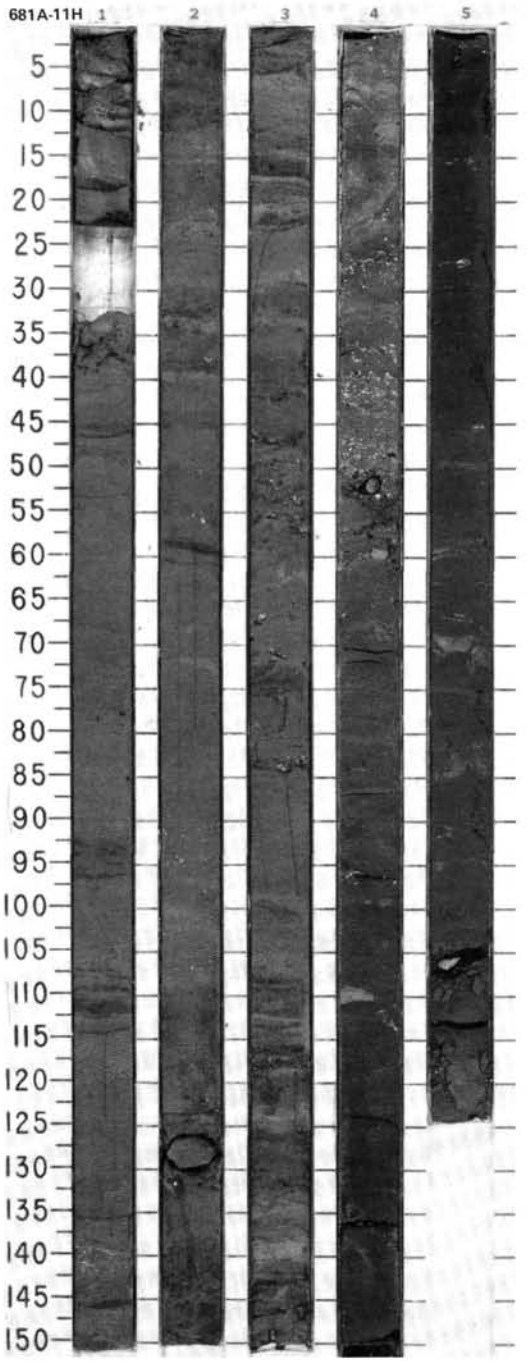

SITE 681 HOLE A CORE 12H CORED INTERVAL 253.5-263.0 mbsl; 101.5-111.0 mbsf

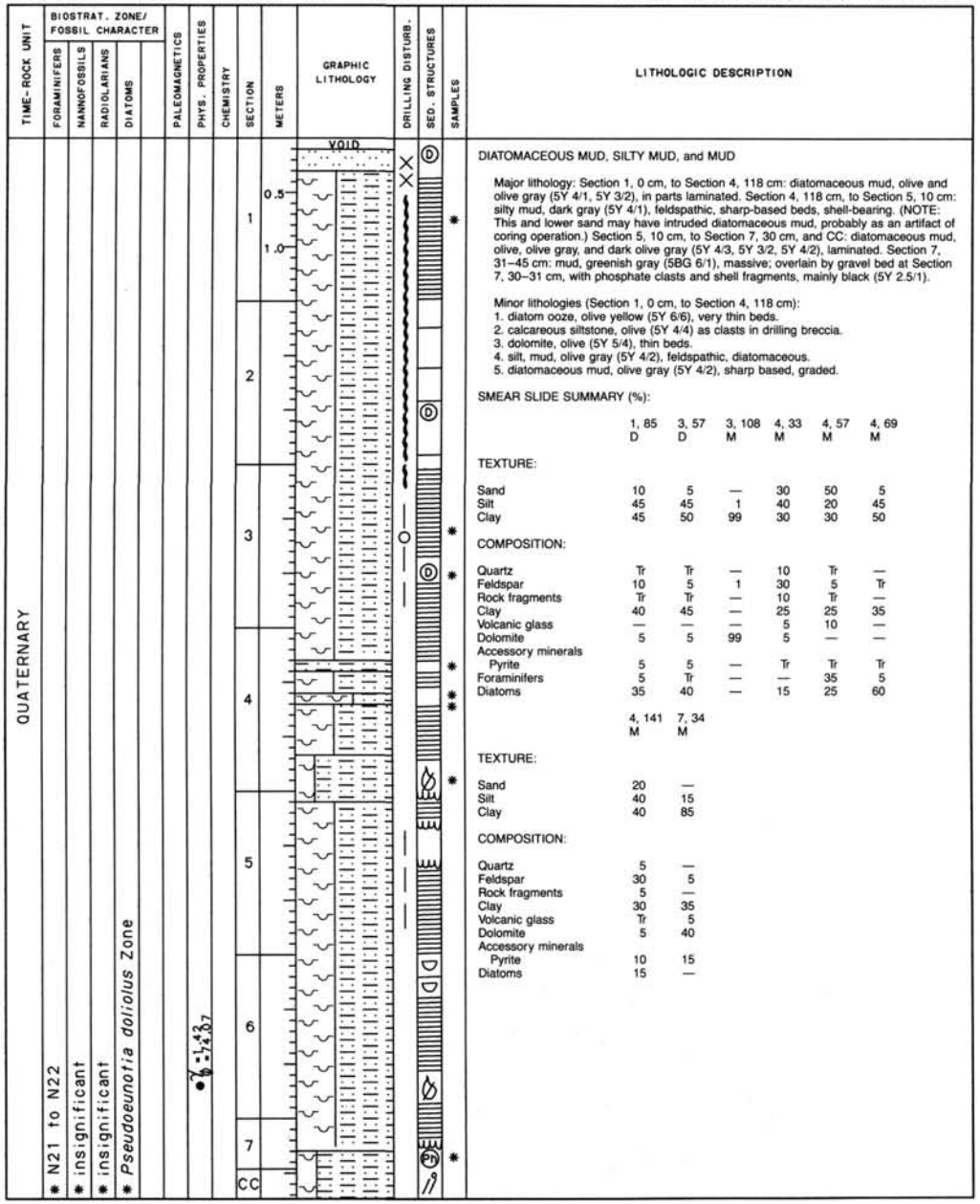

LITHOLOGIC DESCRIPTION

DIATOMACEOUS MUD, SILTY MUD, and MUD

Major lithology: Section 1, 0 cm, to Section 4, 118 cm: diatomaceous mud, olive and olive gray (5Y 4/1, 5Y 3/2), in parts laminated. Section 4, 118 cm, to Section 5, 10 cm: silty mud, dark gray (5Y 4/1), feldspathic, sharp-based beds, shell-bearing. (NOTE: This and lower sand may have intruded diatomaceous mud, probably as an artifact of coring operation.) Section 5, 10 cm, to Section 7, 30 cm, and CC: diatomaceous mud, olive, olive gray, and dark olive gray (5Y 4/3, 5Y 3/2, 5Y 4/2), laminated. Section 7, 31–45 cm: mud, greenish gray (5BG 6/1), massive; overlain by gravel bed at Section 7, 30–31 cm, with phosphate clasts and shell fragments, mainly black (5Y 2.5/1).

Minor lithologies (Section 1, 0 cm, to Section 4, 118 cm):
1. diatom ooze, olive yellow (5Y 6/6), very thin beds.
2. calcareous siltstone, olive (5Y 4/4) as clasts in drilling breccia.
3. dolomite, olive (5Y 5/4), thin beds.
4. silt, mud, olive gray (5Y 4/2), feldspathic, diatomaceous.
5. diatomaceous mud, olive gray (5Y 4/2), sharp based, graded.

SMEAR SLIDE SUMMARY (%):

	1, 85 D	3, 57 D	3, 108 M	4, 33 M	4, 57 M	4, 69 M
TEXTURE:						
Sand	10	5	—	30	50	5
Silt	45	45	1	40	20	45
Clay	45	50	99	30	30	50
COMPOSITION:						
Quartz	Tr	Tr	—	10	Tr	—
Feldspar	10	5	1	30	5	Tr
Rock fragments	Tr	Tr	—	10	Tr	—
Clay	40	45	—	25	25	35
Volcanic glass	—	—	—	5	10	—
Dolomite	5	5	99	5	—	—
Accessory minerals						
Pyrite	5	5	—	Tr	Tr	Tr
Foraminifers	5	Tr	—	—	35	5
Diatoms	35	40	—	15	25	60

	4, 141 M	7, 34 M
TEXTURE:		
Sand	20	—
Silt	40	15
Clay	40	85
COMPOSITION:		
Quartz	5	—
Feldspar	30	5
Rock fragments	5	—
Clay	30	35
Volcanic glass	Tr	5
Dolomite	5	40
Accessory minerals		
Pyrite	10	15
Diatoms	15	—

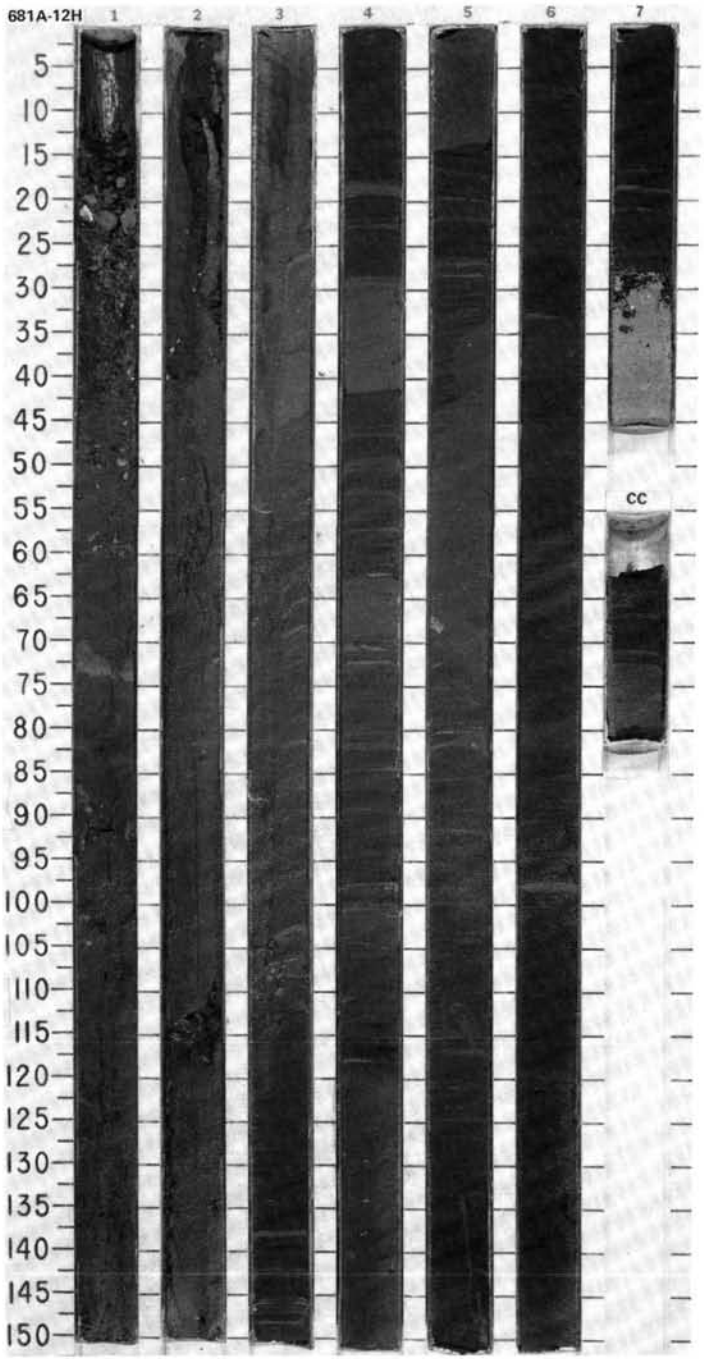

SITE 681 HOLE A CORE 13X CORED INTERVAL 263.0-272.5 mbsl; 111.0-120.5 mbsf

TIME-ROCK UNIT	BIOSTRAT. ZONE/ FOSSIL CHARACTER: FORAMINIFERS	NANNOFOSSILS	RADIOLARIANS	DIATOMS	PALEOMAGNETICS	PHYS. PROPERTIES	CHEMISTRY	SECTION	METERS	GRAPHIC LITHOLOGY	DRILLING DISTURB.	SED. STRUCTURES	SAMPLES
QUATERNARY	* B	* insignificant	* insignificant	* *Pseudoeunotia doliolus* Zone				1, 2, 3, CC	0.5, 1.0				*

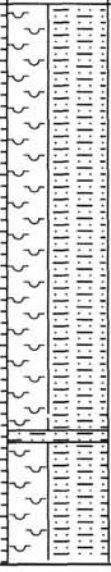

LITHOLOGIC DESCRIPTION

DIATOMACEOUS MUD

Major lithology: diatomaceous mud, olive gray (5Y 4/2), laminated in part.

Minor lithologies:
1. silt, mud, gray (5Y 4/2), thin beds, sharp based.
2. dolomite, dark gray (5Y 5/1), calcareous, cemented.

SMEAR SLIDE SUMMARY (%):

	1, 94 D	3, 77 M
TEXTURE:		
Sand	10	20
Silt	30	40
Clay	60	40
COMPOSITION:		
Quartz	—	Tr
Feldspar	15	30
Rock fragments	5	20
Clay	30	20
Volcanic glass	5	10
Diatoms	45	20

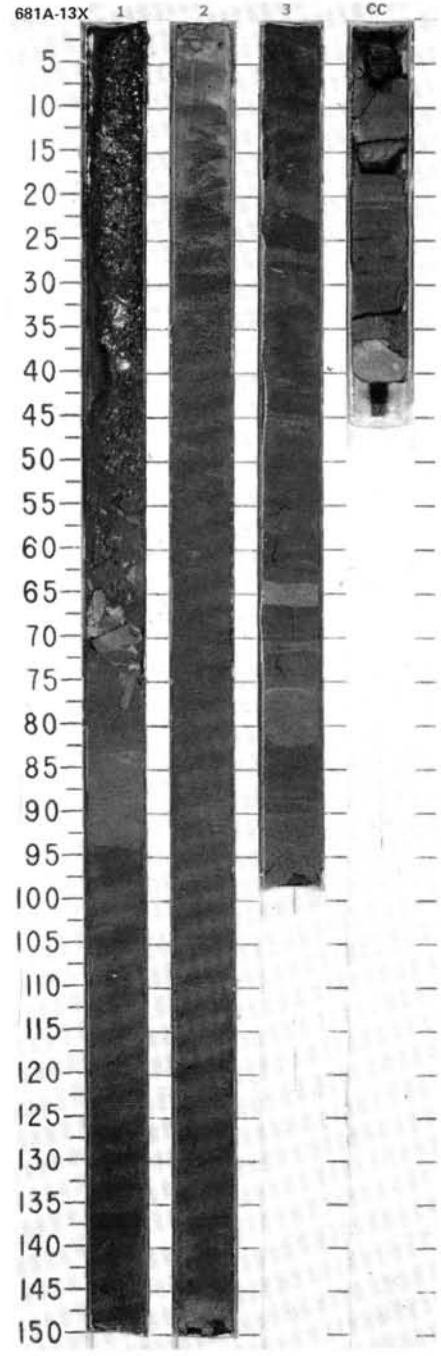

SITE 681 HOLE A CORE 14X CORED INTERVAL 272.5-282.0 mbsl; 120.5-130.0 mbsf

TIME-ROCK UNIT	BIOSTRAT. ZONE/ FOSSIL CHARACTER: FORAMINIFERS	NANNOFOSSILS	RADIOLARIANS	DIATOMS	PALEOMAGNETICS	PHYS. PROPERTIES	CHEMISTRY	SECTION	METERS	GRAPHIC LITHOLOGY	DRILLING DISTURB.	SED. STRUCTURES	SAMPLES
QUATERNARY	*B	*insignificant	*insignificant	*Pseudoeunotia doliolus Zone				1, 2, 3, CC	0.5, 1.0				*

LITHOLOGIC DESCRIPTION

DIATOMACEOUS MUD

Major lithology: diatomaceous mud, olive (5Y 4/3), laminated.

Minor lithology: mud, greenish gray (5BG 5/1), sharp based, massive.

SMEAR SLIDE SUMMARY (%):

	2, 56 D
TEXTURE:	
Silt	50
Clay	50
COMPOSITION:	
Quartz	Tr
Feldspar	5
Rock fragments	5
Clay	35
Dolomite	Tr
Accessory minerals	
Pyrite	5
Foraminifers	5
Nannofossils	Tr
Diatoms	45

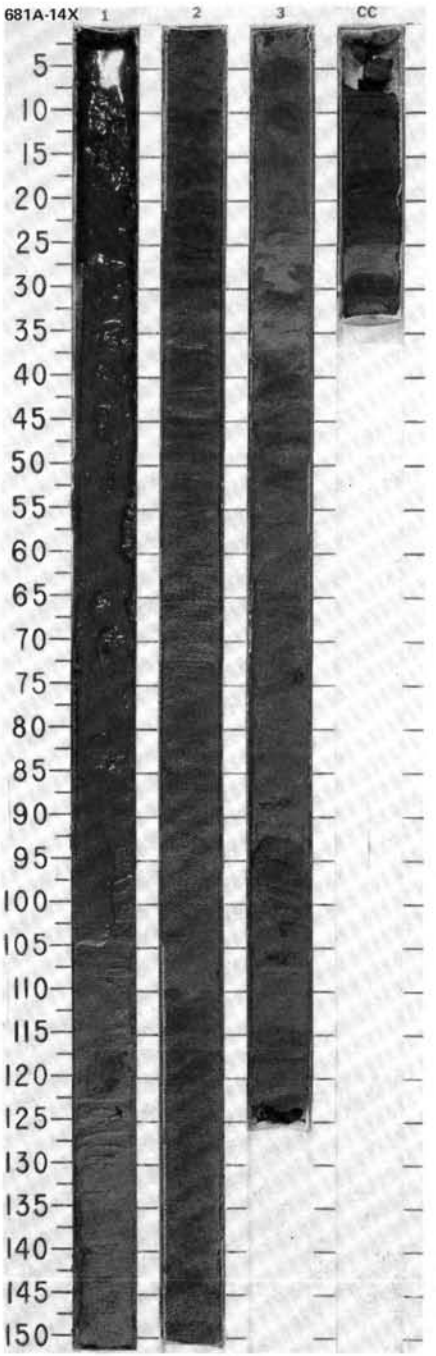

SITE 681 HOLE A CORE 15X CORED INTERVAL 282.0-291.5 mbsl; 130.0-139.5 mbsf

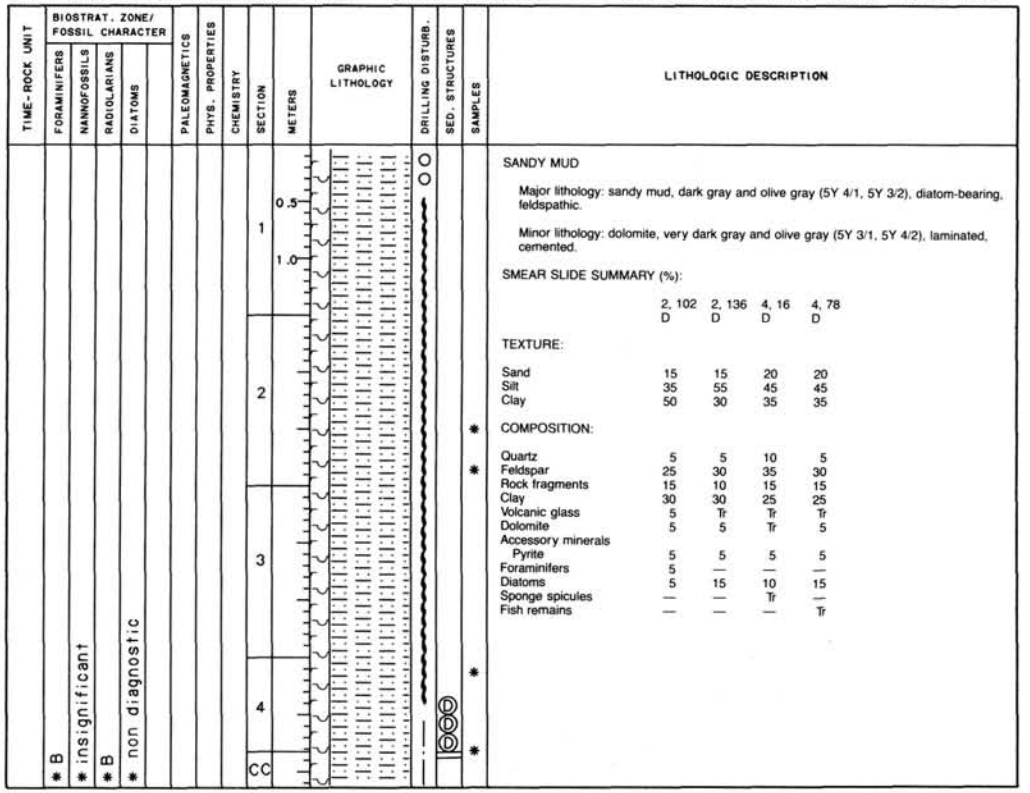

SANDY MUD

Major lithology: sandy mud, dark gray and olive gray (5Y 4/1, 5Y 3/2), diatom-bearing, feldspathic.

Minor lithology: dolomite, very dark gray and olive gray (5Y 3/1, 5Y 4/2), laminated, cemented.

SMEAR SLIDE SUMMARY (%):

	2, 102 D	2, 136 D	4, 16 D	4, 78 D
TEXTURE:				
Sand	15	15	20	20
Silt	35	55	45	45
Clay	50	30	35	35
COMPOSITION:				
Quartz	5	5	10	5
Feldspar	25	30	35	30
Rock fragments	15	10	15	15
Clay	30	30	25	25
Volcanic glass	5	Tr	Tr	Tr
Dolomite	5	5	Tr	5
Accessory minerals				
Pyrite	5	5	5	5
Foraminifers	5	—	—	—
Diatoms	5	15	10	15
Sponge spicules	—	—	Tr	—
Fish remains	—	—	—	Tr

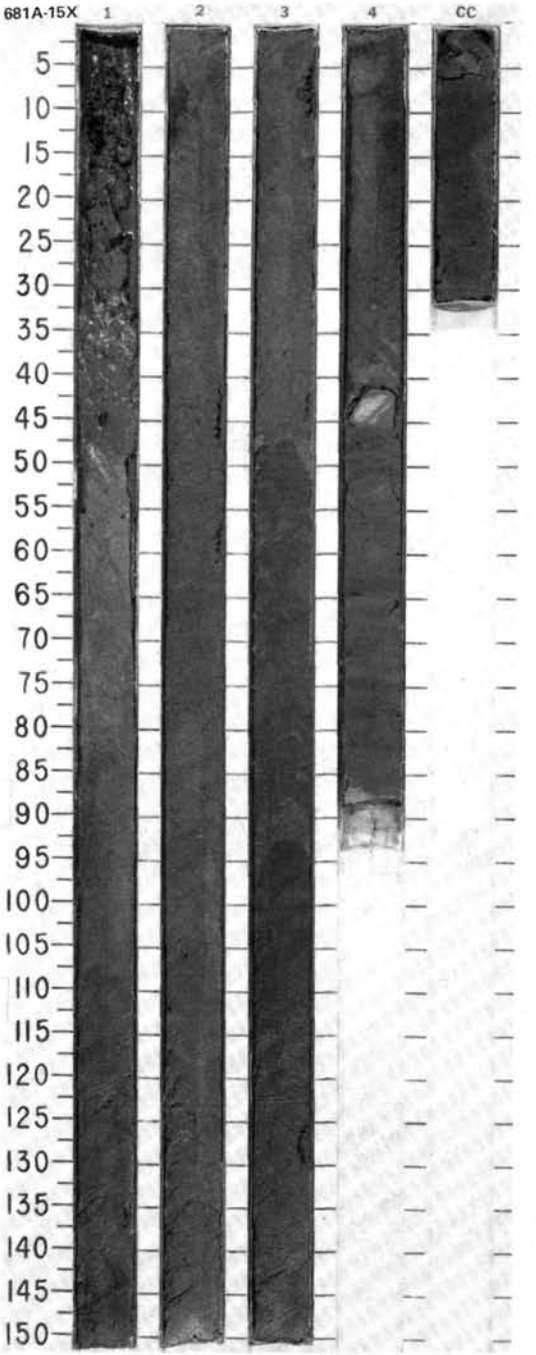

SITE 681 HOLE A CORE 16X CORED INTERVAL 291.5-301.0 mbsl; 139.5-149.0 mbsf

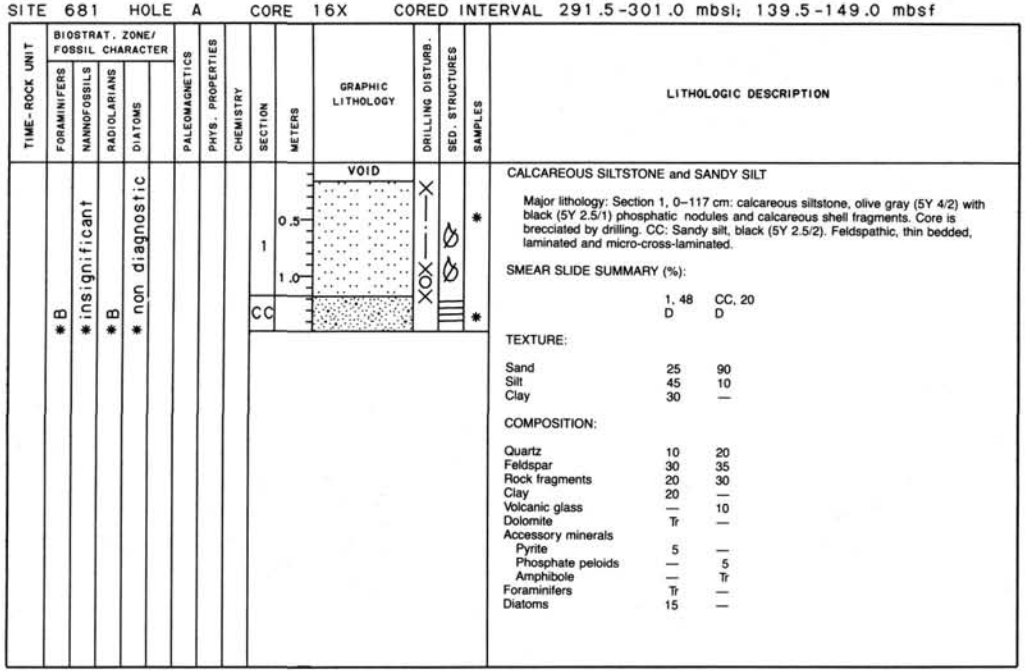

CALCAREOUS SILTSTONE and SANDY SILT

Major lithology: Section 1, 0–117 cm: calcareous siltstone, olive gray (5Y 4/2) with black (5Y 2.5/1) phosphatic nodules and calcareous shell fragments. Core is brecciated by drilling. CC: Sandy silt, black (5Y 2.5/2). Feldspathic, thin bedded, laminated and micro-cross-laminated.

SMEAR SLIDE SUMMARY (%):

	1, 48 D	CC, 20 D
TEXTURE:		
Sand	25	90
Silt	45	10
Clay	30	—
COMPOSITION:		
Quartz	10	20
Feldspar	30	35
Rock fragments	20	30
Clay	20	—
Volcanic glass	—	10
Dolomite	Tr	—
Accessory minerals		
Pyrite	5	—
Phosphate peloids	—	5
Amphibole	—	Tr
Foraminifers	Tr	—
Diatoms	15	—

SITE 681 HOLE A CORE 17X CORED INTERVAL 301.0-310.5 mbsl; 149.0-158.5 mbsf

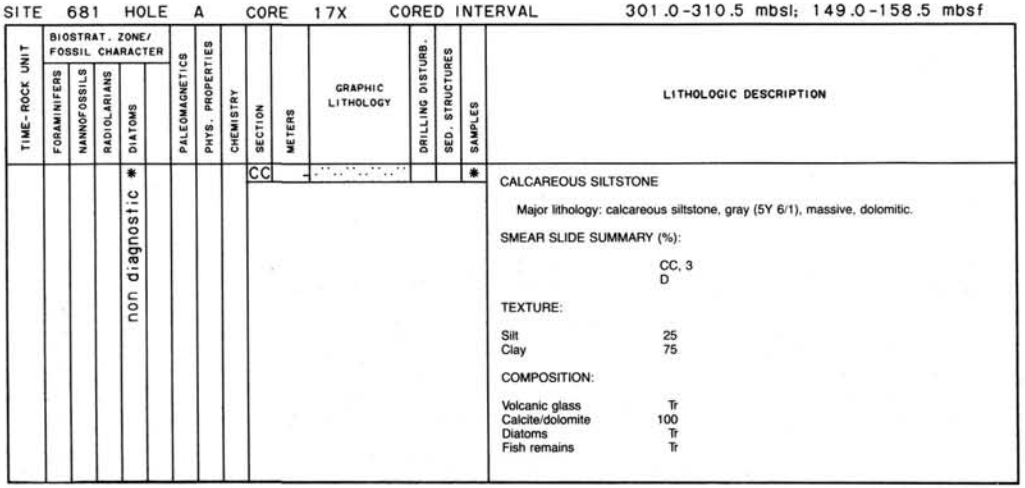

CALCAREOUS SILTSTONE

Major lithology: calcareous siltstone, gray (5Y 6/1), massive, dolomitic.

SMEAR SLIDE SUMMARY (%):

	CC, 3 D
TEXTURE:	
Silt	25
Clay	75
COMPOSITION:	
Volcanic glass	Tr
Calcite/dolomite	100
Diatoms	Tr
Fish remains	Tr

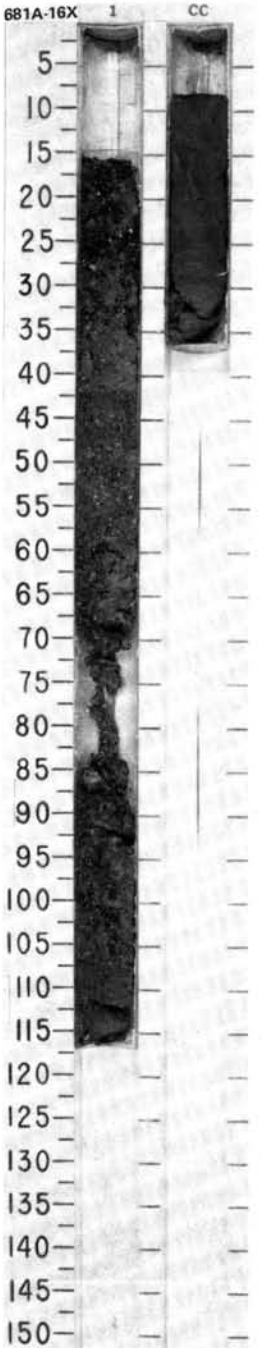

SITE 681 HOLE A CORE 18X CORED INTERVAL 310.5-320.0 mbsl; 158.5-168.0 mbsf

TIME-ROCK UNIT	BIOSTRAT. ZONE/ FOSSIL CHARACTER: FORAMINIFERS	NANNOFOSSILS	RADIOLARIANS	DIATOMS	PALEOMAGNETICS	PHYS. PROPERTIES	CHEMISTRY	SECTION	METERS	GRAPHIC LITHOLOGY	DRILLING DISTURB.	SED. STRUCTURES	SAMPLES	LITHOLOGIC DESCRIPTION
	B *	B *	B *	non diagnostic *				CC			O	D		VERY FINE SAND and DOLOMITE Major lithology: slurry of very fine sand, dark gray (5Y 4/1), and dolomite, olive (5Y 4/3).

SITE 681 HOLE A CORE 19X CORED INTERVAL 320.0-329.5 mbsl; 168.0-177.5 mbsf

TIME-ROCK UNIT	BIOSTRAT. ZONE/ FOSSIL CHARACTER: FORAMINIFERS	NANNOFOSSILS	RADIOLARIANS	DIATOMS	PALEOMAGNETICS	PHYS. PROPERTIES	CHEMISTRY	SECTION	METERS	GRAPHIC LITHOLOGY	DRILLING DISTURB.	SED. STRUCTURES	SAMPLES	LITHOLOGIC DESCRIPTION
PLIOCENE	N23-N21 *	NN15 or older *	insignificant *	*Actinocyclus oculatus* Zone *				CC					*	SILTY SAND Major lithology: silty sand, very dark gray (5Y 3/1), feldspathic, contains shell fragments. SMEAR SLIDE SUMMARY (%): CC, 12 D TEXTURE: Sand 70 Silt 20 Clay 10 COMPOSITION: Quartz 20 Feldspar 35 Rock fragments 25 Dolomite 10 Accessory minerals Amphibole Tr Phosphate peloids 10

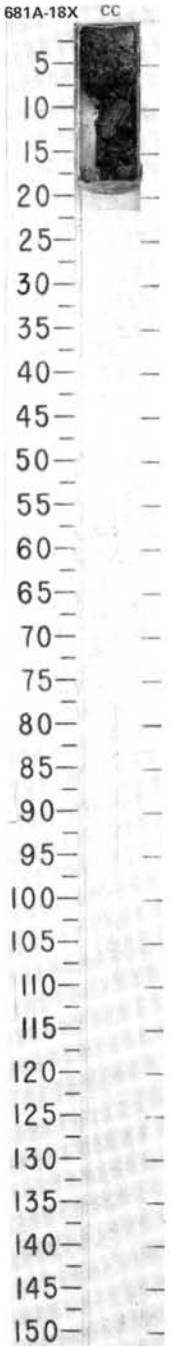

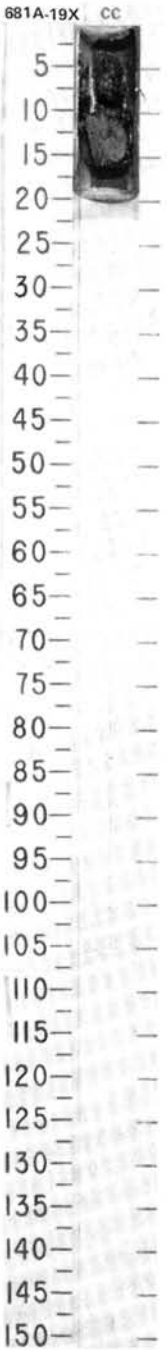

SITE 681 HOLE A CORE 20X CORED INTERVAL 329.5-338.0 mbsl; 177.5-187.0 mbsf

TIME-ROCK UNIT	BIOSTRAT. ZONE/ FOSSIL CHARACTER: FORAMINIFERS	NANNOFOSSILS	RADIOLARIANS	DIATOMS		PALEOMAGNETICS	PHYS. PROPERTIES	CHEMISTRY	SECTION	METERS	GRAPHIC LITHOLOGY	DRILLING DISTURB.	SED. STRUCTURES	SAMPLES	LITHOLOGIC DESCRIPTION
	B *	B *	B *	non diagnostic *					CC			O O		*	

SILTY SAND

Major lithology: silty sand, very dark gray (5Y 3/1), feldspathic.

SMEAR SLIDE SUMMARY (%):

	CC, 29 D

TEXTURE:

Sand	55
Silt	25
Clay	20

COMPOSITION:

Quartz	5
Feldspar	25
Rock fragments	45
Clay	10
Volcanic glass	Tr
Dolomite rhombs.	10
Accessory minerals	
Amphibole	2
Phosphate peloids	3

681A-20X CC

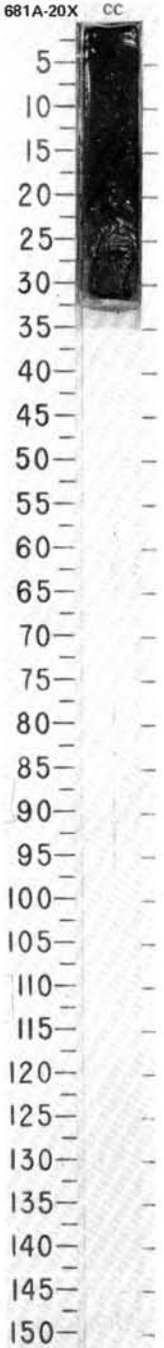

SITE 681 HOLE B CORE 1H CORED INTERVAL 151.4-157.3 mbsl; 0.0-5.9 mbsf

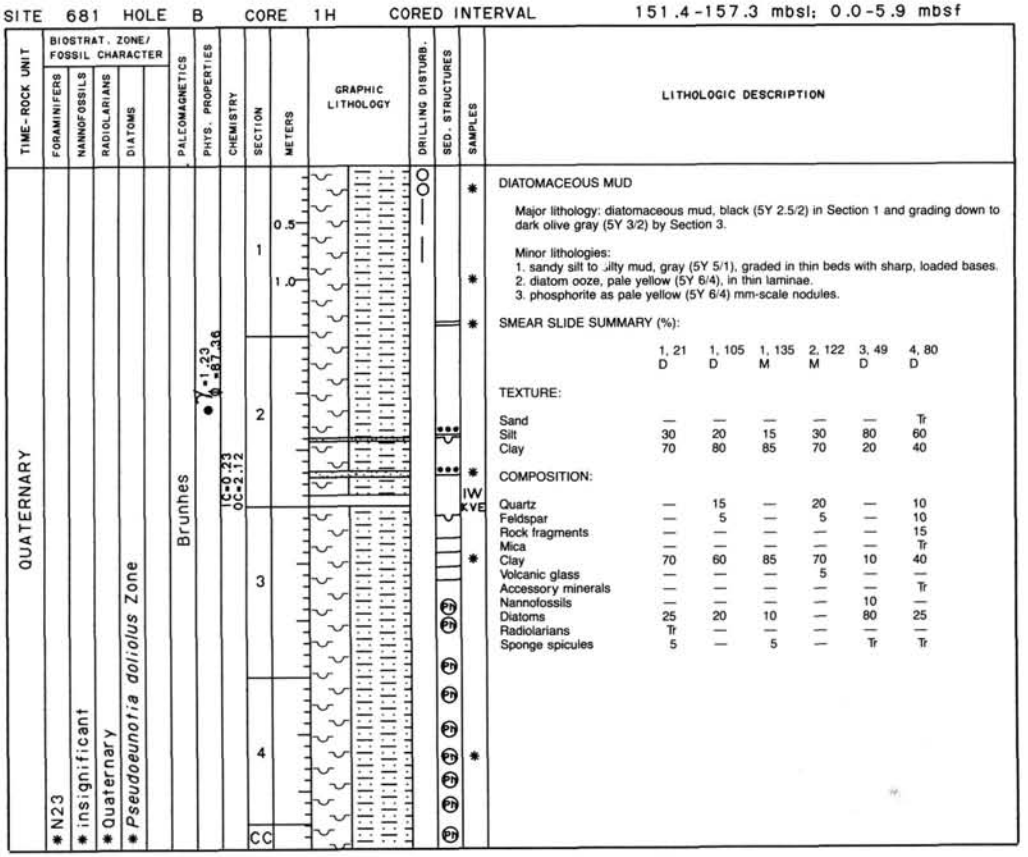

LITHOLOGIC DESCRIPTION

DIATOMACEOUS MUD

Major lithology: diatomaceous mud, black (5Y 2.5/2) in Section 1 and grading down to dark olive gray (5Y 3/2) by Section 3.

Minor lithologies:
1. sandy silt to silty mud, gray (5Y 5/1), graded in thin beds with sharp, loaded bases.
2. diatom ooze, pale yellow (5Y 6/4), in thin laminae.
3. phosphorite as pale yellow (5Y 6/4) mm-scale nodules.

SMEAR SLIDE SUMMARY (%):

	1, 21 D	1, 105 D	1, 135 M	2, 122 M	3, 49 D	4, 80 D
TEXTURE:						
Sand	—	—	—	—	—	Tr
Silt	30	20	15	30	80	60
Clay	70	80	85	70	20	40
COMPOSITION:						
Quartz	—	15	—	20	—	10
Feldspar	—	5	—	5	—	10
Rock fragments	—	—	—	—	—	15
Mica	—	—	—	—	—	Tr
Clay	70	60	85	70	10	40
Volcanic glass	—	—	—	5	—	—
Accessory minerals	—	—	—	—	—	Tr
Nannofossils	—	—	—	—	10	—
Diatoms	25	20	10	—	80	25
Radiolarians	Tr	—	—	—	—	—
Sponge spicules	5	—	5	—	Tr	Tr

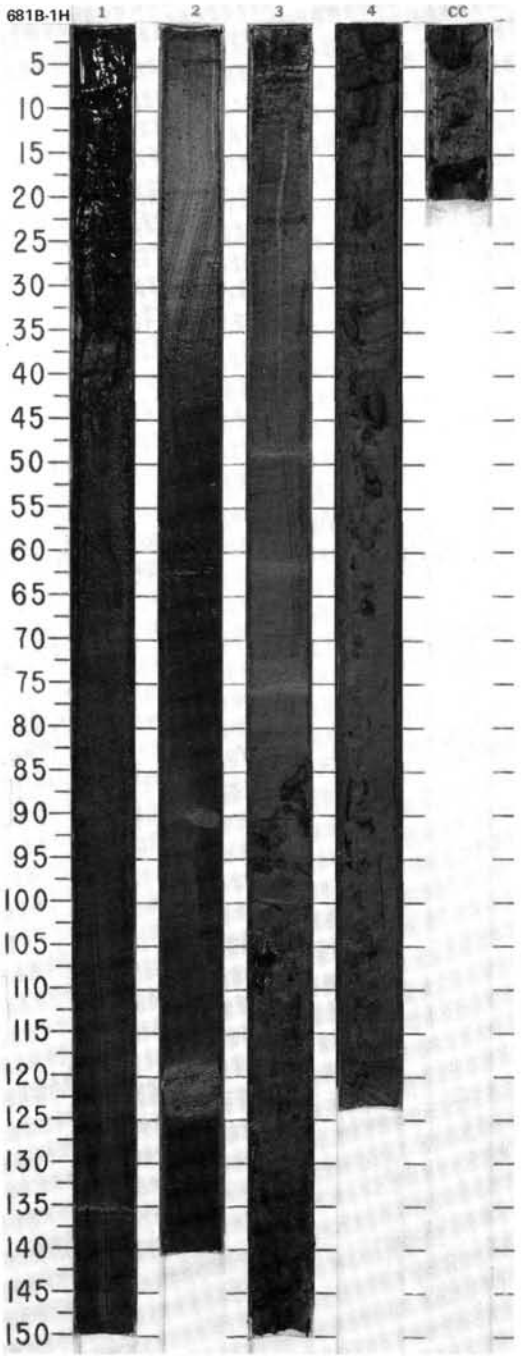

SITE 681 HOLE B CORE 2H CORED INTERVAL 157.3-166.8 mbsl; 5.9-15.4 mbsf

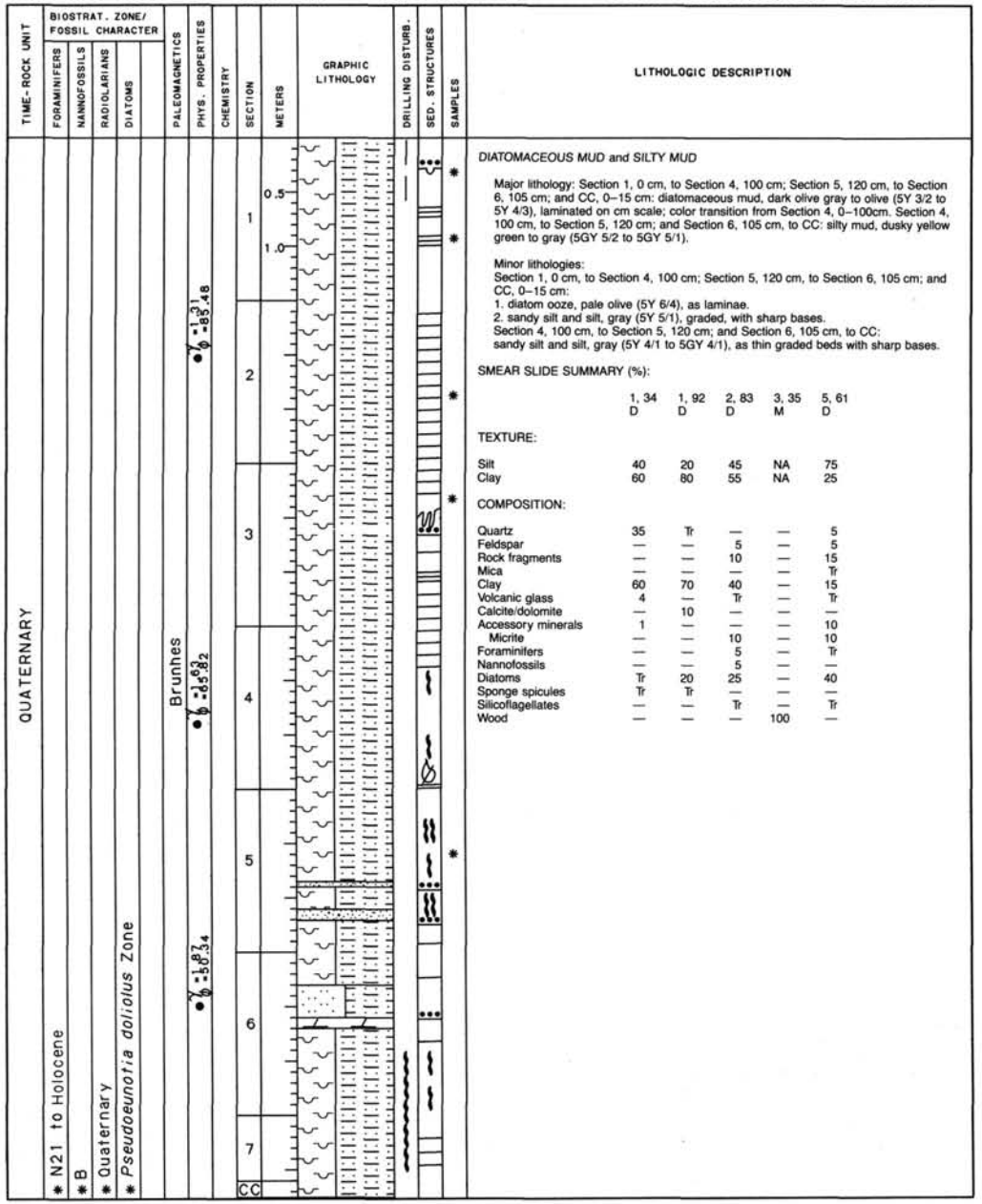

LITHOLOGIC DESCRIPTION

DIATOMACEOUS MUD and SILTY MUD

Major lithology: Section 1, 0 cm, to Section 4, 100 cm; Section 5, 120 cm, to Section 6, 105 cm; and CC, 0–15 cm: diatomaceous mud, dark olive gray to olive (5Y 3/2 to 5Y 4/3), laminated on cm scale; color transition from Section 4, 0–100cm. Section 4, 100 cm, to Section 5, 120 cm; and Section 6, 105 cm, to CC: silty mud, dusky yellow green to gray (5GY 5/2 to 5GY 5/1).

Minor lithologies:
Section 1, 0 cm, to Section 4, 100 cm; Section 5, 120 cm, to Section 6, 105 cm; and CC, 0–15 cm:
1. diatom ooze, pale olive (5Y 6/4), as laminae.
2. sandy silt and silt, gray (5Y 5/1), graded, with sharp bases.
Section 4, 100 cm, to Section 5, 120 cm; and Section 6, 105 cm, to CC:
sandy silt and silt, gray (5Y 4/1 to 5GY 4/1), as thin graded beds with sharp bases.

SMEAR SLIDE SUMMARY (%):

	1, 34 D	1, 92 D	2, 83 D	3, 35 M	5, 61 D
TEXTURE:					
Silt	40	20	45	NA	75
Clay	60	80	55	NA	25
COMPOSITION:					
Quartz	35	Tr	—	—	5
Feldspar	—	—	5	—	5
Rock fragments	—	—	10	—	15
Mica	—	—	—	—	Tr
Clay	60	70	40	—	15
Volcanic glass	4	—	Tr	—	Tr
Calcite/dolomite	—	10	—	—	—
Accessory minerals	1	—	—	—	10
Micrite	—	—	10	—	10
Foraminifers	—	—	5	—	Tr
Nannofossils	—	—	5	—	—
Diatoms	Tr	20	25	—	40
Sponge spicules	Tr	Tr	—	—	—
Silicoflagellates	—	—	Tr	—	Tr
Wood	—	—	—	100	—

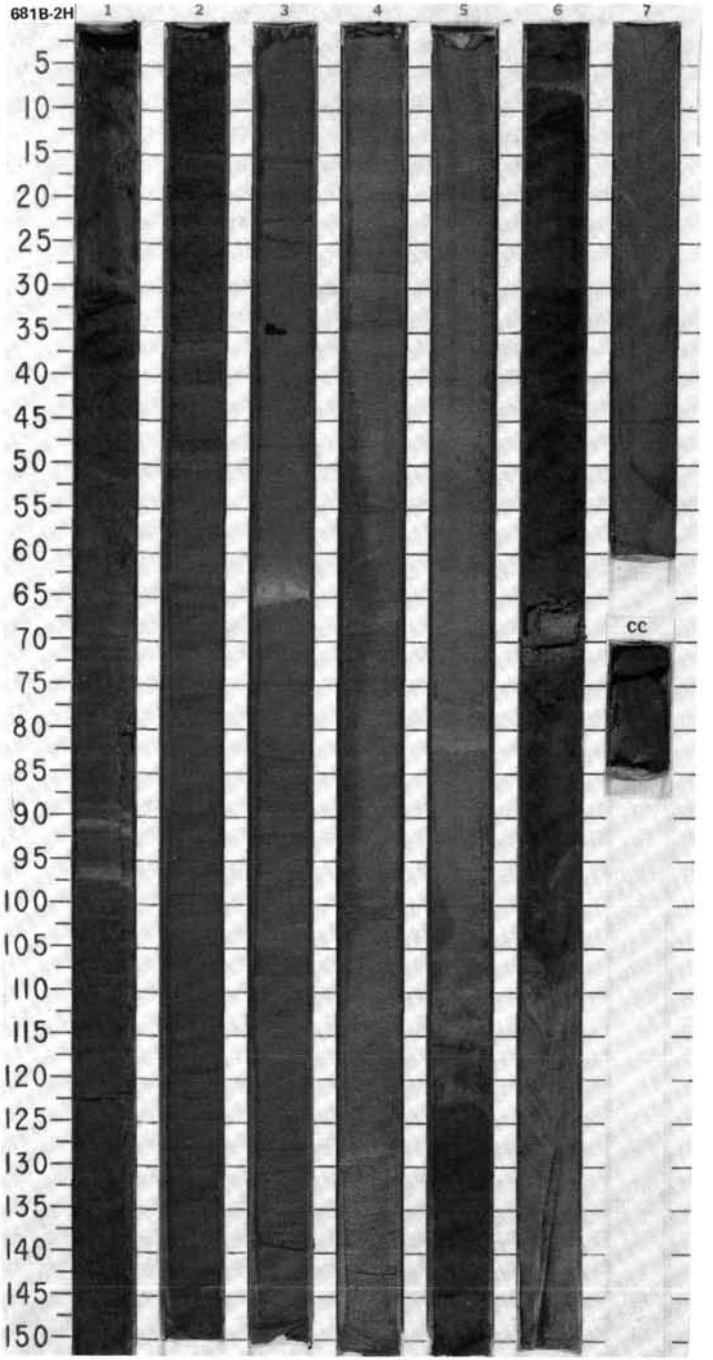

SITE 681 HOLE B CORE 3H CORED INTERVAL 166.8-176.3 mbsl; 15.4-24.9 mbsf

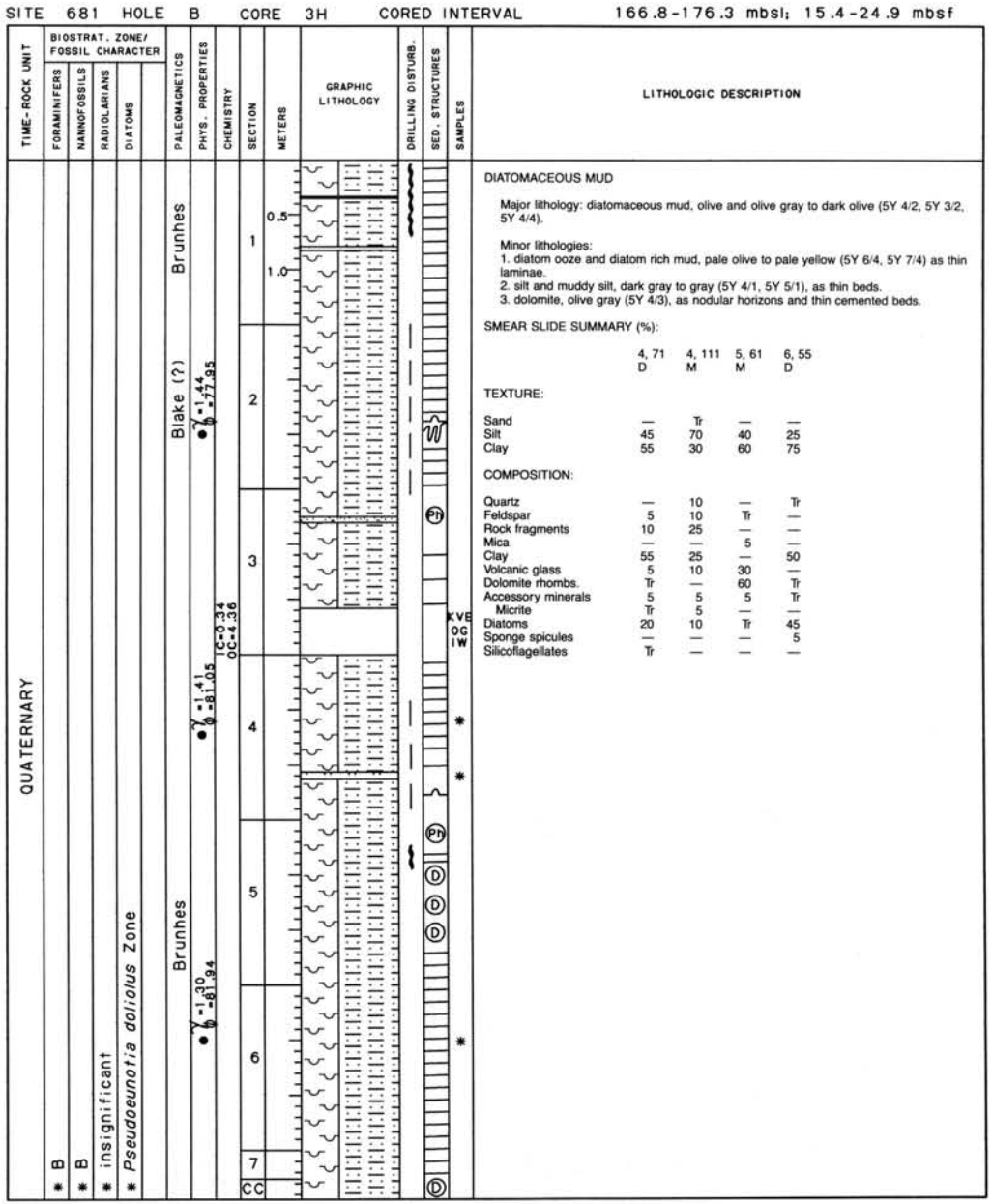

LITHOLOGIC DESCRIPTION

DIATOMACEOUS MUD

Major lithology: diatomaceous mud, olive and olive gray to dark olive (5Y 4/2, 5Y 3/2, 5Y 4/4).

Minor lithologies:
1. diatom ooze and diatom rich mud, pale olive to pale yellow (5Y 6/4, 5Y 7/4) as thin laminae.
2. silt and muddy silt, dark gray to gray (5Y 4/1, 5Y 5/1), as thin beds.
3. dolomite, olive gray (5Y 4/3), as nodular horizons and thin cemented beds.

SMEAR SLIDE SUMMARY (%):

	4, 71 D	4, 111 M	5, 61 M	6, 55 D
TEXTURE:				
Sand	—	Tr	—	—
Silt	45	70	40	25
Clay	55	30	60	75
COMPOSITION:				
Quartz	—	10	—	Tr
Feldspar	5	10	Tr	—
Rock fragments	10	25	—	—
Mica	—	—	5	—
Clay	55	25	—	50
Volcanic glass	5	10	30	—
Dolomite rhombs.	Tr	—	60	Tr
Accessory minerals	5	5	5	Tr
Micrite	Tr	5	—	—
Diatoms	20	10	Tr	45
Sponge spicules	—	—	—	5
Silicoflagellates	Tr	—	—	—

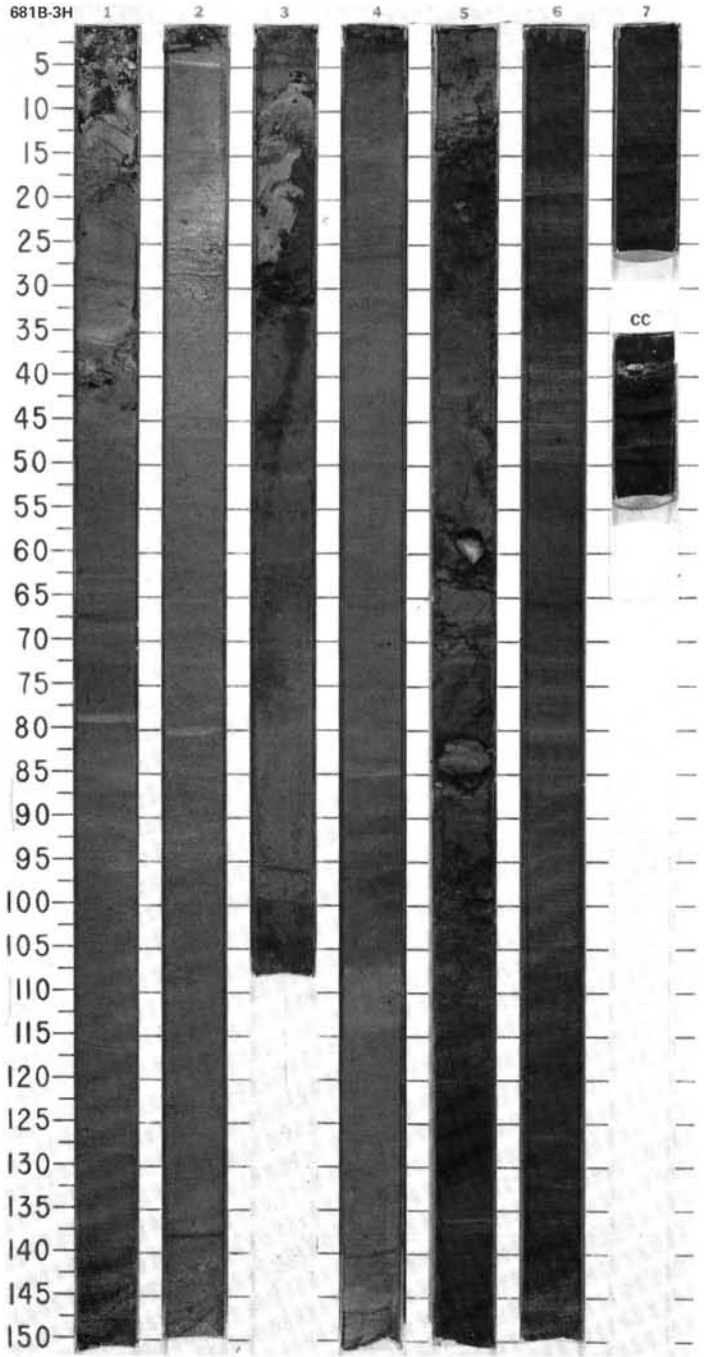

SITE 681 HOLE B CORE 4H CORED INTERVAL 176.3-185.8 mbsl; 24.9-34.4 mbsf

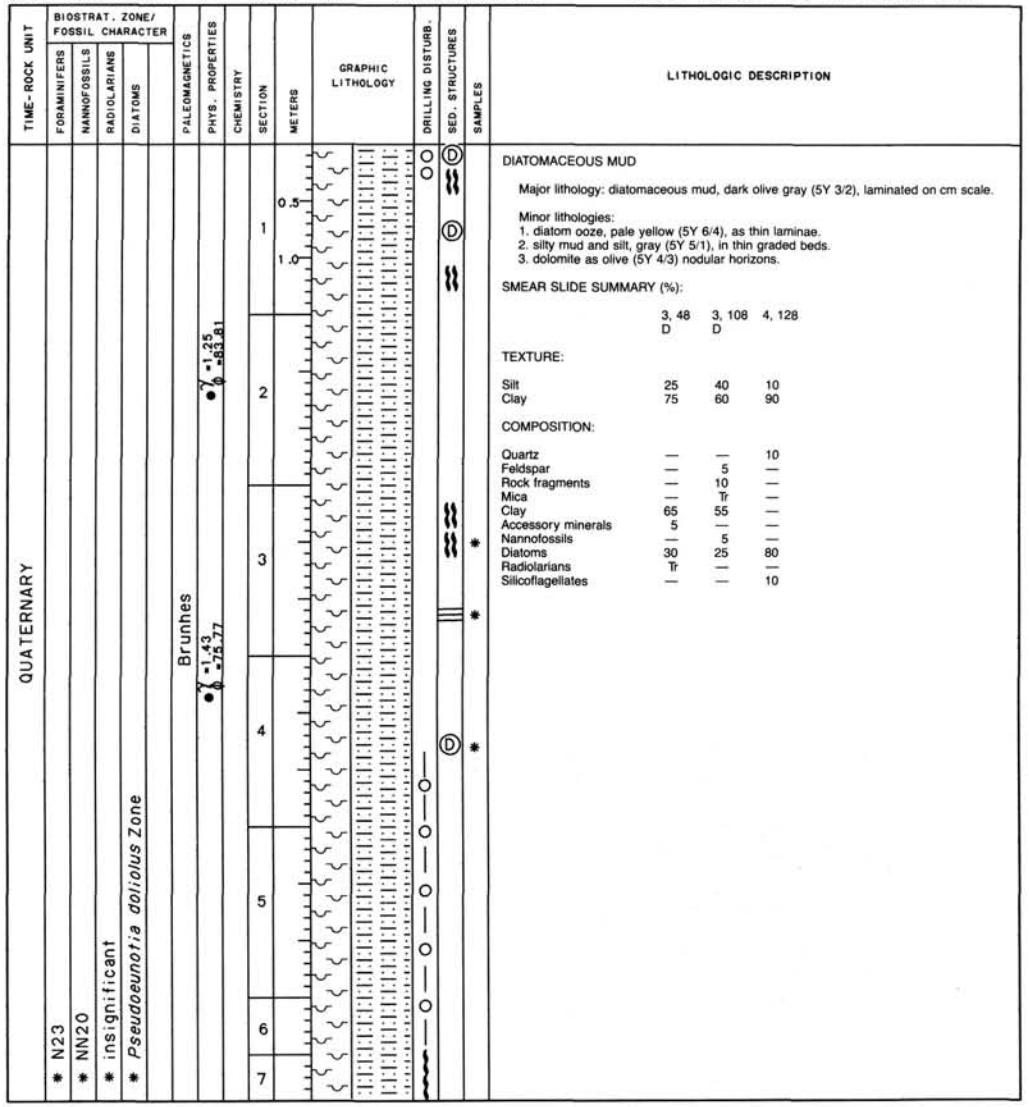

LITHOLOGIC DESCRIPTION

DIATOMACEOUS MUD

Major lithology: diatomaceous mud, dark olive gray (5Y 3/2), laminated on cm scale.

Minor lithologies:
1. diatom ooze, pale yellow (5Y 6/4), as thin laminae.
2. silty mud and silt, gray (5Y 5/1), in thin graded beds.
3. dolomite as olive (5Y 4/3) nodular horizons.

SMEAR SLIDE SUMMARY (%):

	3, 48 D	3, 108 D	4, 128
TEXTURE:			
Silt	25	40	10
Clay	75	60	90
COMPOSITION:			
Quartz	—	—	10
Feldspar	—	5	—
Rock fragments	—	10	—
Mica	—	Tr	—
Clay	65	55	—
Accessory minerals	5	—	—
Nannofossils	—	5	—
Diatoms	30	25	80
Radiolarians	Tr	—	—
Silicoflagellates	—	—	10

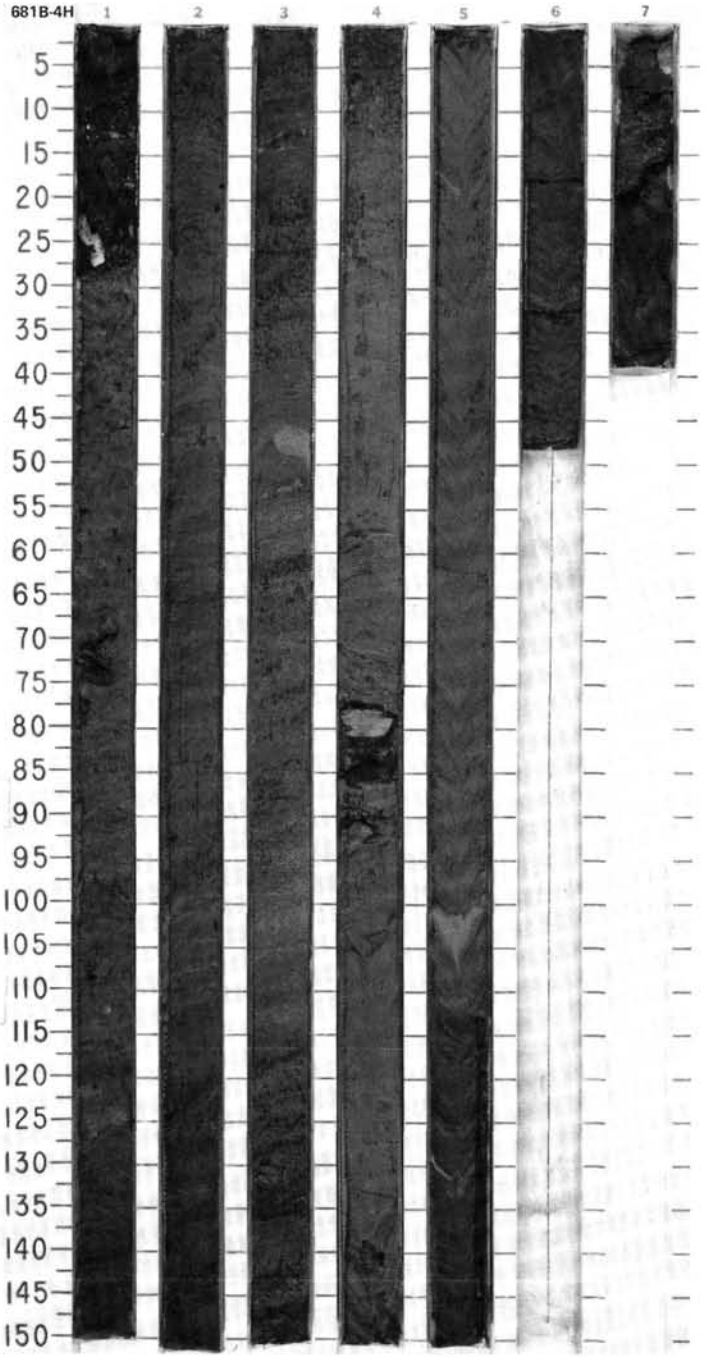

SITE 681 HOLE B CORE 5H CORED INTERVAL 185.8-195.3 mbsl; 34.4-43.9 mbsf

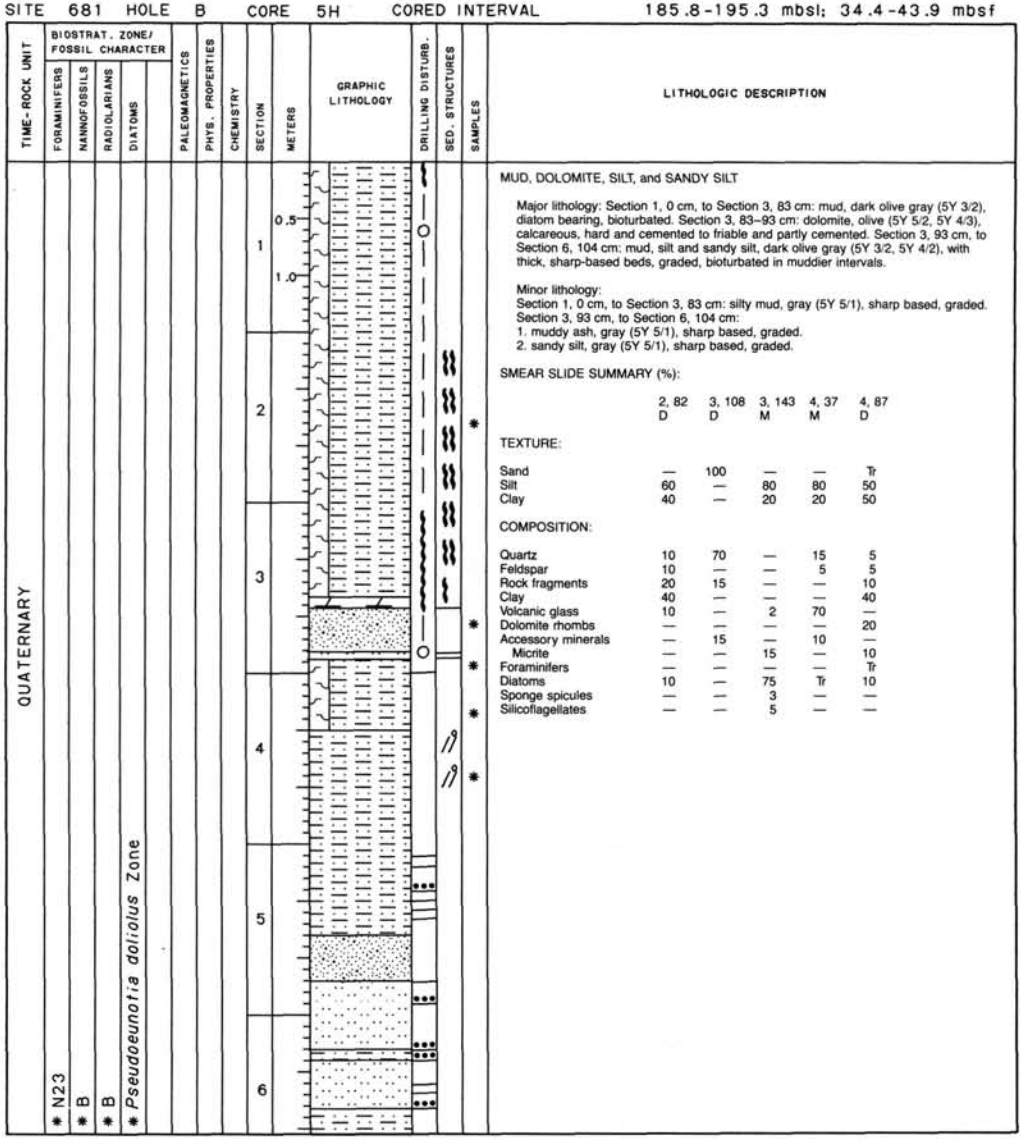

LITHOLOGIC DESCRIPTION

MUD, DOLOMITE, SILT, and SANDY SILT

Major lithology: Section 1, 0 cm, to Section 3, 83 cm: mud, dark olive gray (5Y 3/2), diatom bearing, bioturbated. Section 3, 83–93 cm: dolomite, olive (5Y 5/2, 5Y 4/3), calcareous, hard and cemented to friable and partly cemented. Section 3, 93 cm, to Section 6, 104 cm: mud, silt and sandy silt, dark olive gray (5Y 3/2, 5Y 4/2), with thick, sharp-based beds, graded, bioturbated in muddier intervals.

Minor lithology:
Section 1, 0 cm, to Section 3, 83 cm: silty mud, gray (5Y 5/1), sharp based, graded.
Section 3, 93 cm, to Section 6, 104 cm:
1. muddy ash, gray (5Y 5/1), sharp based, graded.
2. sandy silt, gray (5Y 5/1), sharp based, graded.

SMEAR SLIDE SUMMARY (%):

	2, 82 D	3, 108 D	3, 143 M	4, 37 M	4, 87 D
TEXTURE:					
Sand	—	100	—	—	Tr
Silt	60	—	80	80	50
Clay	40	—	20	20	50
COMPOSITION:					
Quartz	10	70	—	15	5
Feldspar	10	—	—	5	5
Rock fragments	20	15	—	—	10
Clay	40	—	—	—	40
Volcanic glass	10	—	2	70	—
Dolomite rhombs	—	—	—	—	20
Accessory minerals	—	15	—	10	—
Micrite	—	—	15	—	10
Foraminifers	—	—	—	—	Tr
Diatoms	10	—	75	Tr	10
Sponge spicules	—	—	3	—	—
Silicoflagellates	—	—	5	—	—

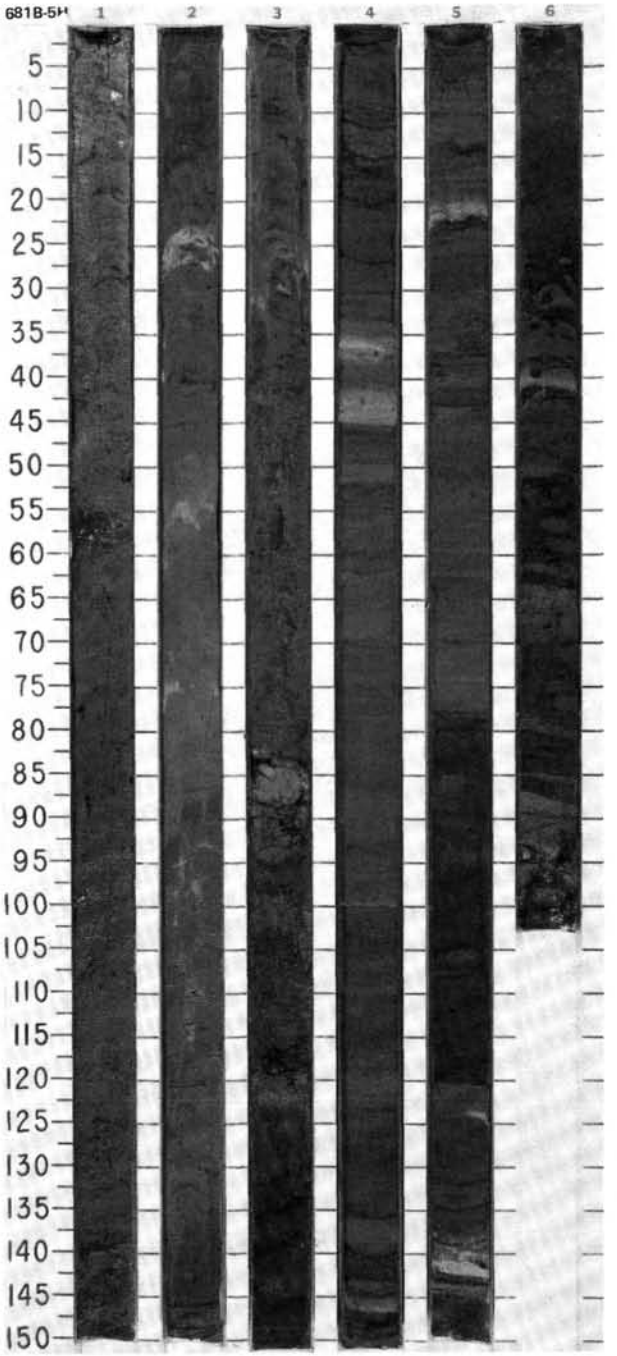

SITE 681 HOLE B CORE 6H CORED INTERVAL 195.3-204.8 mbsl; 43.9-53.4 mbsf

TIME-ROCK UNIT	BIOSTRAT. ZONE/ FOSSIL CHARACTER: FORAMINIFERS	NANNOFOSSILS	RADIOLARIANS	DIATOMS	PALEOMAGNETICS	PHYS. PROPERTIES	CHEMISTRY	SECTION	METERS	GRAPHIC LITHOLOGY	DRILLING DISTURB.	SED. STRUCTURES	SAMPLES	LITHOLOGIC DESCRIPTION
QUATERNARY	*N22	*NN20	*insignificant	*Pseudoeunotia doliolus Zone				1, 2, 3	0.5, 1.0	VOID				DIATOMACEOUS MUD Major lithology: diatomaceous mud, olive gray (5Y 4/2, 5Y 5/1).

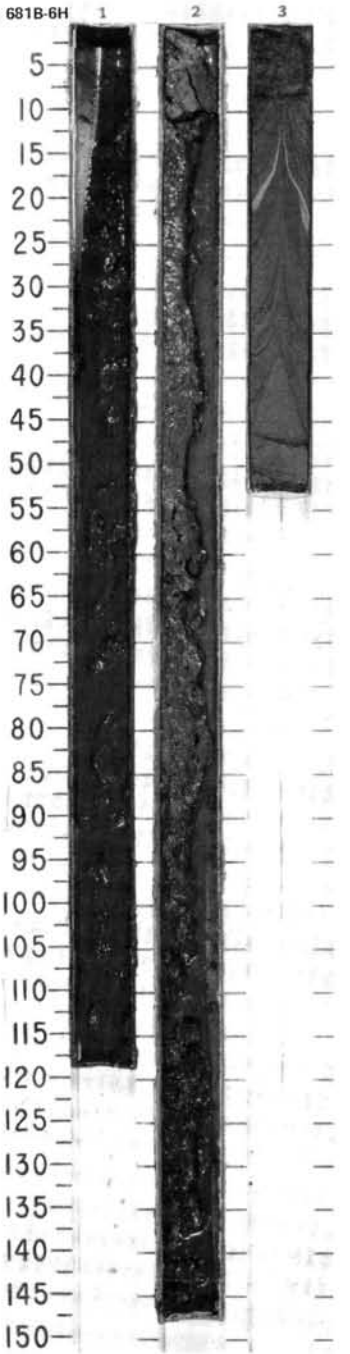

SITE 681 HOLE B CORE 7H CORED INTERVAL 204.8-214.3 mbsl; 53.4-62.9 mbsf

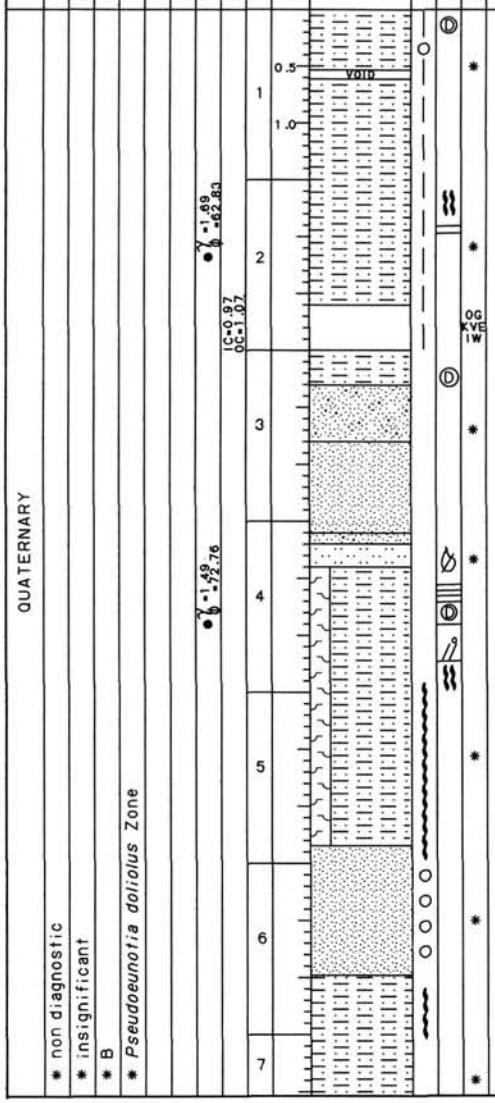

LITHOLOGIC DESCRIPTION

MUD, SAND, SILT, SILTY SAND, and DIATOMACEOUS MUD

Major lithology: Section 1, 0 cm, to Section 3, 50 cm; and Section 6, 99 cm, to Section 7, 57 cm: mud, dark gray (5Y 4/1), slightly calcareous, faintly laminated, bioturbated. Section 3, 50 cm, to Section 4, 40 cm: sand, silt, and silty sand, black, gray, dark olive gray, olive, and dark gray (N 4/, 5Y 4/1, 5Y 3/2, 5Y 4/3, 5Y 3/1). Thin bedded, wood bearing. Section 4, 40 cm, to Section 5, 135 cm: diatomaceous mud, olive (5Y 4/3). Section 5, 135 cm, to Section 6, 99 cm: sand, gray (N 4/1), calcareous. Section 6, 99 cm, to Section 7, 57 cm: mud, gray (5Y 4/1), silty.

Minor lithology: Section 4, 40 cm, to Section 5, 135 cm: dolomite, olive (5Y 4/3), cemented, nodule.

SMEAR SLIDE SUMMARY (%):

	1, 47 M	2, 63 D	3, 69 D	4, 37 M	5, 58 D	6, 57 D	7, 34 D
TEXTURE:							
Sand	45	20	70	NA	—	—	—
Silt	35	40	20	NA	70	80	—
Clay	20	40	10	NA	30	20	100
COMPOSITION:							
Quartz	10	10	20	—	5	30	10
Feldspar	15	15	15	—	—	40	10
Rock fragments	35	20	35	—	—	—	—
Mica	—	5	5	—	—	—	—
Clay	5	40	10	—	20	10	70
Volcanic glass	—	—	—	—	—	10	—
Dolomite rhombs.	—	—	5	—	—	10	5
Accessory minerals	5	Tr	10	—	—	—	—
Micrite	5	—	—	—	10	—	5
Foraminifers	15	10	Tr	—	—	—	—
Nannofossils	10	Tr	—	—	—	—	—
Diatoms	—	Tr	—	—	60	Tr	—
Sponge spicules	—	—	—	—	5	—	—
Wood	—	—	—	100	—	—	—

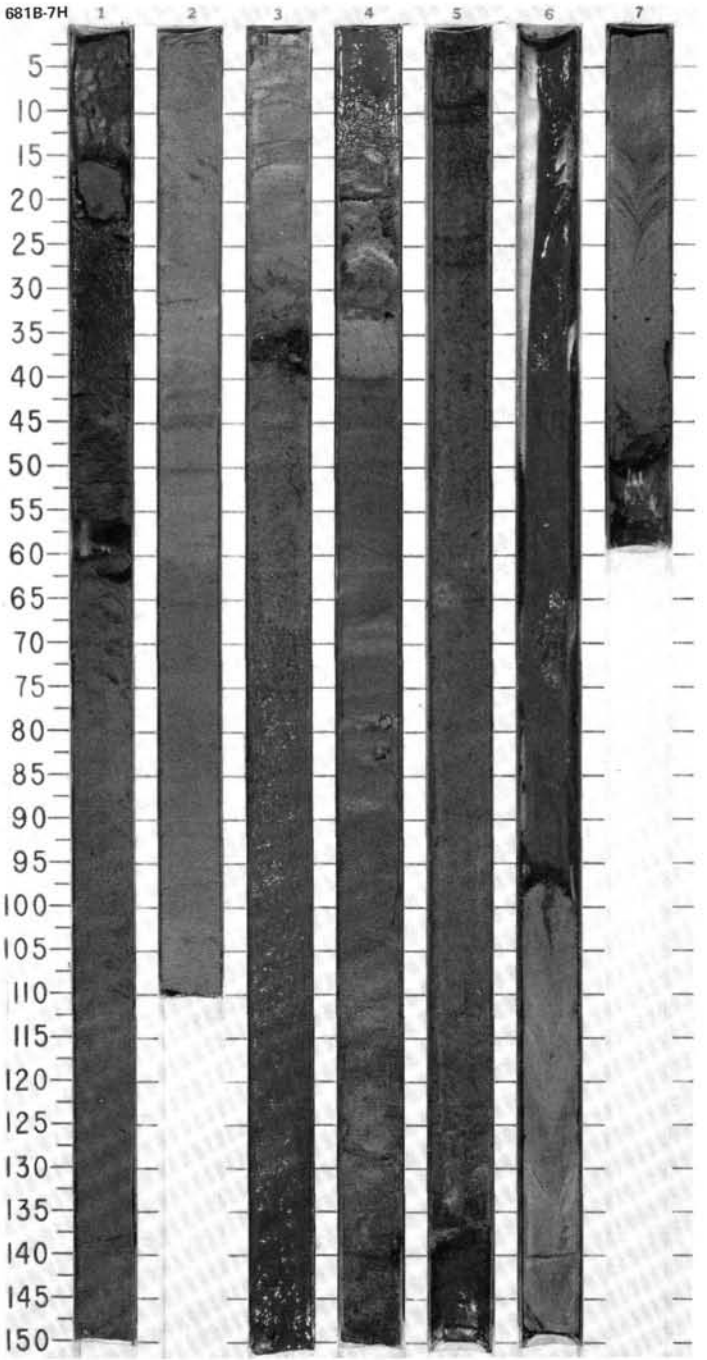

SITE 681 HOLE B CORE 8H CORED INTERVAL 214.3-223.8 mbsl; 62.9-72.4 mbsf

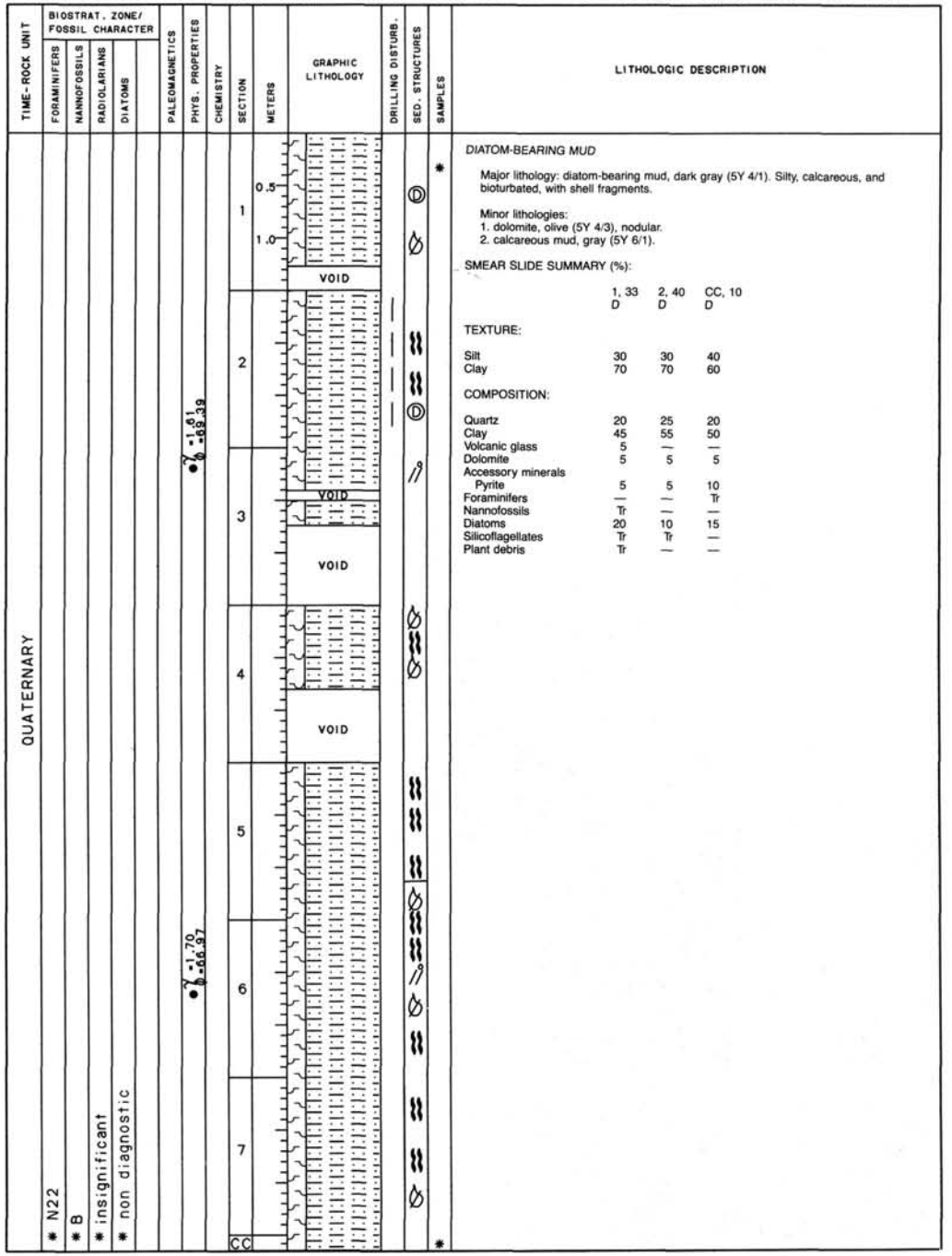

LITHOLOGIC DESCRIPTION

DIATOM-BEARING MUD

Major lithology: diatom-bearing mud, dark gray (5Y 4/1). Silty, calcareous, and bioturbated, with shell fragments.

Minor lithologies:
1. dolomite, olive (5Y 4/3), nodular.
2. calcareous mud, gray (5Y 6/1).

SMEAR SLIDE SUMMARY (%):

	1, 33 D	2, 40 D	CC, 10 D
TEXTURE:			
Silt	30	30	40
Clay	70	70	60
COMPOSITION:			
Quartz	20	25	20
Clay	45	55	50
Volcanic glass	5	—	—
Dolomite	5	5	5
Accessory minerals			
Pyrite	5	5	10
Foraminifers	—	—	Tr
Nannofossils	Tr	—	—
Diatoms	20	10	15
Silicoflagellates	Tr	Tr	—
Plant debris	Tr	—	—

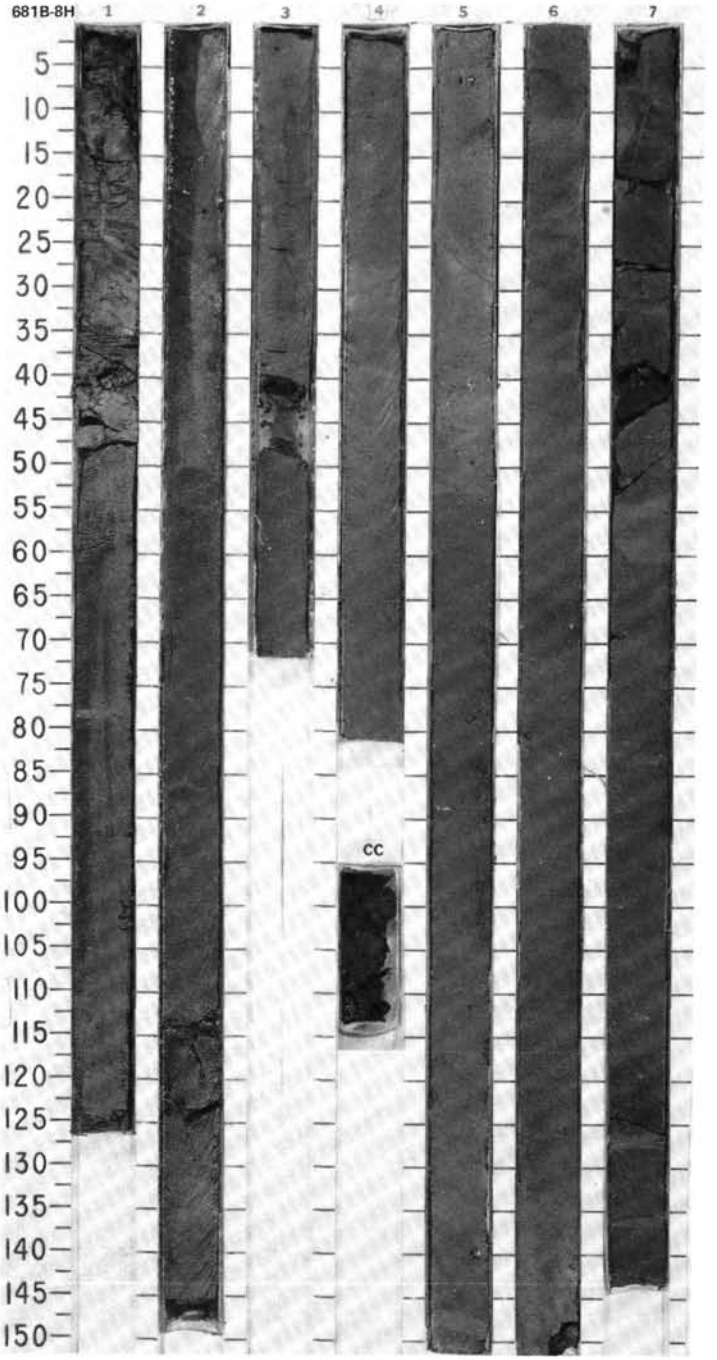

SITE 681 HOLE B CORE 9H CORED INTERVAL 223.8-233.3 mbsl; 72.4-81.9 mbsf

TIME-ROCK UNIT	BIOSTRAT. ZONE/ FOSSIL CHARACTER: FORAMINIFERS	NANNOFOSSILS	RADIOLARIANS	DIATOMS	PALEOMAGNETICS	PHYS. PROPERTIES	CHEMISTRY	SECTION	METERS	GRAPHIC LITHOLOGY	DRILLING DISTURB.	SED. STRUCTURES	SAMPLES
QUATERNARY	* N21 to N22	* NN19	* insignificant	* non diagnostic			IC-0.37 OC-1.20	1, 2, CC	0.5, 1.0			D	OC IW KVE

LITHOLOGIC DESCRIPTION

DIATOM-BEARING MUD

Major lithology: diatom-bearing mud, gray green and dark gray (5GY 4/1, 5Y 4/1). Bioturbated, laminated in part.

Minor lithologies:
1. silt, dark gray (5Y 4/1), sharp based, graded.
2. dolomite, light gray (5Y 7/2), rubbly.

SMEAR SLIDE SUMMARY (%):

	1, 16 D	1, 22 D	CC, 5 D
TEXTURE:			
Sand	5	5	10
Silt	20	30	80
Clay	75	65	10
COMPOSITION:			
Quartz	Tr	10	10
Feldspar	5	10	5
Rock fragments	—	5	—
Clay	20	30	10
Volcanic glass	5	10	—
Dolomite rhombs.	5	5	—
Accessory minerals			
Micrite	—	—	60
Foraminifers	5	Tr	Tr
Diatoms	60	30	15

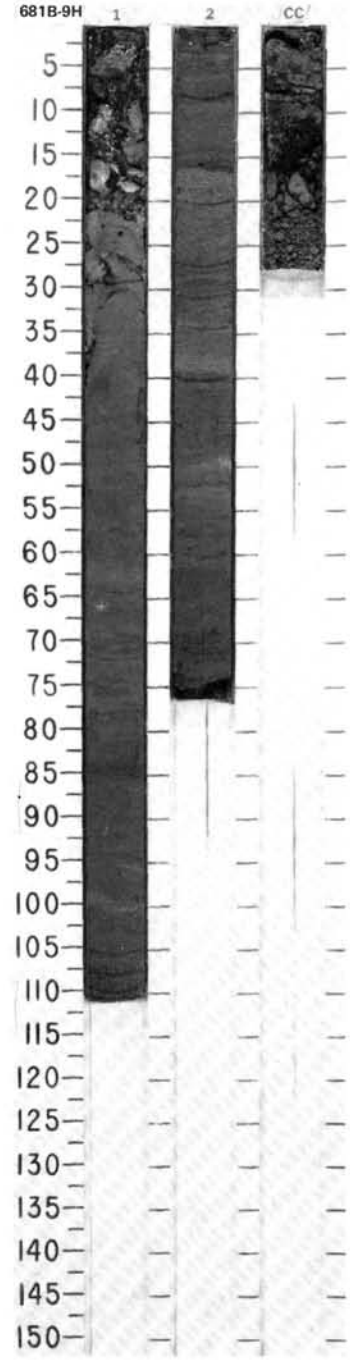

SITE 681 HOLE B CORE 10H CORED INTERVAL 233.3-237.9 mbsl; 81.9-86.5 mbsf

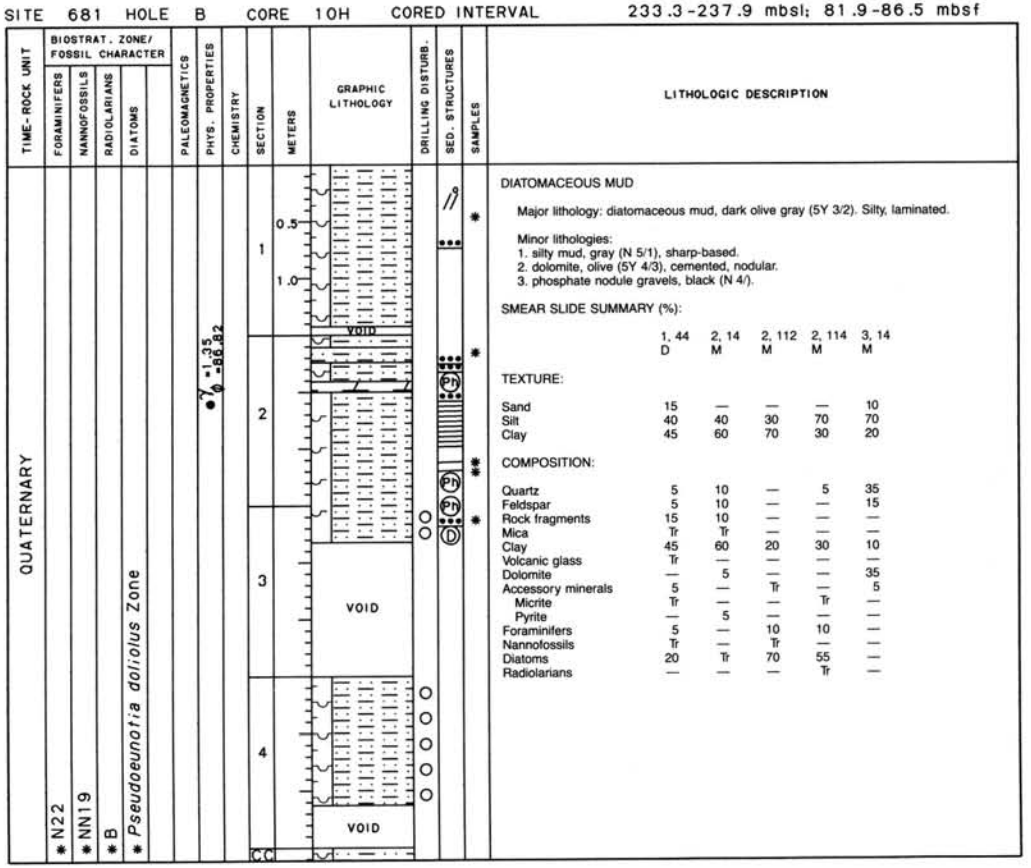

LITHOLOGIC DESCRIPTION

DIATOMACEOUS MUD

Major lithology: diatomaceous mud, dark olive gray (5Y 3/2). Silty, laminated.

Minor lithologies:
1. silty mud, gray (N 5/1), sharp-based.
2. dolomite, olive (5Y 4/3), cemented, nodular.
3. phosphate nodule gravels, black (N 4/).

SMEAR SLIDE SUMMARY (%):

	1, 44 D	2, 14 M	2, 112 M	2, 114 M	3, 14 M
TEXTURE:					
Sand	15	—	—	—	10
Silt	40	40	30	70	70
Clay	45	60	70	30	20
COMPOSITION:					
Quartz	5	10	—	5	35
Feldspar	5	10	—	—	15
Rock fragments	15	10	—	—	—
Mica	Tr	Tr	—	—	—
Clay	45	60	20	30	10
Volcanic glass	Tr	—	—	—	—
Dolomite	—	5	—	—	35
Accessory minerals	5	—	Tr	—	5
Micrite	Tr	—	—	Tr	—
Pyrite	—	5	—	—	—
Foraminifers	5	—	10	10	—
Nannofossils	Tr	—	Tr	—	—
Diatoms	20	Tr	70	55	—
Radiolarians	—	—	—	Tr	—

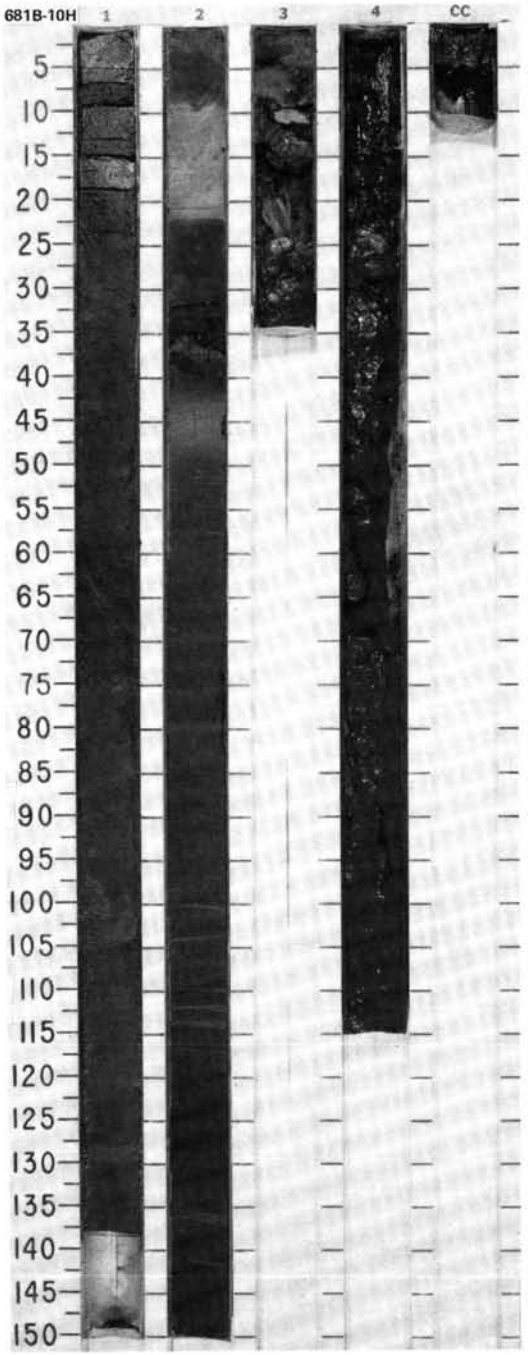

SITE 681 HOLE B CORE 11X CORED INTERVAL 237.9-247.4 mbsl; 86.5-96.0 mbsf

TIME-ROCK UNIT	BIOSTRAT. ZONE/ FOSSIL CHARACTER: FORAMINIFERS	NANNOFOSSILS	RADIOLARIANS	DIATOMS	PALEOMAGNETICS	PHYS. PROPERTIES	CHEMISTRY	SECTION	METERS	GRAPHIC LITHOLOGY	DRILLING DISTURB.	SED. STRUCTURES	SAMPLES	LITHOLOGIC DESCRIPTION
	* non diagnostic	* B	* B	* non diagnostic				1 CC	0.5 1.0	VOID			*	CALCAREOUS SANDY SILT Major lithology: calcareous sandy silt, very dark gray (5Y 3/0). Massive. SMEAR SLIDE SUMMARY (%): CC, 11 D TEXTURE: Sand 25; Silt 65; Clay 10 COMPOSITION: Quartz 20; Feldspar 20; Rock fragments 15; Clay 10; Accessory minerals 5; Micrite 30

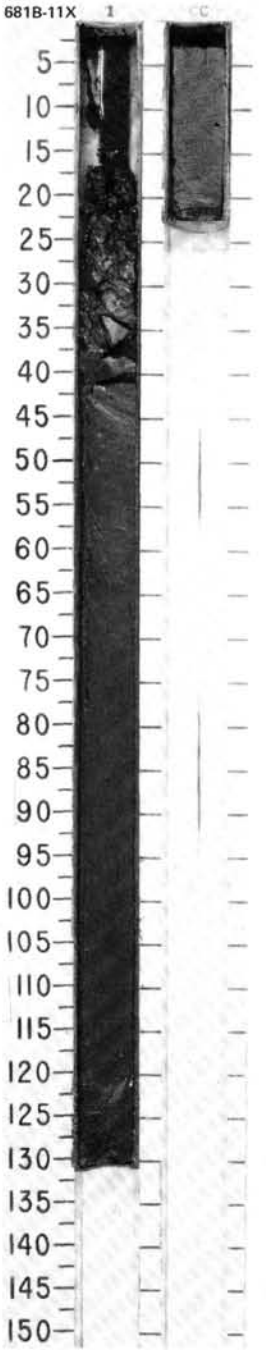

SITE 681 HOLE B CORE 12X CORED INTERVAL 247.4-256.9 mbsl; 96.0-105.5 mbsf

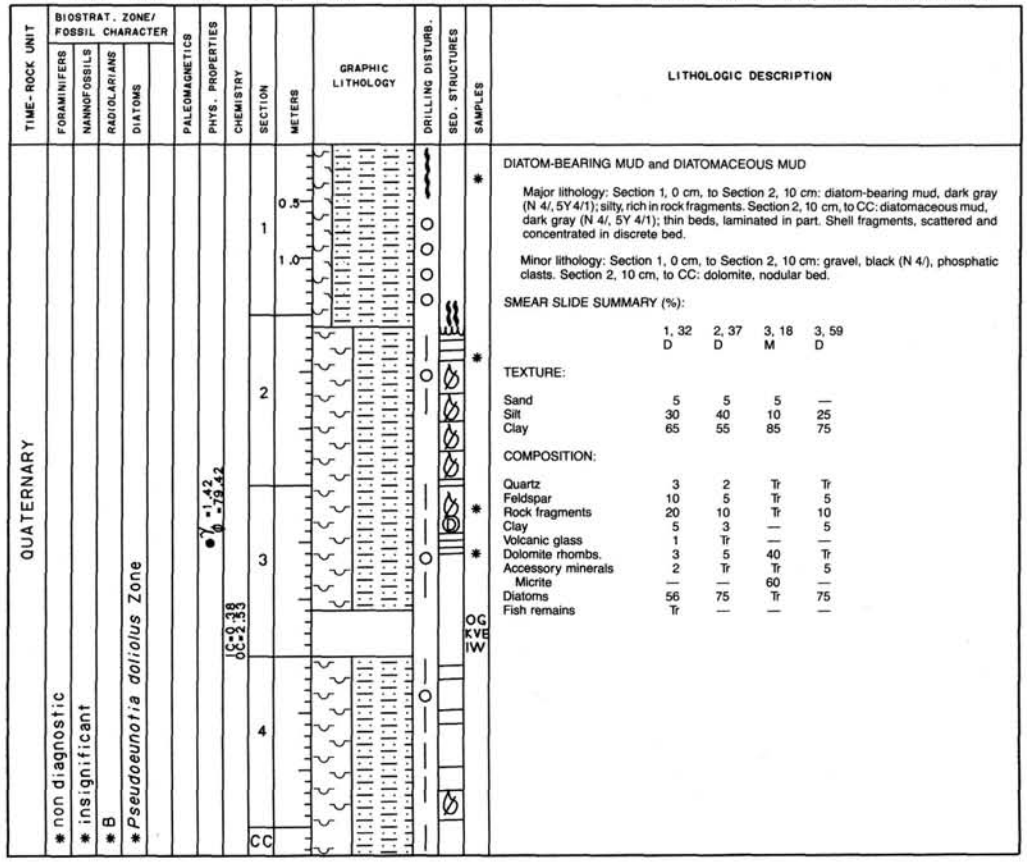

LITHOLOGIC DESCRIPTION

DIATOM-BEARING MUD and DIATOMACEOUS MUD

Major lithology: Section 1, 0 cm, to Section 2, 10 cm: diatom-bearing mud, dark gray (N 4/, 5Y 4/1); silty, rich in rock fragments. Section 2, 10 cm, to CC: diatomaceous mud, dark gray (N 4/, 5Y 4/1); thin beds, laminated in part. Shell fragments, scattered and concentrated in discrete bed.

Minor lithology: Section 1, 0 cm, to Section 2, 10 cm: gravel, black (N 4/), phosphatic clasts. Section 2, 10 cm, to CC: dolomite, nodular bed.

SMEAR SLIDE SUMMARY (%):

	1, 32 D	2, 37 D	3, 18 M	3, 59 D
TEXTURE:				
Sand	5	5	5	—
Silt	30	40	10	25
Clay	65	55	85	75
COMPOSITION:				
Quartz	3	2	Tr	Tr
Feldspar	10	5	Tr	5
Rock fragments	20	10	Tr	10
Clay	5	3	—	5
Volcanic glass	1	Tr	—	—
Dolomite rhombs.	3	5	40	Tr
Accessory minerals	2	Tr	Tr	5
Micrite	—	—	60	—
Diatoms	56	75	Tr	75
Fish remains	Tr	—	—	—

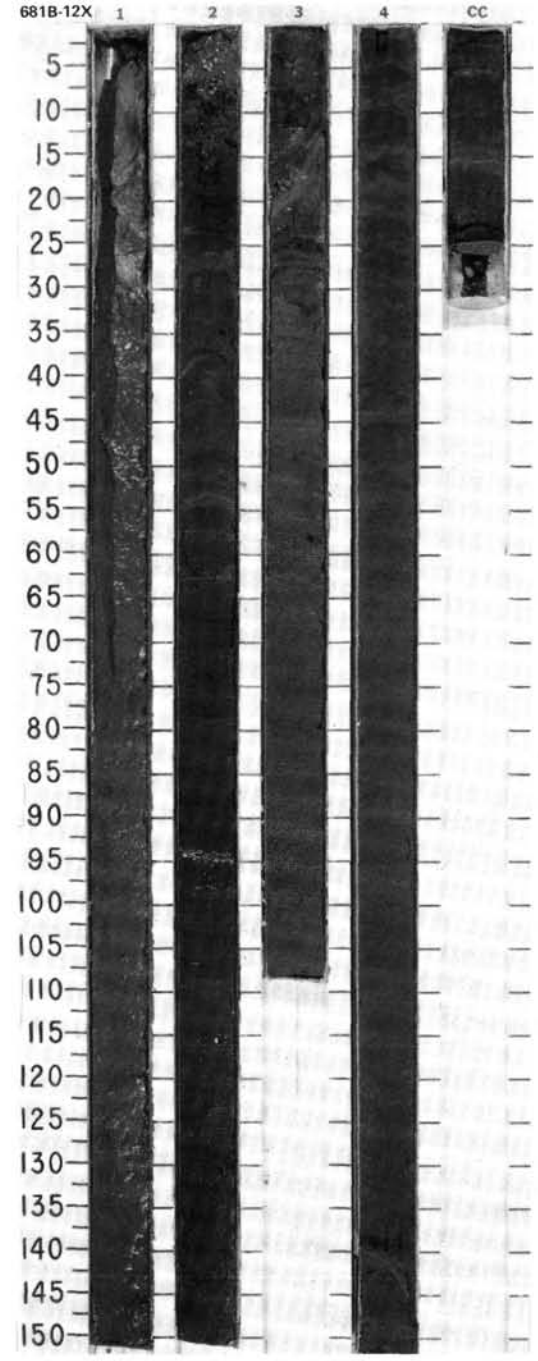

SITE 681 HOLE B CORE 13X CORED INTERVAL 256.9-266.4 mbsl; 105.5-115.0 mbsf

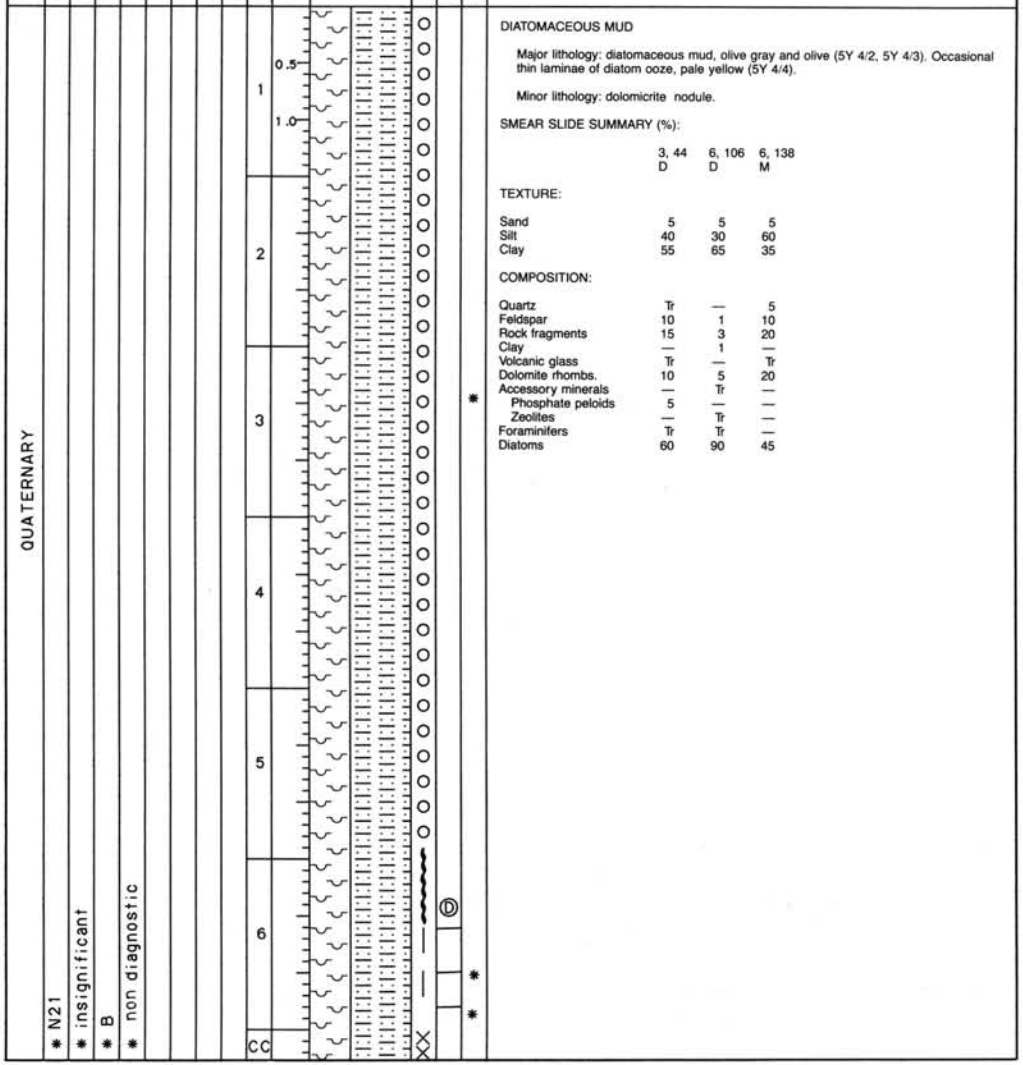

LITHOLOGIC DESCRIPTION

DIATOMACEOUS MUD

Major lithology: diatomaceous mud, olive gray and olive (5Y 4/2, 5Y 4/3). Occasional thin laminae of diatom ooze, pale yellow (5Y 4/4).

Minor lithology: dolomicrite nodule.

SMEAR SLIDE SUMMARY (%):

	3, 44 D	6, 106 D	6, 138 M
TEXTURE:			
Sand	5	5	5
Silt	40	30	60
Clay	55	65	35
COMPOSITION:			
Quartz	Tr	—	5
Feldspar	10	1	10
Rock fragments	15	3	20
Clay	—	1	—
Volcanic glass	Tr	—	Tr
Dolomite rhombs.	10	5	20
Accessory minerals	—	Tr	—
Phosphate peloids	5	—	—
Zeolites	—	Tr	—
Foraminifers	Tr	Tr	—
Diatoms	60	90	45

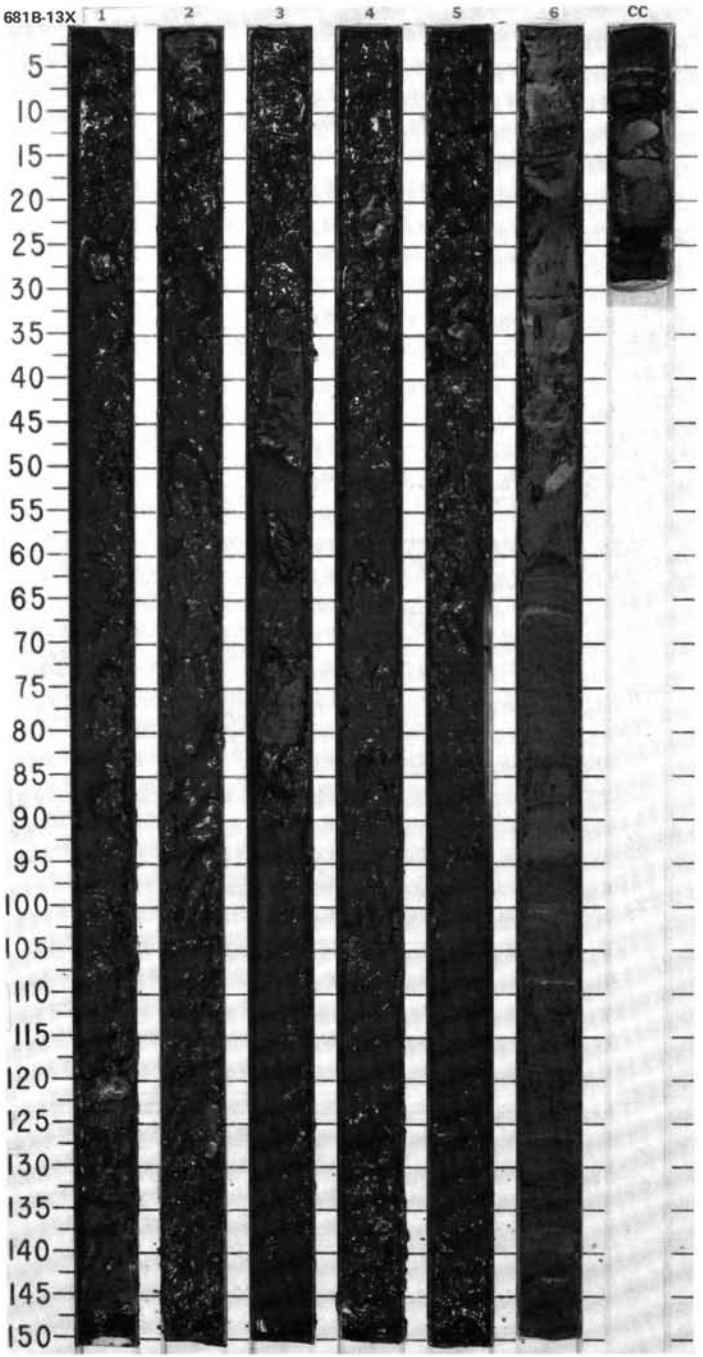

SITE 681 HOLE B CORE 14X CORED INTERVAL 266.4-275.9 mbsl; 115.0-124.5 mbsf

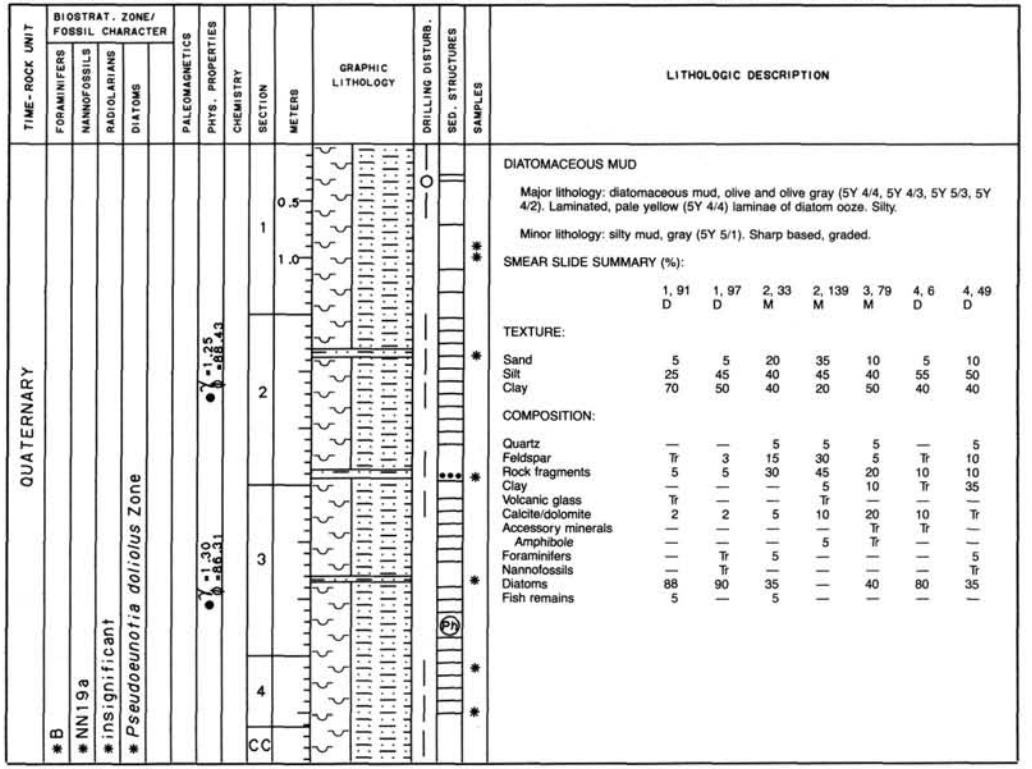

LITHOLOGIC DESCRIPTION

DIATOMACEOUS MUD

Major lithology: diatomaceous mud, olive and olive gray (5Y 4/4, 5Y 4/3, 5Y 5/3, 5Y 4/2). Laminated, pale yellow (5Y 4/4) laminae of diatom ooze. Silty.

Minor lithology: silty mud, gray (5Y 5/1). Sharp based, graded.

SMEAR SLIDE SUMMARY (%):

	1, 91 D	1, 97 D	2, 33 M	2, 139 M	3, 79 M	4, 6 D	4, 49 D
TEXTURE:							
Sand	5	5	20	35	10	5	10
Silt	25	45	40	45	40	55	50
Clay	70	50	40	20	50	40	40
COMPOSITION:							
Quartz	—	—	5	5	5	—	5
Feldspar	Tr	3	15	30	5	Tr	10
Rock fragments	5	5	30	45	20	10	10
Clay	—	—	—	5	10	Tr	35
Volcanic glass	Tr	—	—	Tr	—	—	—
Calcite/dolomite	2	2	5	10	20	10	Tr
Accessory minerals	—	—	—	—	Tr	Tr	—
Amphibole	—	—	—	5	Tr	—	—
Foraminifers	—	Tr	5	—	—	—	5
Nannofossils	—	Tr	—	—	—	—	Tr
Diatoms	88	90	35	—	40	80	35
Fish remains	5	—	5	—	—	—	—

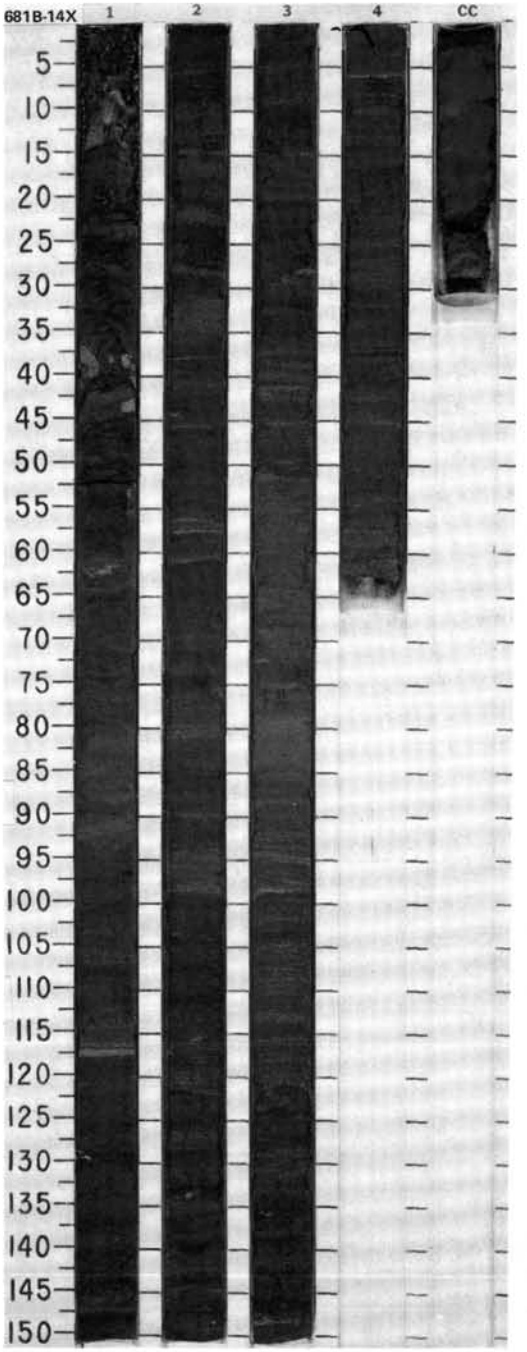

SITE 681 HOLE B CORE 15X CORED INTERVAL 275.9-285.4 mbsl; 124.5-134.0 mbsf

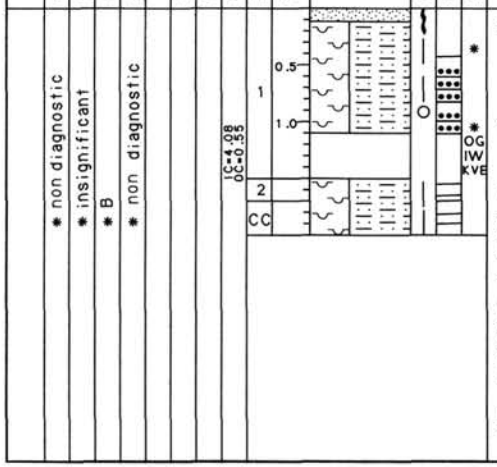

LITHOLOGIC DESCRIPTION

FINE SAND, DIATOMACEOUS MUD, and PHOSPHATIC SAND

Major lithology: Section 1, 0–12 cm: fine sand, dark gray (5Y 4/1). Section 1, 12 cm, to CC: diatomaceous mud, olive and dark olive gray (5Y 3/2, 5Y 5/2, 5Y 4/2, 5Y 4/1), occasional pale yellow (5Y 4/4) laminae of diatom ooze, silty and sandy in part; and phosphatic sand, black (N 4/), grading to dark olive (5Y 3/2); sharp based.

SMEAR SLIDE SUMMARY (%):

	1, 33 D	1, 61 M
TEXTURE:		
Sand	10	100
Silt	30	—
Clay	60	—
COMPOSITION:		
Quartz	Tr	Tr
Feldspar	5	Tr
Rock fragments	20	Tr
Clay	5	—
Dolomite rhombs.	10	—
Accessory minerals		
Zeolites	Tr	—
Phosphate peloids	—	100
Diatoms	60	—
Sponge spicules	Tr	—

SITE 681 HOLE B CORE 16X CORED INTERVAL 285.4-294.9 mbsl; 134.0-143.5 mbsf

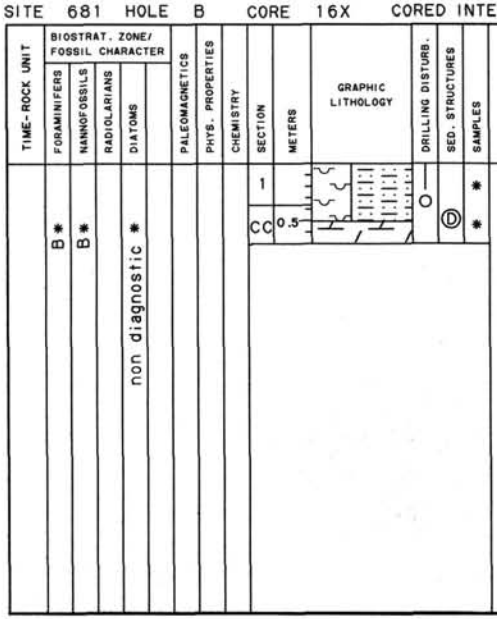

LITHOLOGIC DESCRIPTION

DIATOMACEOUS MUD and DOLOMITIC SILTSTONE

Major lithology: Section 1, 0 cm, to CC, 12 cm: diatomaceous mud, olive gray (5Y 4/2). CC, 12–34 cm: dolomitic siltstone, friable, nodular bed.

SMEAR SLIDE SUMMARY (%):

	1, 16 D	CC, 19 M
TEXTURE:		
Sand	5	Tr
Silt	30	Tr
Clay	65	100
COMPOSITION:		
Feldspar	10	—
Rock fragments	20	—
Clay	Tr	—
Volcanic glass	Tr	—
Dolomite rhombs.	Tr	100
Accessory minerals	5	—
Phosphate peloids	—	Tr
Foraminifers	Tr	—
Diatoms	65	—
Sponge spicules	Tr	—
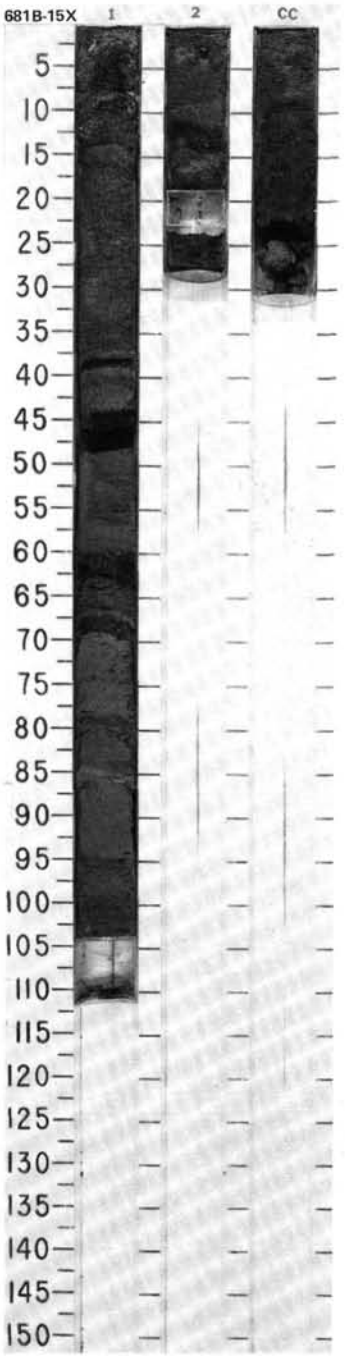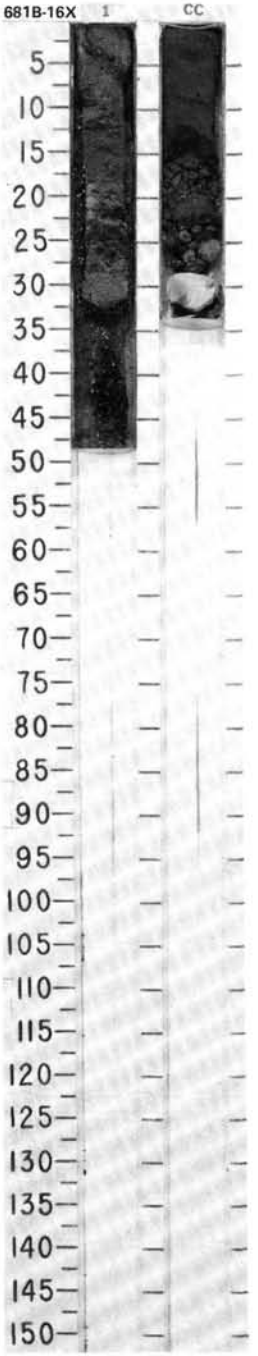
CORES 112-681C-1H TO -10H NOT OPENED